Ingrid Alver Hovsbakken

Kinetic and Isotherm Modelling for the Investigation of Adsorption of Pharmaceuticals onto Suspended Particles in Marine Environmental Conditions

Master's thesis

NTNU
Norwegian University of
Science and Technology

Ingrid Alver Hovsbakken

Kinetic and Isotherm Modelling for the Investigation of Adsorption of Pharmaceuticals onto Suspended Particles in Marine Environmental Conditions

Master's thesis in MIKJ
Supervisor: Alexandron Asimakopoulos
Co-supervisor: Lisbet Sørensen and Mari Creese (SINTEF Ocean)
June 2022

Norwegian University of Science and Technology
Faculty of Natural Sciences
Department of Chemistry

NTNU
Norwegian University of
Science and Technology

Abstract

Pharmaceuticals are emerging pollutants that are currently being released into the marine environment with little care. Adsorption onto suspended particles is believed to contribute to the accumulation of pharmaceuticals in the ocean, which can affect their transport, fate and environmental impact.

Adsorption occurs due to interactions between pharmaceutical molecules and solid suspended particles. Adsorption is a complicated process that depends on many different factors of the adsorbent (the solid particles) and the adsorbate (molecules in the liquid phase). Kaolin is a naturally occurring sediment which has a relatively low adsorption potential, due to its low surface area and low cation exchange capacity compared to other materials. It is however very abundant in our oceans, and understanding its sorption potential can be of importance for assessing the accumulation or transport of organic pollutants.

Adsorption was studied by mixing pharmaceuticals with seawater and kaolin particles for different time intervals and at different initial concentrations. Seawater samples were filtered, diluted and analysed by HPLC-MS/MS. Results revealed that two antidepressants, citalopram and fluoxetine, in addition to the antibiotic ciprofloxacin were among the compounds that adsorbed to kaolin. Their adsorption kinetics over time and their adsorption isotherms were established.

pK_a and log K_{OW} of the adsorbate are said to be important factors for adsorption. However, no clear relationship could be established between these properties and the adsorption, as both acidic and basic, hydrophobic and hydrophilic compounds adsorbed to the kaolin particles.

The optimal isotherm model was chosen on the basis of visual fit, SNE (sum of normalized error) and sizes of different error functions. The HYBRID fractional error function gave the lowest overall error and appeared to visually give a good fit between experimental values and the isotherm model. It was applied to obtain the optimum adsorption model. The kinetics experiments revealed that the adsorption followed the Pseudo-second order rate equation best. The reaction rates increased with increasing amounts of particles in the system. The isotherm experiments revealed that the experimental data fit best to the Sips isotherm, a 3-parameter model. The 2-parameter Langmuir model also fit the data well. The Sips isotherm parameters revealed that the adsorption was favoured at 9 °C more than 4 °C, as the maximum adsorption capacities were higher. The Sips affinity constant was however highest for all compounds at 4 °C.

Sammendrag

Legemidler er nylig oppdagede forurensende forbindelser som slippes ut i det marine miljøet uten særlig omtanke. Man tror at adsorpsjon til suspenderte partikler kan bidra til akkumulering av legemidler i havet, noe som kan påvirke deres transport, skjebne og miljøpåvirkning.

Adsorpsjon oppstår på grunn av interaksjoner mellom legemiddel-molekyler og suspenderte partikler. Adsorpsjon er en komplisert prosess som avhenger av mange forskjellige faktorer som omhandler adsorbenten (de solide partiklene) og adsorbatet (de oppløste molekylene). Kaolin er et naturlig forekommende sediment som har et relativt lavt adsorpsjonspotensiale på grunn av sitt lave overflateareal og lave kationbyttekapasitet. På den andre siden er forekommer det i stor grad i havene våre, og å forstå dets adsorpsjonspotensiale kan være viktig for å adressere akkumuleringen og transporten av organiske forurensinger.

Adsorpsjon ble undersøkt ved å blande legemidler med sjøvann og kaolin-partikler i forskjellige tidsintervaller og ved forskjellige startkonsentrasjoner. Sjøvannet ble deretter filtrert, fortynnet og analysert med HPLC-MS/MS. Resultatene avdekket at blant annet to antidepressiva og en type antibiotika var blant forbindelsene som adsorberte til kaolin. Deres adsorpsjonskinetikk over tid og deres adsorpsjonsisotermer ble fastslått. pK_a og log K_{OW}-verdier for adsorbatet er viktige faktorer for adsorpsjon. Men noe klar sammenheng mellom disse egenskapene og adsorpsjon kunne ikke bli fastslått, da både sure og basiske, hydrofobe og hydrofile forbindelser adsorberte til kaolinpartiklene.

Den optimale isotermmodellen ble valgt på bakgrunn av visuell match, SNE (Sum of normalised error) og størrelsen på feil-funksjonene. HYBRID-feilfunksjonen ga de generelt laveste avvikene og så ut til å gi en visuelt god match mellom de eksperimentelle dataene og isotermmodellen. Den ble brukt til å skaffe den optimale adsorpsjonsmodellen.

Kinetikk-eksperimentene avslørte at adsorpsjonen fulgte en Pseudo første ordens reaksjon best. Reaksjonshastighetene økte med økende mengde partikler i systemet. Isoterm-eksperimentene avslørte at de eksperimentelle dataene passet best til Sips-isotermen, en 3-parameter-modell. 2-parameter-modellen som passet dataene best var Langmuir-modellen. Sips isoterm-parameterne avslørte at adsorpsjonen var favorisert ved 9 °C mer enn 4 °C, fordi den maksimale adsorpsjonskapasiteten var høyere. Sips-affinitetskonstanten var derimot høyere for alle stoffene ved 4 °C.

Preface

This thesis is the product of a 2-year Master's study in Chemical Engineering and Biotechnology (MIKJ), with a specialization in Analytical Chemistry at NTNU Trondheim. This thesis is written in collaboration with SINTEF Ocean in Trondheim. The work in this thesis is a part of the Pharmarine project, an international collaboration project between SINTEF Ocean, UNIS (The University centre of Svalbard), the University of Gdansk, the Medical university of Gdansk and the Institute of Oceanology Polish Academy of Sciences. The project is funded by EEA Poland-Norway Grants, and all expenses and resources used for this thesis (equipment, chemicals, SINTEF staff supervision and instruments) were covered by this funding.

I would like to thank my supervisors who have always been available to help me throughout the project. To Lisbet and Mari, who have helped me throughout both my pre-project and my masters, by always giving good insight, advice and assuring words when things didn't go to plan. An extra thank you to Lisbet who gave me the opportunity to join the project and earn experience that I am sure will come in handy in my upcoming working career. Thank you to Alexandros for always providing helpful feedback to my work. Thank you to Ewa, while not officially my supervisor, but who contributed to my success in terms of helping me with method development, analyses and making sure we got everything done in time.

To all other staff at SINTEF Ocean, especially the laboratory staff, who has always helped me with finding equipment, answering all my questions and helping me with practical challenges related to my laboratory work

Thank you to my friends who have supported and encouraged me when I have been stressed and overwhelmed with work – you know who you are.

Table of contents

x

List of figures

List of tables

Abbreviations

ARE – Average relative error

BET - Brunauer-Emmett-Teller isotherm model

C_0 – Initial concentration

C_e – Equilibrium concentration

CIP - Ciprofloxacin

CIT – Citalopram

D-R - Dubinin-Radushkevich isotherm model

DFT – Density Functional theory

EABS – Sum of absolute errors

ESI – Electrospray ionisation

FLU – Fluoxetine

FT-IR – Fourier transform infrared spectroscopy

HPLC – High performance Liquid Chromatography

HYBRID – HYBRID fractional error

IS – Internal standard

K – Partitioning coefficient

k – rate constant

LC-MS/MS – Liquid chromatography tandem mass spectrometry

LOD – Limit of detection

LOQ – Limit of quantification

MP – Mobile phase

MPSD - Marquardt's percent standard deviation

PFO – Pseudo-first Order

PPCP - Pharmaceuticals and personal care products

PSO – Pseudo-second order

q_e – Equilibrium adsorption capacity

q_{max} – Maximum adsorption capacity

R^2 – Coefficient of determination

RT – Retention time

SNE – Sum of normalised errors

SPE – Solid phase extraction

SSR – Sum of squared residuals

SST – Total sum of squares

WWT(P) – Wastewater treatment (plant)

1 Introduction

A pharmaceutical is a compound meant to prevent, heal or relieve illness, symptoms, pain or to affect physiological functions in humans or animals (The Norwegian Medicines Agency, 2020). Pharmaceuticals are a vital part of sustaining our health and quality of life. The use of plants, clays, minerals and even animals for medicinal purposes began thousands of years ago and have made enormous developments since then. The modern pharmaceutical industry began in the 1800s, with the purification, isolation and synthesis of drugs, and the continuous development of the industry has been essential for the elimination and control of diseases throughout the years (Gill, 2016). The global use of pharmaceuticals is increasing and expected to continue to increase in the future (UNESCO, 2017, IQVIA, 2022).

While pharmaceuticals serve an important purpose for our health and well-being, their release into the environment has caught the attention of scientists and environmental agencies around the world during the last decades (Halling-Sørensen et al., 1998, Kümmerer, 2008). Pharmaceuticals enter the environment via wastewater from urban, domestic and industrial areas, in addition to sewage, aquaculture and agriculture runoff (Bottoni et al., 2010). Pharmaceuticals are being reported in aquatic environments around the world in the ng/L to µg/L range (UNESCO, 2017, Brumovský et al., 2017, Pereira et al., 2016, Kim et al., 2017). Pharmaceuticals and personal care products (PPCPs), along with their metabolites and degradation products, are now considered pollutants of emerging concern, meaning they have relatively recently been discovered in natural streams, their release is poorly regulated by standards and they can potentially cause harmful effects to aquatic life (EPA, 2008). Scientists agree that pharmaceutical emissions need monitoring and more effective removal procedures during wastewater treatment (WWT) in order to prevent them from being released into the environment. However, while there exist water quality guidelines for bacterial content and other polluting compounds such as heavy metals and selected pesticides, there is currently a lack of guidelines and regulations for surveillance of pharmaceuticals (Beiras and Schönemann, 2021, WHO, 2012). Many pharmaceuticals are only partly removed in wastewater and drinking water treatment, meaning small amounts are constantly being excreted into the environment (Verlicchi et al., 2012, Stackelberg et al., 2007)

Scientists are beginning to understand the unwanted effects of pharmaceuticals on the environment, and their potential detrimental effects to aquatic ecosystems. Since pharmaceuticals are designed to have a biological effect in small amounts, even trace amounts

in the environment can cause chronic and unwanted effects in individual organisms, which can in turn affect ecosystems (Pavlovic et al., 2017, Parolini et al., 2010, Gonzalez-Rey et al., 2014). As examples, antibiotic residues have been shown to enhance antibiotic resistance and affect the nutrient recycling in microorganisms, and antidepressants have been shown to affect growth and reproductive abilities in marine organisms in µg/L levels (Näslund et al., 2008, Brooks et al., 2003).

While some pharmaceuticals are easily degradable in environmental conditions, others are more persistent, meaning they are less easily degraded and can stay in the environment for long periods of time. Pharmaceutical degradation is dependent on parameters such as physical and chemical properties of the individual compounds, the environmental matrix they exist in, microbial presence, temperature and sun exposure (Patel et al., 2019). Another factor that affects their fate in the aquatic environment is their sorption to suspended particles, which can alter their bioavailability and degradation potential (Khan et al., 2020). Many pharmaceuticals are already known to be able to adsorb to soil and sediment particles and these mechanisms can act as a sink for accumulation of these compounds (Patel et al., 2019, Ledieu et al., 2021). If pharmaceuticals adsorb and migrate into marine sediments, their persistence can increase in comparison to their persistence in the water column (Hektoen et al., 1995). This can affect their bioavailability and transport pathways. While sorption onto sediments may be an advantage for organisms living in the water column, it can possibly have negative effects on organisms that live in and feed of sediments and other particles. Sub-lethal effects in marine organisms exposed to sediments spiked with pharmaceuticals have been proven (Maranho et al., 2014). Research on the environmental impact of pharmaceuticals has become an important and popular area of study in the last decades, and more research is needed in order to properly understand the full life cycle of pharmaceutical contaminants in the marine environment.

The goal of the Pharmarine project, which this thesis is a part of, is to model and quantify the transport of pharmaceuticals from continental Europe via ocean currents to the Arctic, to assess the pharmaceutical contamination status in the European marine environment and to study the effects of pharmaceutical exposures on Arctic organisms (EEA, 2022). This thesis will look into the adsorption properties of selected pharmaceuticals onto sediment particles, with the aim of generating partitioning coefficients which can help data models better predict the transport of pharmaceuticals from Europe to the European Arctic. By exploring the adsorptive properties of pharmaceuticals onto particles relevant for marine conditions, we can better understand their environmental behaviour and transport potential.
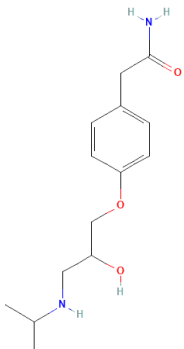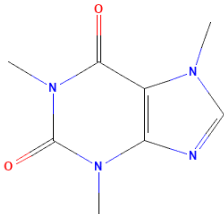
In the fall of 2021, a specialization project was conducted to validate an analytical method using liquid chromatography tandem mass spectrometry (LC-MS/MS) (Hovsbakken, 2021). The method was used to quantify a range of pharmaceuticals and personal care products (PPCPs), select a sample preparation procedure for PPCOs in seawater, investigate their stability in seawater and perform preliminary investigation of their potential to adsorb to inorganic sediment (kaolin) and biological (zooplankton species *Skeletonema Costatum*) particles. For this thesis, the focus has been to investigate the adsorption mechanisms between selected pharmaceuticals and kaolin, through exploring their adsorption kinetics and isotherms.
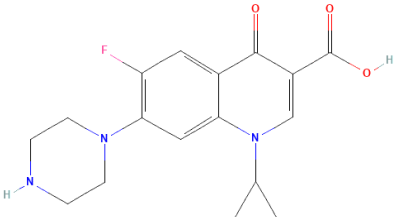
2 Theoretical background
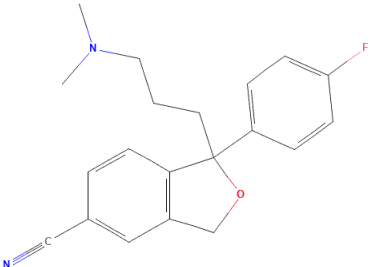
2.1 Pharmaceuticals
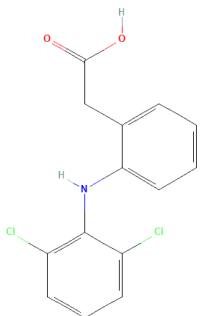
The term "pharmaceuticals" is used to represent a wide variety of compounds, and include many different therapeutic classes, including NSAID's (Non-Steroidal Anti-Inflammatory Drugs), antibiotics, antidepressants, lipid-regulating drugs, anti-epileptic drugs and stimulants. While they are all mostly metabolized in the human liver, their mechanisms in the body vary, from killing unwanted microorganisms to influencing receptors in the brain (Almazroo et al., 2017). Thus, compounds classified as pharmaceuticals can have very different molecular structure, and therefore also have great variety of physical and chemical properties, such as mass, ionizability and polarity. The pharmaceuticals used in this thesis along with some of their properties, are listed in Table 1.
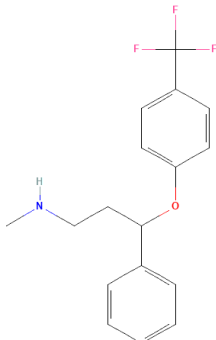
Table 1: Overview of pharmaceuticals in this study, their molecular structures and relevant properties
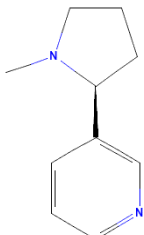
Compound	Type	Structure (National Library of Medicine, 2021)	CAS #	Mass	Chemical formula	pK_A	Log K_{OW} (Williams et al., 2017)
Atenolol	Beta blocker		29122-68-7	266,34	$C_{14}H_{22}N_2O_3$	9,6 [a]	0,16
Caffeine	Stimulant		58-08-2	194,19	$C_8H_{10}N_4O_2$	10,4 [b]	- 0,07
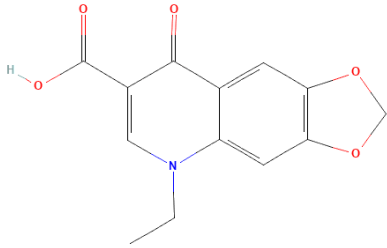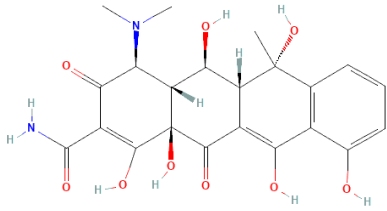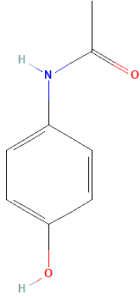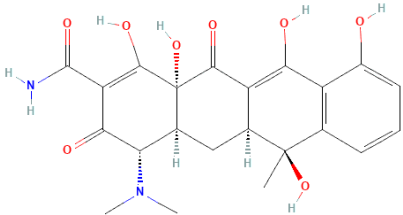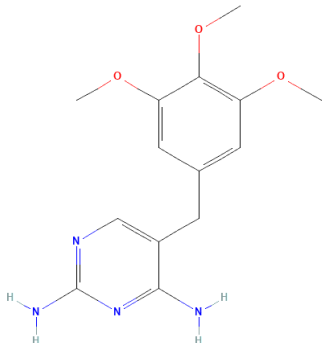
			CAS	MW	Formula	pKa	logP
Ciprofloxacin	Antibiotic		85721-33-1	331,34	$C_{17}H_{18}FN_3O_3$	1: 3,01 2: 6,14 3: 8,70 4: 10,58 [c]	0,280
Citalopram	Anti-depressant		59729-33-8	324,39	$C_{20}H_{21}FN_2O$	9,6 [b]	3,04
Diclofenac	NSAID		15307-86-5	296,15	$C_{14}H_{11}Cl_2NO_2$	4,1 [a]	4,51
Fluoxetine	Anti-depressant		54910-89-3	309,33	$C_{17}H_{18}F_3NO$	10,1 [b]	4,05
Nicotine	Stimulant		54-11-5	162,23	$C_{10}H_{14}N_2$	6,16 [d]	1,17

5

Oxolinic acid	Antibiotic		14698-29-4	261,23	$C_{13}H_{11}NO_5$	5,94 [e]	0,940
Oxytetracycline	Antibiotic		79-57-2	460,43	$C_{22}H_{24}N_2O_9$	1: 3,22 2: 7,46 3: 8,94 [c]	-0,9
Paracetamol	NSAID		103-90-2	151,16	$C_8H_9NO_2$	9,38 [f]	0,460
Tetracycline	Antibiotic		60-54-8	444,43	$C_{22}H_{24}N_2O_8$	1: 3,32 2: 7,78 3: 9,58 [c]	-1,30
Trimethoprim	Antibiotic		738-70-5	290,32	$C_{14}H_{18}N_4O_3$	1: 3,23 2: 6,76 [c]	0,91

a: (Le Guet et al., 2018), b: (Costa Junior et al., 2022), c:(Qiang and Adams, 2004), d: (Akcay and Yurdakoc, 2008), e: (Chemical Abstracts Service, 2021), f: (Dastmalchi et al., 1995)

2.2 Adsorption

Adsorption is a naturally occurring phenomenon which appears in biology, chemistry, physics and environmental science (Dabrowski, 2001). Adsorption processes are also important in many industrial fields such as catalysis, carbon capture, separation processes and gas and water purification, in addition to being deployed in wastewater treatment plants (WWTPs) to remove contaminants from water (Singh et al., 2018).

Adsorption can be defined as the process where a vapor, gas, liquid or suspended/dissolved substances (the adsorbate) within these phases comes in contact with a solid material (the adsorbent) and is captured either on its surface or within its pores (Chen, 2017a, Wang and Guo, 2020a). The reversed process is called desorption. These two processes take place simultaneously, and thermodynamic properties such as pressure and temperature, in addition to properties of the adsorbate and adsorbent, favour either of the processes over the other (Dabrowski, 2001). Favourable adsorbents are characterised by high stability and robustness and are often porous materials with large surface areas, which yield them high adsorption capacities. For example, activated carbon has a very large surface area per mass, which contributes to it being a very effective adsorbent (Chen, 2017b).

Adsorption can take place by different adsorption mechanisms. Three of these are shown in Figure 1. The figure describes chemical, physical and ion exchange adsorption mechanisms, and the process occurring in a given system depends on the strength and the mechanism of the bond formation between the adsorbate and the adsorbent (Sims et al., 2019). Chemical adsorption, or chemisorption, implies that the adsorbate binds to the adsorbent through covalent bonds or through sharing or donation of electrons between the adsorbate and the adsorbent. This results in a monolayer of adsorbate on the adsorbent, which in time will reach a maximum amount of the adsorbed species, because there is a limited number of sites for the adsorbate to adsorb to (Wang and Guo, 2020a). Physical adsorption, also called physisorption, occurs when London, dipole-dipole and van Der Waal interactions are formed between the adsorbent and the absorbate. These types of interactions can result in multilayer adsorption, where several layers of adsorbate molecules can be stacked on the adsorbent. Often, the binding between the adsorbate and the adsorbent becomes weaker as more layers build, but it theoretically never reaches a maximum limit. Physisorption also includes weak electrostatic interactions, such as ion exchange, where the binding is driven by the opposite charges of the adsorbate molecules and the adsorbent surface. Since physisorption is a product of weak forces, it is reversible and bonds can easily be broken (Al-Ghouti and Da'ana, 2020). The mechanism of adsorption in a

specific system depends on the affinity between the adsorbent and the adsorbate, which is dependent on both chemical properties of the adsorbate and adsorbent, in addition to factors in their environment. In porous materials, diffusion of molecules into the pores of the adsorbent can also contribute significantly to the adsorption reaction (Chen, 2017b)
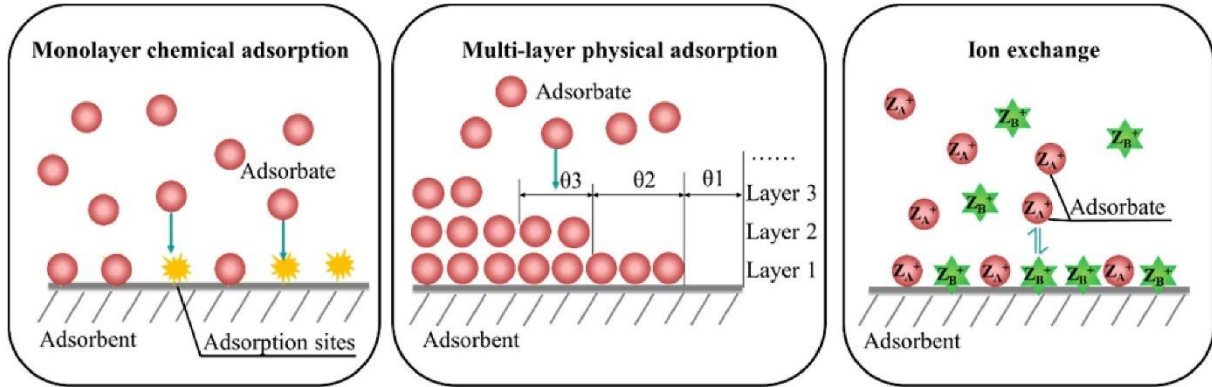
Figure 1: Adsorption mechanisms (Wang and Guo, 2020a)

The amount of a compound adsorbed to an adsorbent suspended in a liquid solution can be calculated from equation 1 (Couto Jr et al., 2015). The q_t is a necessary parameter to obtain in order to study the kinetics of the adsorption reaction and explore the adsorption mechanisms.

$$q_t = \frac{(C_0 - C_t) \times V}{M} \tag{1}$$

q_t (mg/g) is the amount of adsorbate adsorbed at a time t, C_0 is the initial concentration of adsorbate in solution (mg/L), C_t is the adsorbate concentration remaining in solution (mg/L) after a time t, V is the volume of the adsorbate solution (L) and M is the mass of adsorbent (g). q_t is often given the unit mg/g, mmol/g or mmol/kg, depending on the suitable units of the parameters in the equation. An adsorbent is said to have a maximum adsorption capacity, but this depends on the mechanism of the adsorption process and the adsorbent being studied. The maximum adsorption capacity is referred to as the q_{max}. In kinetics modelling, the adsorbed amount of adsorbate at equilibrium is often referred to as the q_e.

Another way of approximating the amount of removed compound from a solution it the sorption percentage, also referred to as % removed (Pavlovic et al., 2017). It is calculated based on the initial and the remaining concentration of the compound in the solution after a given time. It

can be used to estimate the adsorption of compounds from solution onto solid particles. The equation for the sorption percentage is given in equation 2.

$$Sorption\ percentage = \frac{C_0 - C_t}{C_0} \times 100\% \qquad (2)$$

The sorption percentage must though be used with caution, as studies have shown that it can have some limitations to its use, and the resulting plot must not be confused with an adsorption isotherm (Tran et al., 2017). The sorption percentage does not take into consideration the amount of adsorbent in the system and cannot be used to calculate adsorption kinetic parameters, but it can be useful for approximating the total percentage of adsorbate removed over time.

A partitioning coefficient, or distribution coefficient, describes the ratio of a compound that is distributed between different phases in a system. Partitioning coefficients are specific to the system under investigation, and are dependent on temperature, pressure and other physical and chemical factors of the elements in the system. In the case of this thesis, the coefficient can be used to describe the distribution of an adsorbate in a solid-aqueous system. The equation for the distribution coefficient (K) in a solid-liquid system is given in equation 3:

$$K = \frac{q_e}{C_e} \qquad (3)$$

Here, q_e is the amount of adsorbate on the solid adsorbent surface at equilibrium (mg/g) and Ce is the equilibrium concentration in the liquid phase (mg/L). This gives K the unit of L/g, unless other units are used for q_e and C_e.

The partitioning of an adsorbate between the liquid and solid phase in a system is dependent on many factors, such as the initial concentration of adsorbate and adsorbent, hydrophobicity/hydrophilicity, contact time, pH, ionic strength, particle size and temperature (Li and Zhang, 2017, Pavlovic et al., 2017).

2.2.1 Chemical properties influencing adsorption

Properties of the adsorbate

Chemical properties of the adsorbate and the adsorbent will heavily affect the adsorption mechanism. The pK_a of a substance determines at which pH the compound is ionized, which in turn will affect its sorption to particles. Acidic drugs, such as diclofenac (pK_a = 4,1), are

expected to be deprotonated and anionic at neutral pH and be primarily in the water phase of the adsorption system, and their adsorption is expected to increase with lower pH. For example, the low pK_a of diclofenac is one of the reasons it is not removed efficiently in WWTPs (Wastewater treatment plants), as it does not adsorb effectively to sludge (Fent et al., 2006).

The K_{OW} (or more commonly used, Log K_{OW}) is the octanol-water distribution coefficient and describes the hydrophilicity or hydrophobicity of a compound by determining its distribution between polar (water) and non-polar (octanol) phases. A hydrophobic compound will tend to partition more in a non-polar phase more than a hydrophilic compound. Hydrophilic compounds with low or negative log K_{OW} will tend to stay in the water phase and not be adsorbed onto particles, in comparison to hydrophobic compounds which might tend to "escape" the water phase (Wang et al., 2021). Studies have found that pK_a and Log K_{OW} are among the most important parameters determining the partitioning of compounds between liquid and solid phases (Al-Khazrajy and Boxall, 2016).

Properties of the adsorbent

The PZC (point of zero charge) is the pH where the net surface charge on the surface of an adsorbent is zero. This means that the amount of positive and negative charges in its surface are equal, giving it a neutral net surface charge (Appel et al., 2003). If the pH of the system is higher than the PZC, the net surface charge will become negative, and the particles will have an increased ability to exchange cations with its surrounding environment.

The CEC (cation exchange capacity) is a measure of a soil or clay particle's ability to retain cations on its surface(Ma and Eggleton, 1999). It is often used to describe soils in order to predict their ability to retain nutrients in the form of minerals and ions. The CEC is, like the PZC, dependent on the pH of the system.

The size and surface area of the adsorbent particles is important for the adsorption mechanisms. The CEC is also dependent on the particle size of the adsorbent. Studies have found that a decrease in particle size of clay minerals can increase the CEC due to an increase of broken bonds on the particle edges (Ma and Eggleton, 1999), which means that the adsorbent can have more interactions with adsorbate molecules. The same is true for pores on the adsorbent; more pores provide a larger surface area and can increase the adsorption capacity (Chen, 2017a). The

sizes and types of pores can contribute to different adsorption mechanisms taking place, but this is outside the scope of this thesis.

2.2.2 Environmental physiochemical parameters influencing adsorption

Temperature

Temperature can greatly affect adsorption, and the optimum temperature for adsorption is likely dependent on both the nature of the adsorbent and the adsorbate. An increase in temperature has been shown to increase the adsorption of dye onto both clay minerals and natural adsorbent fibres (Umpuch and Sakaew, 2013, Marques et al., 2018). The increased adsorption to clay was attributed to the adsorbent particles experiencing a swelling effect from the increase in temperature, which made it possible to retain even more adsorbate in the clay structure. In addition, in systems with porous adsorbent particles where diffusion into pores play an important role in adsorption, the diffusion of adsorbate into the pores increase with temperature. The increased adsorption to the natural adsorbent fibres was attributed to an increased activity of the dye when temperature increased, leading to more collisions between dye molecules and the adsorbent. Studies on the adsorption of pharmaceuticals onto activated carbon has also come to the same conclusions, which was thought to be due to increased diffusion in and out of the pores of the adsorbent (Nam et al., 2014). A study of the sorption of ciprofloxacin on sediments (Pavlovic et al., 2017) showed that the distribution coefficient (K_D) decreased with higher temperatures, indicating that the adsorption is favoured in lower temperatures. This was attributed to the increase of solubility of the adsorbate with higher temperatures, because of the slightly hydrophilic nature of ciprofloxacin. The same effect was found by Hu et al, when studying the adsorption of atenolol onto kaolin (Hu et al., 2015). This has also been the case with the adsorption of lead and cadmium ions (Horsfall and Spiff, 2005). A study on the adsorption of microcystins (toxins from bacteria) onto different sediments found that one sediment had a positive correlation between temperature and adsorption, while another sediment had a negative correlation (Wu et al., 2011). This was dependent on the organic matter content of the sediments. The sediment with the lowest organic matter content had a negative correlation between temperature and adsorption. It is therefore evident that the effect of temperature on adsorption is dependent on many factors of the system, and there is no equal effect for all adsorbents and adsorbates.

Salinity and presence ions

The cation content of the system affects adsorption, as cations can act as bridges for the binding of pharmaceuticals onto clays (Parolo et al., 2012). Several studies have found that high salt content can decrease the adsorption of pharmaceuticals. Li et al studied the adsorption of trimethoprim on natural marine sediments and found that high salinity decreased the adsorption of trimethoprim (Li and Zhang, 2017). This was due to the sediment having PZC above the experimental pH, meaning that an increase in anions from salt would occupy adsorption sites on the net positively charged sediment surface. Increased hardness of water has also been shown to decrease the adsorption of caffeine onto activated carbon, which was attributed to an increase in solubility, which caused caffeine to prefer the liquid phase more over the adsorbed state (Couto Jr et al., 2015).

pH

The pH of the adsorption system can affect whether the compounds are ionized or not, affecting their binding potential. pH can also affect the surface properties of the adsorbent. For example, tetracycline has four ionizable groups. This means that at different pH's, a different number of these groups will be deprotonated, affecting the binding potential of the molecule. Under neutral conditions, tetracycline will act as a zwitterion (Parolo et al., 2012). Depending on the pK_a values of the different molecules under study, different molecules will be ionized at the experimental pH, and their binding potential will vary. The solubility of the compounds under study will also change due to their ionization. A neutral drug will be more lipid soluble than an ionized drug, which will be more water soluble.

pH can also affect the binding sites on the surface of the adsorbent (Li and Zhang, 2017). This study concluded that when trimethoprim was more in its zwitterionic form (at pH 6,9), the adsorption to the sediment was higher than when it was mostly anionic (at pH 8,1) due to the sediment having the highest amount of positively charged binding sites at the lowest pH, and fewer at the highest pH.

Presence of additional substances in the system

Studies have shown that when the liquid in a liquid-solid adsorption system contain more than one organic adsorbate, competitive sorption can occur (Wang and Wang, 2018). This means that adsorbates compete for adsorption sites on the adsorbent. While hydrophobicity (high log K_{OW}) cannot solely explain which compounds will "win" the competition, it could sometimes be a fairly good indicator (Bakir et al., 2012). Studies have also shown that the adsorption of some pharmaceuticals can increase with the addition of others, due to dimer-formation and co-binding between compounds, making sorption of an otherwise non-adsorbing pharmaceutical possible (Luo et al., 2022). A study on the adsorption of the antibiotics ciprofloxacin and tetracycline showed that the number of adsorption sites was limited. When the compounds were in a singular system, their individual adsorption capacities were about the same as the combined adsorption capacity when they were in a binary system. Each of the compounds adsorption capacity in the binary system were equal, meaning no competition occurred. In that study, the hydrophobicity was not a good indicator of the adsorption, as ciprofloxacin is more hydrophobic than tetracycline, but they had close to equal adsorption when they were in a mixture (Wu et al., 2019)

Adsorption is also dependent on the presence of other components, such as organic matter or humic substances. The content of organic matter is also known to affect the sorption of pharmaceuticals onto sediments by either interacting with the sediments or contribute to mobilization of organic compounds from the sediments to the solution (Le Guet et al., 2018, Wu et al., 2011). The presence of organic substances did not have a uniform effect on all pharmaceuticals, as some pharmaceuticals adsorbed more and some less with the presence of organic humic compounds, according to Le Guet et al. Wu et al found that organic matter could both increase and decrease the adsorption of organic adsorbates, as organic matter could take up adsorption places on the adsorbent, but also enhance the adsorption when exceeding a certain concentration level of organic matter.

Initial concentration of adsorbate and adsorbent

The concentration range of adsorbate and adsorbent in the system of the adsorption experiments can highly affect the outcome of the study (Ángel et al., 2022, Fallou et al., 2016). A study on adsorption of diclofenac on biochar showed that an increase in adsorbent dosage increased the

percentage of diclofenac removed, but had a negative effect the adsorption capacities, q (Maged et al., 2021). The same has been shown for dye removal studies (Marques et al., 2018). This is due to the increase of available adsorption area, but relatively low concentration of adsorbate, leaving many available adsorption sites or surface area free, and therefore not being able to increase the amount removed relative to the amount of adsorbent.

2.3 Adsorption kinetics

Adsorption kinetics are the measuring of the rate of an adsorption reaction over time, at a constant pressure and a given initial concentration (Chen, 2017b). Adsorption kinetic models can be used to predict behaviour and to quantify rate constants and other parameters for the system under investigation. Many different models exist, but in the last decades the most used ones have been the pseudo-first and second order rate laws (PFO and PSO) (Revellame et al., 2020, Ho and McKay, 1999). The rate at which a reaction takes place, and the time it takes for it to reach equilibrium, can be described by rate equations, according to the most suitable rate law, which are described in Table 2.

Table 2: Adsorption kinetic models

Model	Equations	
PFO	$q_t = q_e(1 - e^{-k_1 t})$	(4)
PSO	$q_t = \dfrac{k_2 q_e^2 t}{1 + k_2 q_e t}$	(5)

The constants k_1 (h^{-1}) and k_2 (g*mg/h) are the rate constants of the first and second order equations, respectively. The higher the value of k, the faster the adsorption reaction takes place and reaches equilibrium. k is dependent on the initial concentration of the absorbate (Putro et al., 2021). Wang and Gou found that the PFO was preferred for describing external and internal diffusion at high initial concentrations, while PSO was best at modelling adsorption on adsorbents with many active sites at low initial concentrations (Wang and Guo, 2020b).

2.4 Adsorption isotherms

Adsorption can be described using adsorption isotherm models which show the relationship between the amount of adsorbate in the bulk aqueous phase and the amount adsorbed onto a given amount of adsorbent (Stumm and Morgan, 1996). Adsorption is visualized by plotting q_e, the concentration of adsorbate on the adsorbent at equilibrium, versus C_e, the equilibrium concentration of adsorbate in solution. In order to estimate adsorption parameters such as the distribution coefficients, binding energy and adsorption capacity, the experimental data can be fitted to mathematical adsorption models. Several different models have been developed throughout the years, and many have successfully been used to describe pharmaceutical adsorption onto solid particles. The Langmuir model is the most used model, followed by the Freundlich model, when it comes to pharmaceutical adsorption (Wang and Guo, 2020a). In addition, the Sips and Temkin models have been used for modelling the adsorption of pharmaceuticals. The different models have different assumptions about the adsorption system, and the best fit between a model and experimental data can provide information on the adsorption mechanism. An overview of the adsorption models used in this thesis is given in Table 3, and a more thorough explanation of the models is given below.

Table 3: Overview of adsorption models used in this thesis

Model name	Equation (Wang and Guo, 2020a)		Parameters
Linear (Henry's law)	$q_e = K_D \times C_e$	(6)	K_D = partitioning coefficient (L/g)
Langmuir	$q_e = q_{max} \times \dfrac{K_L \times C_e}{1 + K_L \times C_e}$	(7)	K_L = Langmuir constant (L/mg)
Freundlich	$q_e = K_F \times C_e^{\frac{1}{n}}$	(8)	K_F = Freundlich constant ($L^{1/n} * mg^{1-1/n}/g$) n = measure of non-linearity (Freundlich exponent)
Sips	$q_e = \dfrac{q_{max} \times K_s \times C_e^n}{1 + K_s \times C_e^n}$	(9)	K_s = affinity constant ($L^n * mg^{-n}$), related to adsorption energy n = heterogeneity descriptor
Temkin	$q_e = \dfrac{RT}{b} \times \ln(K_T \times C_e)$	(10)	K_T = binding constant (L/mg) b = Temkin constant (J/mol) R = ideal gas constant

To obtain the model, the adsorption parameters in the model needs to be optimized to achieve a model that fits the experimental data in the best way possible. The linearized forms of the models are frequently used, because of their easy application and estimation of model parameters by linear regression, but non-linear fitting is said to have the least amount of error (Wang and Guo, 2020b).

The linear adsorption model

The linear adsorption model (or Henry's law) is a model that has been successfully used to describe adsorption of adsorbate, given that the initial concentration is relatively low. It is the simplest of the adsorption models and describes adsorption that is unlimited and has no maximum capacity. The larger the value of K_L, the stronger the adsorption (Wu et al., 2019).

The Langmuir model

The Langmuir model is the most used isotherm model (Wang and Guo, 2020a). The Langmuir model assumes that the adsorbate adsorbs as a monolayer, and that the adsorbent has a limited number of adsorption sites, meaning that when all available spaces on the adsorbent have been occupied, there is no more adsorption taking place, and the maximum adsorption capacity, q_{max}, has been reached. The Langmuir model is based on the mechanism of chemisorption between the adsorbate and the adsorbent (Wang and Guo, 2020a). A flaw of the Langmuir isotherm is that it assumes a homogenous adsorbent surface and that all adsorption sites have the same adsorption energy, which might not always be the case (Al-Ghouti and Da'ana, 2020, Jin et al., 2017).

The Freundlich model

The Freundlich model is common for describing physisorption (Wang and Guo, 2020a). It assumes that a multilayer adsorption mechanism takes place, with no maximum adsorption capacity, but takes into consideration that the adsorption energy declines as the strongest adsorption sites are occupied. This means that in theory, a Freundlich system can adsorb an infinite amount of adsorbate, but at a declining rate at higher adsorbate concentrations. The Freundlich model often fits better for heterogenous solid surfaces than the Langmuir isotherm

(Stumm and Morgan, 1996). The factor *n* in the Freundlich model estimates if the adsorption is favourable or not. If n is greater than 0, the adsorption is favourable, but when it is below 0, it is unfavourable. An n-value of 1 means that it is irreversible, and the model equals Henry's Law (Al-Ghouti and Da'ana, 2020)

The Temkin isotherm model

The Temkin adsorption model has been used to estimate the adsorption of pharmaceuticals onto iron-modified clay, in addition to dyes and PAHs from aqueous solutions (Wu et al., 2019, Shikuku et al., 2018). Equal to the Freundlich model, it presumes a multi-layer adsorption process (Wang and Guo, 2020a). It ignores very high and low concentrations of adsorbate, and assumes a linear decrease in adsorption strength as more layers of adsorbate bind to the adsorbent (Shikuku et al., 2018).

The Sips isotherm model

The Sips isotherm model is a 3-parameter hybrid model that combines the Langmuir and the Freundlich models. It can be used to describe both homogenous and heterogenous systems. The Sips model has been used to assess the adsorption of fluoxetine onto various bio-adsorbents like cork and bark (Silva et al., 2020). The Sips model is a 3-parameter model, unlike Langmuir and Freundlich which are 2-parameter models. It is therefore expected to better predict the adsorption parameters for the equilibrium data, and it is proven to be a good model for estimating monolayer adsorption (Saadi et al., 2015) (Wang and Guo, 2020a). When the adsorbate concentration is low, the model reduces to the Freundlich model, and when the concentration is high or the n value is equal to 1, it reduces to the Langmuir model.

2.5 Error functions

In order to estimate the best fitting isotherm model, and from that, the best adsorption parameters, error functions can be implemented in the isotherm modelling in order to quantify the variations between the experimental and the modelled q_e values (Kumar et al., 2008). The isotherm model can be fitted to the experimental data by minimizing the error function of choice. The lower the value of the error function, the better the isotherm model is expected to

fit the data. The choice of error function can massively impact the fitting and choice of the optimal isotherm model and the adsorption parameters (Gimbert et al., 2008, Ho, 2004). The most used error function used for adsorption of organic compounds from liquid phases onto solid particles is the coefficient of determination (R^2) which can be calculated using the total sum of squares (SST) and the sum of squared residuals (SSR) (Wang and Guo, 2020a). Other functions that are extensively used in adsorption studies are the hybrid fractional error function (HYBRID), Marquardt's percent standard deviation (MPSD), Sum of absolute errors (EABS) and Average relative error (ARE) (Gimbert et al., 2008, Ng et al., 2002). The equations for these error functions are presented in Table 4.

To establish which adsorption isotherm is the best fit for the experimental data, the error of the data set needs to be considered. The size of the error-function, the visual fit and the physical description of the isotherm model must all be considered when choosing the optimal isotherm model for the system. In the following error functions in Table 4, $q_{e,exp}$ refers to the experimental q_e value calculated using equation 1, while $q_{e,model}$ refers to the value calculated by the model (Gimbert et al., 2008). The factor n represents the number of data points used in the calculation while p represents the number of parameters in the isotherm model. For Langmuir, Freundlich and Temkin models, p is equal to 2, while Henrys Law has $p = 1$ and Sips had $p = 3$. Subtracting p from n gives the degrees of freedom for the system (Kumar et al., 2008)

Table 4: Error functions used in this thesis

Error function	Equation (Gimbert et al., 2008)	
SST (total sum of squares)	$$SST = \sum_{i=1}^{n}\left(q_{e,exp} - \overline{q_{e,exp}}\right)^2$$	(11)
SSR (Sum of squared residuals)	$$SSR = \sum_{i=1}^{n}\left(q_{e,exp} - q_{e,model}\right)^2$$	(12)
R^2 (Coefficient of determination)	$$R^2 = 1 - \frac{SSR}{SST}$$	(13)

MPSD (Marquardt's percent standard deviation)	$100 \times \sqrt{\dfrac{1}{n-p} \sum_{i=1}^{n} \left(\dfrac{q_{e,exp} - q_{e,model}}{q_{e,exp}} \right)^2}$	(14)
HYBRID (Hybrid fractional error function)	$\dfrac{100}{n-p} \sum_{i=1}^{n} \left[\dfrac{(q_{e,exp} - q_{e,model})^2}{q_{e,exp}} \right]$	(15)
EABS (Sum of absolute errors)	$\sum_{i=1}^{n} \left| q_{e,model} - q_{e,exp} \right|$	(16)
ARE (Average relative error)	$\dfrac{100}{n} \sum_{i=1}^{n} \left| \dfrac{q_{e,model} - q_{e,exp}}{q_{e,exp}} \right|$	(17)

The R^2 is a way of expressing the fraction of explained variance in the data set and is one of the most used ways of estimating the fit of experimental adsorption data to both kinetics and isotherm models (Helbæk, 2011, Wang and Guo, 2020b). R^2 is however not statistically valid for non-linear models, as the SST and SSR are not the same for a linear and a non-linear model (Spiess and Neumeyer, 2010). Despite this, it is still one of the most used ways of assessing fit of adsorption models to experimental data (Wang and Guo, 2020a) MPSD has been proved to be a good indicator for isotherm fitting when it comes to two-parameter models (Kumar et al., 2008, Fallou et al., 2016). The HYBRID function is said to improve the error at low adsorbate concentrations (Gimbert et al., 2008). ARE attempts to normalize the error across the entire concentration range, but has shown to have weaknesses when applied to low-concentration adsorption isotherms (Fallou et al., 2016). EABS is known to bias the fit toward the highest concentration range of the data (Ng et al., 2002). All in all, the different error functions have pros and cons when applied for different purposes and concentrations ranges.

2.5.1 SNE

Gimbert et al. implements an SNE value (Sum of Normalized Errors) to decide which error function produces the smallest overall variations between the experimental and the modelled isotherm data (Gimbert et al., 2008). The SNE is calculated by optimizing each individual error function, while recording the error values for the other functions. When this is performed for all error functions, all the values are normalized towards the highest value obtained for each

error function and the normalized values are added together. The error function yielding the smallest sum can be assumed to give the overall best fit of the isotherm to the experimental data.

2.6 Choice of the optimal isotherm model

The use of error functions is, as mentioned, very convenient for minimizing the deviations between the experimental data and the calculated isotherm. The use of each error function can however yield different isotherm parameters, and it is challenging to know which error function and parameters describe the system the best. The choice of isotherm should not only be based on the size of the error function(s), but also on the visual fit of the isotherm and the nature of the isotherm and the assumptions it carries (Kumar et al., 2008).

2.7 Adsorption in the environment

In the aquatic environment, pharmaceutical concentrations are dependent on photodegradation, bioaccumulation, biodegradation and hydrolysis processes, in addition to adsorption. Pharmaceuticals are known to adsorb to sediments, in addition to soil, colloids and other suspended particles in the aquatic environment (Bavumiragira et al., 2022). The fate of pharmaceuticals in the aquatic environment is highly dependent on the adsorption processes taking place.

2.7.1 Kaolin

Kaolin (or kaolinite) is a clay mineral with the chemical formula $[Al_2Si_2O_5(OH)_4]$. It consists of alternating layers of tetrahedral silica (SiO_4) and octahedral alumina (AlO_6) as shown in Figure 2 (Hounfodji et al., 2021). The two sheets share oxygen atoms, and every pair of sheets are tightly bound by hydrogen bonds between oxygen atoms in the silica layer and hydroxyl groups in the alumina layer (Hounfodji et al., 2021) (Nesse, 2000). Unlike other clay minerals, kaolin does not contain cations between the layers, which gives it relatively low cation-exchange capacity (CEC) compared to other clay minerals (Nesse, 2000) (Cheng and Heidari, 2018). This also contributes to kaolin not being categorized as a swelling clay, as it also has a low ability to retain water molecules between the layers. The cation exchange capacity of kaolin is however dependent on pH, as a higher pH will contribute deprotonating hydroxyl groups on

the surface and allowing more cations to bind to the kaolin surface, increasing its CEC (Ma and Eggleton, 1999). pH can therefore greatly affect kaolin's adsorption characteristics. Studies have shown that kaolin has a Point of Zero Charge (PZC) of between 2,7 and 4,1, depending on the analytical method, which means it has a net negative surface charge at neutral pH (Appel et al., 2003). Kaolin often has a lath, or layered, structure, shown in Figure 3 (Schoonheydt et al., 2018). Compared to other clay minerals, kaolin has a low surface area of around $4 - 20$ m^2/g, while materials like active carbon can have surface area of over 2000 m^2/g (Hu et al., 2015, Song et al., 2019, Chen, 2017a).
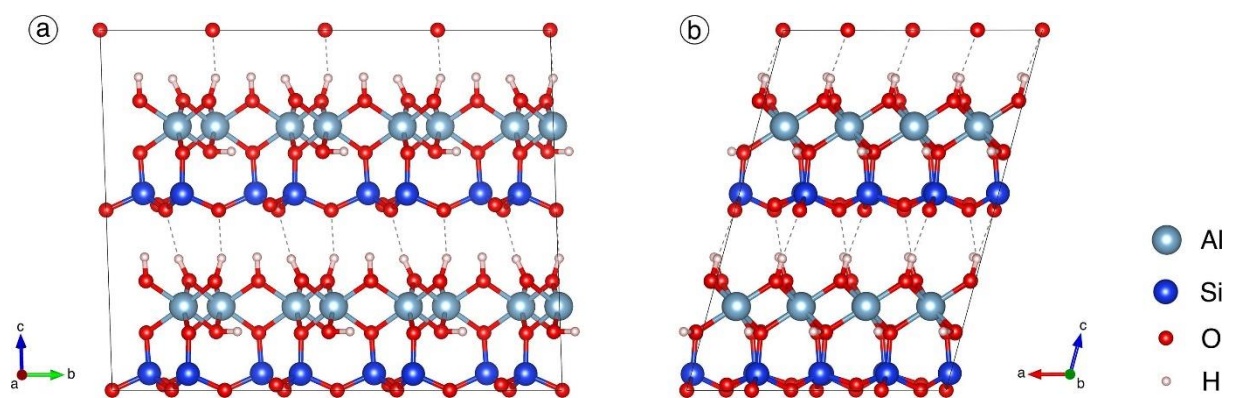
Figure 2: The molecular structure of kaolin (Hounfodji et al., 2021)
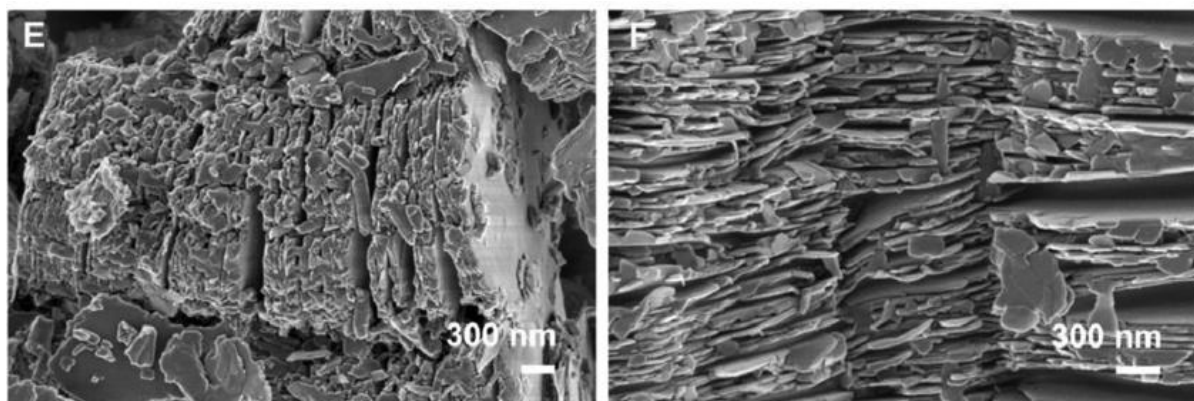
Figure 3: Electron microscope images of kaolin particles (Ivanić et al., 2015)

Kaolin is among the most abundant clay minerals in marine sediments in the northern hemisphere, where it typically accounts for between 10-20 % of the sediment composition (Zuther et al., 2000, Veerasingam et al., 2014). In lake areas, the amount has been found to be even higher than in marine areas (Zhou et al., 2014). However, local variations are common due to the locations of weathering sources and river outlets, in addition to temperatures, sea

conditions and the different particle sizes being considered in the scientific measurements (Rateev et al., 2011). Kaolin also has a tendency to accumulate in the equatorial zone, and in some arctic seas, it is not present at all (Kalinenko, 2001).

Research into the adsorptive properties of kaolin has been performed using both batch studies and computational methods. The latter has proven to be fairly accurate and to give a good representation of the mechanisms that occur (Hounfodji et al., 2021). It is, however, important to remember that environmental research include many more factors that will influence adsorption, such as pH, ionic strength, presence of organic substances will affect the adsorption greatly (Parolo et al., 2012).

Kaolin has been shown to be effective in removing dyes from aqueous solutions (reference needed) It has also shown to be effective for adsorbing some pharmaceuticals. Some studies on the adsorption of pharmaceuticals onto kaolin and other minerals and materials are listed in chapter 2.8. One study found that pharmaceuticals containing amine groups had especially high sorption to kaolin, suggesting that electrochemical affinity plays an important role in the sorption of pharmaceuticals onto kaolin (Yamamoto et al., 2016).

2.8   Pharmaceutical sorption to particles

An overview of literature regarding the adsorption of pharmaceuticals from aqueous phases onto solid particles is given in Table 5. Attempts were made to include studies researching the adsorption to kaolin, but this was not always possible to find, and thus other adsorbents were included. This includes other sediments, soil, activated carbon and other bio-adsorbents like carbon from plants.

The adsorption of pharmaceuticals is expected to be low compared to swelling clays with higher CEC's, but since kaolin is a constituent of many sediments, it is still useful to know of its adsorption capacities and mechanisms (Li et al., 2011). Notice that the units of q_{max} can vary between studies, as some use the unit mol instead of g when describing the amount of adsorbate. Notice also that some of the matrixes only say water; some studies did not specify which type of water the solutions were made in, only states that it is an aqueous solution.

Table 5: Overview of available literature on adsorption studies on pharmaceuticals

Compound	Adsorbent	Liquid phase	Analytical method	Results/main findings	Reference
Atenolol	Kaolin	Water	Fluorescence spectro-photometry	$q_e = 2,5 * 10^{-5}$ mol/g	(Rakić et al., 2013)
	Kaolin	Milli-Q water	UV-Vis	PSO kinetics $k_2 = 0,1$ kg/mmol*h $q_e = 25$ mmol/kg Langmuir model fit $q_{max} = 40$ mmol/kg ($\approx 6,7$ mg/g) $K_L = 1,25$ L/mmol ($\approx 4,69$ L/g)	(Hu et al., 2015)
	Natural river sediment (France)	Milli-Q water	UHPLC-MS/MS	Freundlich best fit $K_F = 99$ L$^{1/n}$*mg$^{1-1/n}$ /kg $n_F = 1,11$	(Le Guet et al., 2018)
Caffeine	Bentonite	Water	UV	Freundlich and Langmuir fit $q_{max} = 41,667$ mg/g $K_L = 0,7186$ L/mg $K_F = 18,5097$ mg/g $n_F = 2,805$	(Lenzi et al., 2020)
	Activated carbon	Water	UV-Vis	High pH dependency (low pH -> high adsorption) Freundlich and Langmuir fit Hardness of water decrease adsorption	(Couto Jr et al., 2015)
	Natural river sediment (Brazil)	0,01 M CaCl$_2$	HPLC-PAD	PFO kinetics (R^2=0,99) $k_1 = 0,4$ h^{-1} $q_e = 18,4$ µg/g Freundlich fit $K_F = 1,8$ mL/g n = 0,7	(Costa Junior et al., 2022)
Ciprofloxacin	Kaolin	Water	UV-Vis	Langmuir fit (pH 3-4,5) $q_{max} = 19$ mmol/kg (6,3 mg/g) $K_L = 262$ L/mmol (790,8 L/g)	(Li et al., 2011)
	Montmorillonite	Water	HPLC-UV	PSO kinetics $k_2 = 28,91$ g/mmol*h (=0,0873 g/mg*h) $q_e = 0,92$ mmol/g (=304,8 mg/g) Langmuir fit q_{max} (single) = 1,04 mmol/g (344,6 mg/g), close to CEC of adsorbent (0,953), indicating that ion exchange is most important mechanism	(Wu et al., 2019)
	Carbon from plants	Water	HPLC-PAD	Eq.time 48 hours Langmuir best fit $q_{max} = 104,2 – 133,3$ mg/g Max adsorption @pH 6	(El-Said Ibrahim, 2012)

Citalopram	Soils		UHPLC-MS/MS	Freundlich fit K_F = 1838 cm^3/g (1,838 L/g) n = 1	(Klement et al., 2018)
	Natural river sediment (Brazil)	0,01 M CaCl$_2$	HPLC-PAD	PFO and PSO fit (R^2=0,99) k_1 = 0,3 h^{-1} $q_{e,1}$ = 47,2 µg/g k_2 = 0,007 g/µg*h $q_{e,2}$ = 54,4 µg/g (R^2=0,99) Freundlich fit K_F = 4,2 mL/g n = 2,3 R^2 = 0,91	(Costa Junior et al., 2022)
Diclofenac	Natural river sediment (France)	Milli-Q water	UHPLC-MS/MS	Freundlich best fit K_F = 17 L$^{1/n}$*mg$^{1-1/n}$/kg n = 0,68 R^2 = 0,987	(Le Guet et al., 2018)
	Organo-modified kaolin	Water	UV-Vis	Langmuir fit K_L = 8 L/mmol (27,0 L/g) at lowest modification level q_{max} = 13 mmol/kg (3,85 mg/g)	(Sun et al., 2017)
	Kaolin	Water	DFT (Density functional theory)	Exothermic Diclofenac poorly adsorbed	(Hounfodji et al., 2021)
Fluoxetine	Natural river sediment (Brazil)	0,01 M CaCl$_2$	HPLC-PAD	PFO and PSO fit (R^2=0,99) k_1 = 0,4 h^{-1} $q_{e,1}$ = 43,6 µg/g k_2 = 0,01 g/µg*h $q_{e,2}$ = 51,4 µg/g Freundlich isotherm fit K_F = 7,5 mL/g n = 1,4 R^2=0,96	(Costa Junior et al., 2022)
	Pine bark	Distilled water	UHPLC-DAD	Sips isotherm best fit R^2 = 0,991 q_{max} = 6,53 mg/g Ks = 15,8 L/g n = 6,74	(Silva et al., 2020)
Nicotine	Bentonite	0,01 M CaCl$_2$	UV-Vis	D-R isotherm best fit (R^2=0,98) q_{max} = 53,36 mmol/g (8657 mg/g)	(Akcay and Yurdakoc, 2008)
	Activated carbon	Distilled water	UV-Vis	Langmuir best fit (R^2 = 0,989) q_{max} = 552 mg/g (30°C) K_L = 0,0053 L/mg (=5,3 L/g)	(Pi et al., 2015)
Paracetamol	Kaolin	Water	DFT	Exothermic	(Hounfodji et al., 2021)

				Paracetamol strongly adsorbed, H-bonding main mechanism	
	Alumina and silica	Nanopure water	UV-Vis	No significant sorption at neutral pH	(Lorphensri et al., 2006)
Oxolinic acid	Sand (France)	Seawater	HPLC	Freundlich fit ($R^2 = 0,98$) $K_F = 0,3$ L/kg $1/n = 0,74$	(Pouliquen and Le Bris, 1996)
Oxytetracycline	Sand (France)	Seawater	HPLC	Freundlich fit ($R^2 = 0,99$) $K_F = 0,3$ L/kg $1/n = 0,97$	(Pouliquen and Le Bris, 1996)
	Kaolin	0,01 M $CaCl_2$	HPLC-UV	PSO best fit $k_2 = 0,044 - 0,149$ g/mg*h $q_e = 0,2088 – 7,692$ mg/g Langmuir best fit ($R^2 = 0,965$ @298 K) $q_{max} = 8,749$ mg/g $K_L = 0,137$ L/mg q_e increases with temperature	(Song et al., 2019)
Tetracycline	Kaolin	Water	UV-Vis	Cation exchange important mechanism Langmuir fit ($R^2 = 0,993$) $q_{max} = 9$ mmol/kg (4,0 mg/g) $K_L = 89$ L/mmol (0,20 L/mg)	(Li et al., 2010)
	Montmorillonite	Water	HPLC-UV	PSO best fit $k_2 = 28,29$ g/mmol*h $q_e = 0,94$ mmol/g Langmuir fit ($R^2 = 0,99$) $q_{max} = 1,06$ mmol/g, close to CEC of adsorbent (0,953), indicating that ion exchange is most important mechanism	(Wu et al., 2019)
Trimethoprim	Natural river sediment (France)	Milli-Q water	UHPLC-MS/MS	High adsorption, $K_d = 282$ L/kg Langmuir best fit $K_L = 2$ L/mg $q_{max} = 222$ mg/g $R^2 = 0,995$	(Le Guet et al., 2018)
	Natural sea sediment (China)		HPLC-UV	PSO best fit $k_2 = 0,860$ /mg*min (10 mg/L C_0) $q_e = 18,0$ mg/g Both Langmuir and Freundlich fit For 30% salinity, pH 6,9 and most adsorbing sediment: Langmuir: $q_{max} = 1,12$ mg/g $R^2 = 1,0$ $K_L = 13,3$ L/kg Freundlich: $K_F = 13,7$ L/kg $R^2 = 0,999$	(Li and Zhang, 2017)

According to the literature review above, the most used models for visualising the adsorption of pharmaceuticals onto sediment particles is the Langmuir and Freundlich models. This is confirmed by Al-Ghouti and Da'ana and Wang and Gou, with the latter also mentioning the linear model (Henry's law), Sips, Toth, BET (Brunauer-Emmett-Teller), Temkin and D-R (Dubinin-Radushkevich) models for pharmaceuticals and organic pollutants (Wang and Guo, 2020a, Al-Ghouti and Da'ana, 2020).

The literature overview reveals that the analytical methods used is a mix of chromatographic and spectrophotometric methods. Some studies also include FT-IR (Fourier-transform infrared spectroscopy) to look for changes in the types of bonds present to characterize the type of binding between pharmaceuticals and particles, but the isotherm measurements themselves are collected using chromatographic and spectrophotometric methods. Most studies include some pre-treatment of sediments, like drying, crushing and sieving in order to sort out specific particle sizes.

It is important to note that many articles only fit the results to one model, without comparing between different ones. Some also found several models to be good fits, indicating that several adsorption mechanisms can be present in the systems, and emphasizes that adsorption is a complicated phenomenon that is affected by many different factors. It could also be due to the use of naturally derived adsorbents, like real river sediments with a variety of components.

2.9   Instrumentation and methods

2.9.1   Liquid chromatography

Liquid (column) chromatography is a well-known and widely used separation technique that is based on a compound's relative affinity to the liquid mobile phase and the stationary phase inside the chromatographic column. In the late 1960s, smaller packing materials were introduced, which made separations better, but required higher pressures in the system to achieve reasonable flow rates (West et al., 2014). High pressure (today: performance) liquid chromatography (HPLC) became the new norm.

HPLC is now being used in a variety of scientific fields and has become one of the most important tools for analysis of organic compounds in aquatic matrices (Lundanes et al., 2014, Meierjohann et al., 2017, West et al., 2014). Reversed phase HPLC is the most popular

technique for aquatic matrices, in which the mobile phase often is a mix of polar solvents, and the stationary phase is non-polar. That allows for aqueous samples to be analysed, and performs well for polar analytes. Stationary phase materials are typically silica based materials, often derivatised to alter their polarity and stability (Poole, 2003). For relatively small molecules, alkyl bonded silica particles (C8 or C18) are often preferred (Ciborowski and Silberring, 2016). LC-MS is versatile and often has a less complicated sample preparation approach, than gas chromatography (GC), as it might require derivatization of pharmaceutical compounds (Fatta et al., 2007). Organic contaminants are also often not volatile, which is problematic for GC analyses.

The mobile phase of HPLC separation is important, and it can be altered in several ways to give the best possible separation (Liang et al., 2013). The use of gradient elution is popular, a method where the composition of the mobile phase changes throughout the analysis to achieve optimal separation between compound peaks. It is normal for a gradient in reversed phase analysis to begin with a weak solvent (often water), and finish with a stronger, organic solvent to enhance elution of strongly retained (often hydrophobic) analytes that might be highly retained by the stationary phase (Poole, 2003). The mobile phase can also have additional compounds added, like salts, bases or acids, to help with ionisation of sample compounds or to make sure the target compounds exist in a chemical form in which they are well analysed and detected (Liang et al., 2013).

2.9.2 Mass spectrometry

Mass spectrometric techniques represent versatile and powerful tools within analytical chemistry, as they allow for identification and quantification of complex analyte mixtures (West et al., 2014). Mass spectrometry is based on the principle that sample molecules are ionized by applying energy. The ions are then separated based on their mass/charge ratios, and the number of different ions are added together and result in a mass spectrum.

For mass analysis to work, analytes need to be ionized by applying energy to the analyte molecules and giving them a net charge. Many different ionization methods have been developed for the various chromatographic techniques out there, but ESI (electrospray ionisation) is a popular choice for RP-HPLC analyses (Wang et al., 2016). ESI is a soft ionization technique that can create both positively and negatively charged adducts, and it

works well for relatively polar molecules of a large variety of molecular masses (Lundanes et al., 2014). It is widely used with HPLC due to its suitability for liquid samples.

A widely used detector in mass spectrometry and environmental/analytical chemistry is the triple quadrupole (Ferrer et al., 2010, West et al., 2014). This is due to its high sensitivity, making it able to detect environmental pollutants at ultra-low concentrations. A quadrupole works by applying an electric current to four opposing rods, and passing analyte ions through. By varying the current applied to the rods, ions with selected mass/charge ratios and certain stable trajectories are able to pass through. When a triple quadrupole is being used, three consecutive quadrupoles are combined. The first quadrupole is usually used as a mass analyser or a mass filter, meaning it only lets certain ions pass through. The second quadrupole is the collision cell which induces fragmentation, before entering the last quadrupole, or the second mass filter, that can be set to only let certain product ions pass through. This way, the triple quadrupole brings an additional level of certainty to the analysis.

Hyphenated methods

When combining chromatography and mass spectrometry, they make a powerful analytical tool. HPLC-ESI-MS/MS, especially reversed phase, is among the go-to methods for analysis of environmental samples, especially polar organic pollutants in aqueous matrices (Meierjohann et al., 2017, Lundanes et al., 2014, Fatta et al., 2007). A drawback of the method, however, is that it often requires clean-up of heavily contaminated environmental samples. The ESI source is sensitive with regard to contaminants and sensitivity of the analysis can quickly become affected by dirt, contaminants and salt. However, since ESI can operate with liquid samples, it is a very useful tool for HPLC.

2.10 Quantitation and quality assurance

Retention time

When compounds move through the chromatographic column, they will eluate at different times due to their interactions with the mobile and the stationary phase. The time at which a

compound eluate through the column and its peak appears in the chromatogram is called the retention time (RT) and is related to the relative affinity of the compound with the two phases. The retention time of a compound is specific to the method and instrumental parameters used.

Matrix effects

Matrix effects occur when interfering compounds in the sample matrix contribute to the enhancement or suppression of the analyte response. They occur in both GC- and LC-MS, in both single and 2-dimentional MS (Hao et al., 2007). Matrix effects can originate from co-eluted compounds with similar masses being detected by the MS, or by compounds in the matrix that interfere with the ionization of compounds in the ionization chamber. The latter is often observed in ESI-instrumentation and is a big problem in environmental sample analyses, as they often contain sodium or other ions which can enhance of suppress the analyte signal (Kloepfer et al., 2005, Hao et al., 2007). To account for matrix effects, pure solvent can be spiked with the same amount of analyte as the sample matrix to compare analyte responses and quantify the contribution from the matrix. The use of internal standards will also contribute to reducing matrix effects, as a change in instrument response is expected to be equal for the analyte and the IS.

Calibration and internal standards

Calibration is a necessary step in analytical chemistry in order to determine the relationship between analyte concentration and signal intensity (West et al., 2014). A known and predictable relationship between analyte signal and the concentration is necessary in order to quantify the unknown analyte level in samples. Calibration curves will often lose some linearity at high concentrations. This could be due to the column or detector being saturated with the analyte, or simply because there is a maximum signal intensity possible to produce by the instrument (Yuan et al., 2012). The linear range describes the range where the calibration curve has satisfactory linearity.

The internal standard (IS) method is the preferred method for calibration, compared to external calibration, because it can account for matrix effects and provide better precision (Lundanes et al., 2014). Internal standards can account for loss of analytes during sample preparation, depending on the time of addition of the IS. The IS can also account for variations in

instrumental analysis, such as variations in ionization efficiency, as loss in signal is expected to be equal for the internal standard as the analyte (Gros et al., 2012). An IS is thus very important for quantitation purposes. Popular IS are deuterated forms of the analyte compounds, meaning they will be chemically and physically similar to the analyte, but will be separable when using MS detection (Lundanes et al., 2014).

Limit of detection and quantification

The limit of detection (LOD) is an important aspect of analytical chemistry and environmental science. It describes the lowest concentration where an analyte can be confidently detected and confirmed to be a signal rather than background noise. The LOD varies with compound, instrument and analytical method of choice, and is especially important for environmental samples where concentrations can be quite low. The limit of quantification (LOQ) is related to the LOD and is the limit where an analyte can be quantified with a certain level of confidence. There are many ways of calculating LOD and LOQ, and they can vary with analytical method and desired sensitivity for the analysis. (Armbruster and Pry, 2008)

One way of establishing an LOD, which will be used in this thesis, is by observing the calibration curve and assessing the accuracy at different levels. The LOD and LOQ can be set to the lowest concentration level where the accuracy is within ± 20% of the real concentration, and where the S/N ratio is above 3 or 10 respectively for LOD and LOQ.

Standard deviation

The standard deviation is a way of expressing the variation between data in a dataset. It is used to assess the precision of our data. A large standard deviation implies that our data points have a large variance which could imply that our method is unreliable. The standard deviation of a data set is given in equation 18, where n is the number of observations in our dataset, x_i is the value of a given observation i and $\bar{x}$ is the mean values of the observations (West et al., 2014).

$$SD = \sqrt{\frac{\sum_{i=1}^{n}(x_i-\bar{x})^2}{n-1}} \qquad (18)$$

The relative standard deviation is calculated by comparing the standard deviation to the mean of the data set, shown in equation 19, which gives a standard deviation relative to the mean of the data.

$$RSD = \frac{SD}{\bar{x}} \times 100\% \qquad (19)$$

The limit of acceptable deviation will vary with the purpose of the experiment being conducted.

Standard deviation of calculated values

The accumulated standard deviation is a way of calculating the standard deviation of calculated values. For example, when calculating the standard deviation of a calculated value, equations 20 and 21 can be used to calculate the standard deviation of the calculated value.

$$y = a + b - c \qquad s_y = \sqrt{s_a^2 + s_b^2 + s_c^2} \qquad (20)$$

$$y = a \times \frac{b}{c} \qquad \frac{s_y}{y} = \sqrt{\left(\frac{s_a}{a}\right)^2 + \left(\frac{s_b}{b}\right)^2 + \left(\frac{s_c}{c}\right)^2} \qquad (21)$$

Accuracy

Accuracy is an important measure for confirming that the value is close enough to the real or expected concentration of the sample. Accuracy is best assessed by reference material, but suitable organic reference materials are seldom available (Lundanes et al., 2014). The magnitude of accepted accuracy varies with the method and the goal of the analyses. In this thesis, for example, accuracy deviations within ± 20% of the real or expected sample concentrations of quality control samples and calibrations standards were acceptable.

3 Materials and methods

3.1 Chemicals and materials

HPLC-grade methanol, pharmaceuticals as pure, standards (either solid or as pre-dissolved from manufacturer) and kaolin (CAS 1332-58-7) were all purchased from Merck. Ultra-pure water was provided by a Millipore Milli-Q (MQ) ultra-pure water system. Seawater was provided by SINTEF's own seawater intake from the Trondheim fjord at approximately 80 m depth and was sterile filtered through a Sterivex^{TM} 0,22 µm filter (Merck) before use.

3.2 Preparation of standards

Standard solutions of pharmaceuticals and deuterated internal standards (atenolol_d7, ciprofloxacin_d8, diclofenac_d4, fluoxetine_d6, paracetamol_d4 and tetracycline_d6) were prepared by weighing solid standard, transferring to a volumetric flask and dissolving in suitable solvent. Methanol was mostly used as solvent, but in some cases the standards were made in other solvents, such as ethanol or HCl. This is specified in Appendix 7.1, Table 15.

3.3 Adsorption kinetics experiments

The adsorption kinetics experiments were conducted at three different temperatures (4, 9 and 18 °C). Sampling was performed at 8 different time intervals, from 1 hour to 10 days. Kaolin was weighed and transferred to 250 mL Pyrex bottles to have final concentrations of 5 and 10 g/L (1,25 ang 2,5 g kaolin, respectively). 250 mL sterile filtered seawater was measured and added to each bottle. Control samples without kaolin were also included. Bottles were spiked with 250 µL of a 50 µg/mL mixture of the 12 target pharmaceuticals presented in Table 1 to a final concentration of 50 ng/mL. Sample bottles were placed on a rotational incubator at 1 RPM. An overview of the samples is given in Table 6.

Table 6: Sample overview of the kinetics experiments

Hours	Blank	Control	5 g/L kaolin	10 g/L kaolin
1	3	3	3	3
3	-	3	3	3
6	-	3	3	3

24 (1 d)	-	3	3	3
48 (2 d)	-	3	3	3
72 (3 d)	-	3	3	3
144 (6 d)	-	3	3	3
240 (10 d)	3	3	3	3

3.4 Adsorption isotherm experiments

Based on initial tests, three pharmaceuticals (citalopram (CIT), ciprofloxacin (CIP) and fluoxetine (FLU)) were selected for determination of adsorption isotherms. The adsorption isotherm experiments were conducted at three different temperatures (4, 9 and 18 °C). Sampling was performed after 48 hours.

Experimental stock solutions were made by dilution of pharmaceuticals in 250 mL volumetric flasks; one for each individual compound, and one for control where all three pharmaceuticals were mixed. Standard solutions of pharmaceuticals in methanol were added to the flasks and diluted in sterile filtered seawater to a final concentration of 1000 ng/mL. The further concentrations were made by mixing different ratios of the stock and seawater. 100 mg kaolin was measured directly in 22 mL glass vials (final concentration of 5 g/L). 20 mL of pharmaceutical solutions of different concentrations were added into the vials. Three blanks only containing seawater, and three blanks containing kaolin and seawater were also prepared. Sample vials were placed on a rotational incubator rotating at 1 RPM. An overview of the samples is provided in Table 7.

Table 7: Sample overview of the isotherm experiment

Concentration	Control (mix)	CIT + Kaolin	CIP + Kaolin	FLU + Kaolin
Blank (0 ng/mL)	3	-	-	-
8 ng/mL	3	3	3	3
16 ng/mL	3	3	3	3
31 ng/mL	3	3	3	3
63 ng/mL	3	3	3	3

125 ng/mL	3	3	3	3
250 ng/mL	3	3	3	3
500 ng/mL	3	3	3	3
1000 ng/mL	3	3	3	3

3.5 Sampling

The rotational incubator is shown in Figure 4. Sampling was performed by removing the bottles/vials from the rotating incubator, shaking well and transferring 1 mL of sample using an Eppendorf pipette to a 1,5 mL Eppendorf centrifuge vial. For kinetics experiment, sample bottles were placed back onto the carousel after sampling. The samples were then centrifuged at the experimental temperature (4, 9 or 18 °C) at 4500 RPM for 10 minutes, to provoke sedimentation of particles. The supernatant was removed using a glass Pasteur pipette and transferred to a plastic syringe (CODAN 1 or 2 mL) with a syringe filter (JT Baker, 13 mm, 0,2 µm, H-PTFE). The sample was filtered and 90 µL of filtered sample was transferred to a 2 mL GC vial with a 250 µL vial insert. Samples were kept frozen until the day of analysis. They were then

Figure 4: The rotational incubator used for sample mixing

thawed and added 10 µL internal standard to a total concentration of 25 ng/mL.

3.6 Analysis

The mobile phases were methanol and Milli Q water, both with 5 mM ammonium formate (pH 8,5). pH adjustments were made for some analyses if the column used did not manage a pH of 8,5. The pH was adjusted by first adding the 5 mM ammonium formate, and then acidifying with formic acid. The pH was controlled by a pH-meter until a pH of 7,3 was reached. The different columns used and the mobile phase pH is described in detail in appendix X.

Samples were analysed using an Agilent 1200 HPLC and an Agilent 6470 Triple Quadrupole. The column was a 50 mm Agilent Poroshell column. A few different versions of this column were used throughout the analyses. The different columns used are listed in appendix 7.1, Table 16. Other instrumental parameters are listed in Table 8. Quantification parameters are listed in Table 9. The separation of the quantification ions is shown in Figure 24 in appendix 7.1.

The worklist was randomized prior to analysis to avoid biased results due to analytical trends.

The mobile phase was held at 99% water for one minute before changing to 99% methanol gradually over a 10-minute period. It was held at 99% methanol for two more minutes before instantly switching back to 99% water and keeping it there until the end of the run. The mobile phase flow was 0,6 mL and the sample injection volume was 5 µL.

Table 8: Instrumental parameters for the HPLC-ESI-MS/MS analysis

Parameter	Value
Column oven temperature	50 ℃
Gas temperature	250 ℃
Gas flow	8 L/min
Sheath gas temp	300 ℃
Sheath gas flow	10 L/min
Capillary voltage	4000 V
Nozzle voltage	0
Nebulizer	35 psi

Table 9: Analytical and quantification parameters for target compounds and internal standards.

Compound	RT*	Precursor ion	Quantifier ion	Qualifier ion	Collision energy (quantifier/ qualifier)	Fragmentor voltage (quantifier/ qualifier)
Atenolol	4,582	267,2	145,1	190,1	29/21	155
Atenolol_*d*7	4,496	274,2	123,1	152,1	21/29	155
Caffeine	3,847	195,1	138,1	110,1	21/30	130

Ciprofloxacin	3,827	332,1	288,1	231,1	17/45	165
Ciprofloxacin_d8	3,767	340,1	296,1	322,1	17/20	165
Citalopram	8,119	325,2	109,0	262,1	33/21	150
Diclofenac	7,229	296,0	215,0	250,0	21/13	85
Diclofenac_d4	7,203	300,0	219,0	254,0	21/13	85
Fluoxetine	8,624	310,1	148,1	117,1	5/40	95
Fluoxetine_d6	8,603	316,2	154,2	123,0	5/40	95
Nicotine	5,477	163,1	130,1	117,1	25/33	110
Oxolinic acid	3,260	262,1	244,1	216,1	21/33	125
Oxytetracycline	3,982	461,2	426,2	264,9	21/37	150
Paracetamol	1,124	152,1	110,1	65,1	17/37	125
Paracetamol_d4	1,113	156,1	114,1	69,1	17/37	125
Tetracycline	5,423	445,2	154,0	410,2	29/21	140
Tetracycline_d6	5,322	451,2	416,2	160,0	21/29	140
Trimethoprim	5,265	291,2	230,1	123,1	25/29	160

*Retention times are for the Agilent Poroshell 120 EC-C18 column with MP pH of 8,5. Retention times varied slightly with different columns and mobile phase pH used for different analyses.

3.7 Data processing

Analytical raw data was processed using the Agilent MassHunter Quantitative Analysis software. Calibration curves were assessed using linear calibration, and internal standard calibration was used for compounds where they were available. External calibration was used for the rest. Processed data was exported and organized in Microsoft Excel and plotted using Excel or R in RStudio. The linear kinetics and isotherm models were fitted using the Excel LINEST function and deriving the adsorption parameters from the regression line to calculate the predicted q_e values from the model. Non-linear kinetics and isotherm model calculations were performed using the Excel Solver add-in.

4   Results and discussion

4.1   Analytical method assessment and quality assurance

4.1.1   Choice of analytical technique

Many adsorption studies use spectrometric methods for the detection of pharmaceuticals, either alone or as a detector in combination with chromatographic separation. Pharmaceuticals generally have one or more aromatic rings in their structure, meaning they can be detected using relatively simple UV-Vis detection. However, the sensitivity of UV-Vis analyses is lower than for chromatographic methods. In the literature overview in chapter 2.8, some of the studies using spectrometric detection reported detection limits of several hundred ng/mL, which is too high in order to analyse samples with as low concentrations as in this thesis (Li et al., 2011, Silva et al., 2020). In addition, spectrophotometric methods might fail when analysing mixtures of compounds, as the adsorption peaks can interfere. The choice of HPLC-MS/MS instead of simpler analysis methods such as UV-Vis spectrometry was a good choice for working with low concentration samples in this project.

4.1.2   Revision of analytical method

During the specialisation project conducted in the fall of 2021, 37 pharmaceuticals, pesticides and personal care products were analysed by HPLC-MS/MS. The analytical method was used on both SPE-extracted samples and "unprocessed" seawater samples using direct injection, and two different mobile phases were tested (Hovsbakken, 2021). However, the method had several drawbacks, including long analysis time and poor sensitivity for some analytes. The LC column used in the specialization project was subject to some wear-and-tear, and didn't perform to the needed level of sensitivity for this thesis.

Several improvements could be made to the method for the analyses in this thesis. The development of the "new" method was inspired by EPA method 1694 (Ferrer et al., 2010). Since the number of samples was large, the project could benefit from using a shorter column and a stronger mobile phase gradient compared to in the specialization project, in order to elute the analytes quicker and save analysis time. This was especially favourable due to the large number of samples, over 500, planned to be analysed. The column was changed from a 150 mm to a 50 mm long column. In addition, switching from a mobile phase consisting of water and methanol with ammonium fluoride or formic acid, which was used in the specialisation project, the addition of ammonium formate to the mobile phases proved to give an overall better

response for the target analytes. As there was limited time for this project, there was not enough time to assess the method completely and have it work optimally for all compounds, before having to start analysing samples. Having a universal method for a diverse mixture of acidic, neutral and basic compounds with large structural variations is near impossible. The change of method especially affected the analysis of tetracycline and oxytetracycline, which were among the compounds that did not gain higher responses using the new mobile phase additive. Their peaks were wide and tailing, which made quantification difficult. Though, they had also been unstable during the specialization project and showed signs of degradation during the 14-day degradation experiment, so their implementation for kinetics experiments over 10 days was already difficult (Hovsbakken, 2021).

4.1.3 Direct analysis of seawater

Many studies analysing pharmaceuticals by HPLC, which were assessed in the specialisation project, are based on extensive pre-treatment or extraction for sample clean-up and concentration (Hovsbakken, 2021). Because of the large number of samples planned to be included in this thesis, SPE or other extraction methods were not possible to perform given the time and resources available. It was therefore decided to do direct analysis of seawater samples without pre-treatment, besides filtering to remove particles. This was also tested in the pre-project and worked well for most analytes. The direct analysis of the amount of seawater samples in this project turned out to be too many for the HPLC system to handle, likely due to the amount of salt being injected into the system, and it was therefore necessary to dilute the samples in Milli-Q water before analysis. If this had been known beforehand, higher concentrations of pharmaceuticals could have been added in order to be more confident that the compounds yielded sufficient responses to be quantified.

4.1.4 Calibration and matrix effects

The analysis of seawater was expected to increase the risk of matrix effects, as additional ions in the samples can affect their ionisation. The calibration curve was therefore initially prepared in seawater in order to account for matrix effects in the seawater samples. As mentioned, after analysis of the first sample batch (kinetics at 9 °C) there were signs that the column didn't handle all the seawater being injected. This was seen by reduced signal for some compounds (especially tetracycline and oxytetracycline) as the analysis proceeded, and the peaks were

getting wider and drifting outside of the retention time window so that quantification became impossible. This was possibly due to the stationary phase being decomposed due to the salt and not being able to retain the compounds consistently throughout the analysis. It could also be due to the salt building up in the ion source, lowering the ionization of the compounds and therefore affecting the signal intensities. The mobile phase pH was initially 8,5, which was also at the pH tolerance limit of the column. The combination of these factors impacted the analysis to such an extent that it was decided to dilute samples in Milli-Q water before analysis, to reduce the build-up of salt. The mobile phase was also pH adjusted down to 7,3 in an attempt to preserve the stationary phase. This would hopefully improve the sensitivity of the analysis. Samples were therefore diluted 1:9 in Milli-Q water before analysis, and calibration standards were also prepared and run in MQ water instead.

4.1.5   Internal standard variations

Internal standards were added to account for matrix effects and variations in signal from the instrument. In the case of dilution of the samples, the IS was also useful for accounting for dilution errors, as any error in pipetting is expected be equal for the analyte and for the internal standard.

For some compounds, the internal standard signal became varying and/or reduced throughout the analysis. This problem was especially clear for tetracycline and oxytetracycline. This can be seen as relatively large standard deviations, for example for the sorption percentage calculations described later.

For some compounds, the concentrations at 9 and 4 °C are not equal, e.g for diclofenac. This might be due to a different batch of IS being added to the 9 °C samples, which was older than the IS used for 4 °C samples, and might have been prone to some degradation. The deviations could also be from deviation in spiking, as the IS volume to be added to the samples was 10 µL, which is very low and could lead to error. In cases where the internal standard calibration made deviations between sample triplicates bigger rather than smaller, external calibration was used instead.

4.1.6 Quality control and assurance

In order to assess the performance of the analysis throughout the analyses, QC samples with concentrations of 25 ng/mL were included every 10 samples, in addition to pure MQ samples to rise out the system and account for carry-over. The worklist was randomized before the analysis in order to exclude any analytical trends impacting the analysis, for example ion source contamination and difference in signal intensities throughout the analysis. The randomization could have contributed to larger variations between sample triplicates due to some being analysed early and some later in the sequence, but it minimized the chances of trends appearing wrongfully because of sample placement in the sequence.

Blanks were included in order to assess contamination and carry-over. Blanks can be used to set the LOD and LOQ, and this method was used in the specialisation project. Some pharmaceuticals were prone to carry-over, and in the case of blanks being analysed after standards or samples of relatively high concentrations, blanks could get "contaminated" and the method LOQ would suffer. A different way of assessing the LOQ was therefore used in this thesis than in the specialisation project.

Quality control data from the analyses are available in appendix 7.3. Samples were run in separate batches, one batch being either kinetics or isotherm samples at one temperature. The QC data therefore suffers from some inconsistencies due to different sets of calibration standards being ran for each batch, and some analyses including calibration standards of lower concentrations. Since the first sample batch (kinetics samples at 9 °C) were not diluted, the lowest calibration standard was set to be 0,1 ng/mL. When samples were later diluted in MQ water, calibration standards of 0,05 and 0,02 ng/mL were also included to be able to quantify even lower concentrations in the samples. The LOQ for each analyte was set to be the lowest calibration standard that yielded an accuracy of 80-120 % and had a signal-to-noise ratio of 10 or higher. All calibration curves were linear in the given ranges with an $R^2 > 0,99$.

Because of the need to dilute samples before injection, the sensitivity of the analysis was sometimes not good enough to account for both dilution and adsorption of the lowest sample concentrations in the isotherm experiment (8 ng/ml). For example, the analysis of the 4 °C isotherm experiment samples had an LOQ of 1 ng/mL for fluoxetine, and some of the samples were blow this limit. They are however still included in the isotherm calculations.

4.2 Experimental design

4.2.1 Choice of pharmaceuticals

The compounds for inclusion in this thesis were based on a combination of factors. Four compounds were selected by the Pharmarine project partners to be of most interest to use for modelling. These are tetracycline, simvastatin, fluoxetine and diclofenac. Other compounds included were those that were analysed well and/or showed adsorption tendencies to kaolin during the specialization project. The chosen compounds are those that were presented in Table 1. Originally, simvastatin was among the compounds, but was very unstable and degraded quickly. It was also not analysed well in the specialization project, as it did not show up in the analyses, either in SPE extracts or using direct analysis of seawater samples during the specialization project. (Hovsbakken, 2021).

Due to the large number of samples needed for the isotherm experiments, three compounds were chosen to include. The compounds selected for the isotherm experiments were based on which compounds adsorbed to kaolin, had low detection limits and were easily analysed and quantified. The compounds included in the kinetic and isotherm modelling experiments, and some of their properties, are repeated in Table 10.

Table 10: Repetition of type and chemical properties of compounds used in the isotherm experiments

Compound	Type	pKa	Log K_{ow}
Ciprofloxacin	Antibiotic	1: 3,01	0,280
		2: 6,14	
		3: 8,70	
		4: 10,58	
Citalopram	Antidepressant	9,6	3,04
Fluoxetine	Antidepressant	10,1	4,05

4.2.2 Choice of isotherm models

The choice of isotherm models to study for this thesis was based on the literature overview in chapter 2.8, in addition to the review article from Wang and Guo (Wang and Guo, 2020a). In addition to the Langmuir and the Freundlich models, which are the most extensively used models, the Sips model was chosen due to it being a combination of the two others, and a 3-parameter model which could give some more accurate parameter estimations. The Temkin

model had been successfully used to study the adsorption of antibiotics onto clay, which is why that was also included.

Additional models were considered to include, such as the D-R (Dubinin-Radushkevich) model. The D-R model requires information on the solubility of the adsorbates. Since the experiments were performed in seawater, the solubility is unknown, and it was therefore not included.

4.2.3 Experimental sources of error

There are several factors about the experimental set-up that may have contributed to some errors and inaccuracies in the results. This includes preparation of the kaolin. It was observed that the kaolin had a range of different particle sizes, as some particles sank quickly to the bottom of the bottles/vials and some stayed suspended in the aqueous phase for a longer period of time. To ensure that the kaolin was more homogenous, pre-treatment of the kaolin could have been considered. This could have included procedures such as sieving and drying, in order to have the particles be within the same size range and making sure no water was bound to the kaolin.

During sampling, it was observed that kaolin tended to clump together and accumulate in the corners of the bottles and vials, at the bottom and around the cap. This could have contributed to variance in the amount of kaolin particles available for the pharmaceuticals to adsorb to, which could be a source of error and lack of precision.

The degradation of compounds over time is a factor that could contribute to inaccurate results. During the specialisation project, stability of compounds was tested over a period of 14 days. Most compounds were stable, with the exception of oxytetracycline, tetracycline and caffeine. There is also the possibility that compounds adsorb to the glass walls of the containers. Glass and plastic containers were compared in the specialisation project, and according to those results, glass containers provided less loss of pharmaceuticals. There was however no reference material with zero adsorption to compare to, so the absolute loss of pharmaceuticals due to glass adsorption is unknown.

The experiments were performed in temperature-controlled rooms. The temperature for the 9 °C experiments varied from 8,0 to 10,1 °C and the 4 °C experiments varied from 4,0 to 5,1°C, according to temperature measurements made every 10 minutes during the experiment execution. pH was not controlled or adjusted during experiments, but pH of samples was confirmed to be 7 using a pH test strip.

Samples in the isotherm experiments were prepared by manually pipetting different amounts of a 1000 ng/mL solution of the individual pharmaceuticals, and pure seawater, op obtain the lower concentrations. The manual pipetting was faster than mixing them in volumetric flasks, and due to the large number of samples, some precision had to be sacrificed in order to have time to prepare the samples in a reasonable amount of time.

4.2.4   Data processing sources of error

Majority of the data processing was performed using the Agilent MassHunter Quantitative Analysis software by assessing the calibration curve linearity, accuracy and manually integrating peaks that were not well integrated by the software. The manual integration step can introduce some error due to small changes in peak integration leading to large peak area variations, but it was sometimes necessary in order to quantify some peaks. This was especially a problem after samples were diluted, as some peaks became lower and wider, and the software was not always able identify and quantify the peak.

Calculations of sorption percentage and kinetics- and isotherm data were performed in Microsoft Excel, and RStudio was used to plot some of the figures. A drawback of using the Solver algorithm in Excel for parameter optimisation is that it needs an initial "guess" in order to optimize the values and find the best global minimum for the error function. It is possible for an error function to have several local minimums, and it can therefore be challenging to find the optimal global solution if the initial guess is not good enough.

4.3   Adsorption kinetics

The adsorption of the pharmaceuticals over time was assessed by calculating the concentrations in control samples and samples containing kaolin at different time intervals, and the results were plotted using RStudio and are presented in Figure 5. The sorption percentage at different times was calculated using the mean concentrations of the triplicate samples and equation 2. These are presented in Table 13 as numbers, and in Figure 6 as plots. The three compounds that were included in the isotherm experiments were also the ones being assessed with regard to the non-linear PFO and PSO kinetic models (ciprofloxacin (CIP), citalopram (CIT) and fluoxetine (FLU)). The choice of focusing on the three same compounds was done in order to save time and to be able to compare both kinetic and isotherm model results for these compounds.
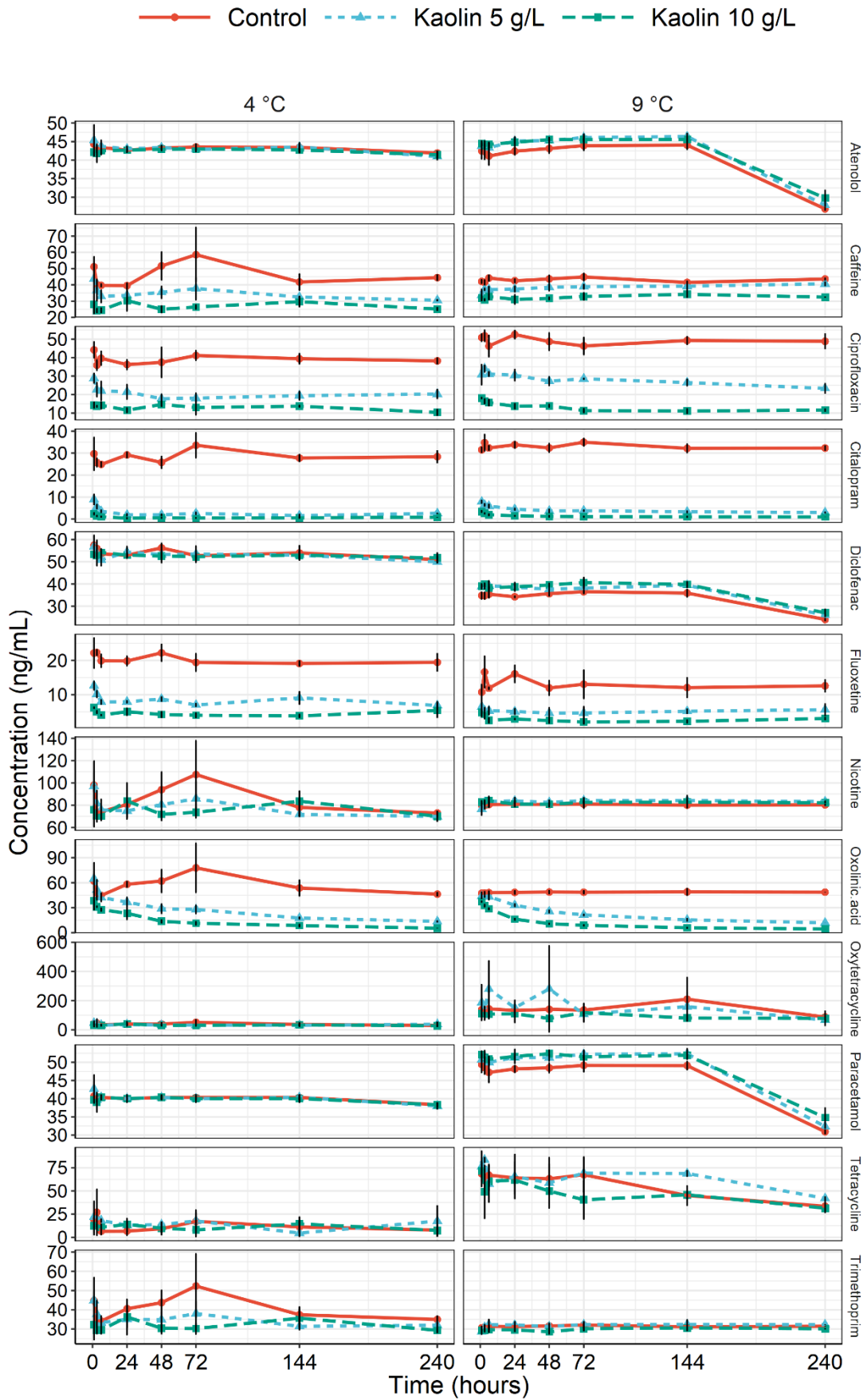
Figure 5: Plots showing concentration over time for the 12 pharmaceutical compounds

From the plots in Figure 5, it is clear which compounds adsorb to the kaolin or not. For example, atenolol, diclofenac and paracetamol appear to not adsorb to the kaolin due to the control samples and the samples containing kaolin having equal concentrations over time. In addition, tetracycline and oxytetracycline seems to not adsorb as well, but due to analytical difficulties for these compounds which were mentioned previously, the results are not very reliable. They did show adsorption potential in the specialization project adsorption experiment, but from the data in this thesis it is difficult to reach a conclusion on their adsorption potential. For the adsorbing compounds, increasing the amount of kaolin in the samples seems to increase the amount of adsorbate adsorbed, which is as expected, as more available surface area will increase the amount of adsorbed compound.

The adsorption of pharmaceuticals onto kaolin were estimated using the sorption percentage, which are shown in Figure 6. The raw data for the concentrations used for and sorption percentage calculations are found in appendix 7.4. The sorption percentage is calculated using equation 2, the means of the triplicates of the control samples and the mean of the triplicate kaolin samples. The standard deviations are calculated using a combination of equations 20 and 21. The equilibrium time of the pharmaceuticals varied extensively. For example, citalopram seemed to have reached equilibrium after less than 24 hours. Over 70% of the compound was adsorbed after 1 hour and the concentrations did not change significantly after around 24 hours. Other compounds, such as oxolinic acid, seemed to still adsorb to the kaolin after 6 days (144h), and might not yet have reached equilibrium even after 10 days. There is a possibility that the rotation of the samples was too slow for liquid and the solid phases to have enough contact time, and that a more "violent" stirring could have made oxolinic acid reach equilibrium faster. Oxolinic acid has been shown to reach equilibrium after 24 hours when in contact with natural sediments (Pouliquen and Le Bris, 1996). This could however be attributed to different shaking intensities, and therefore differences in contact time.
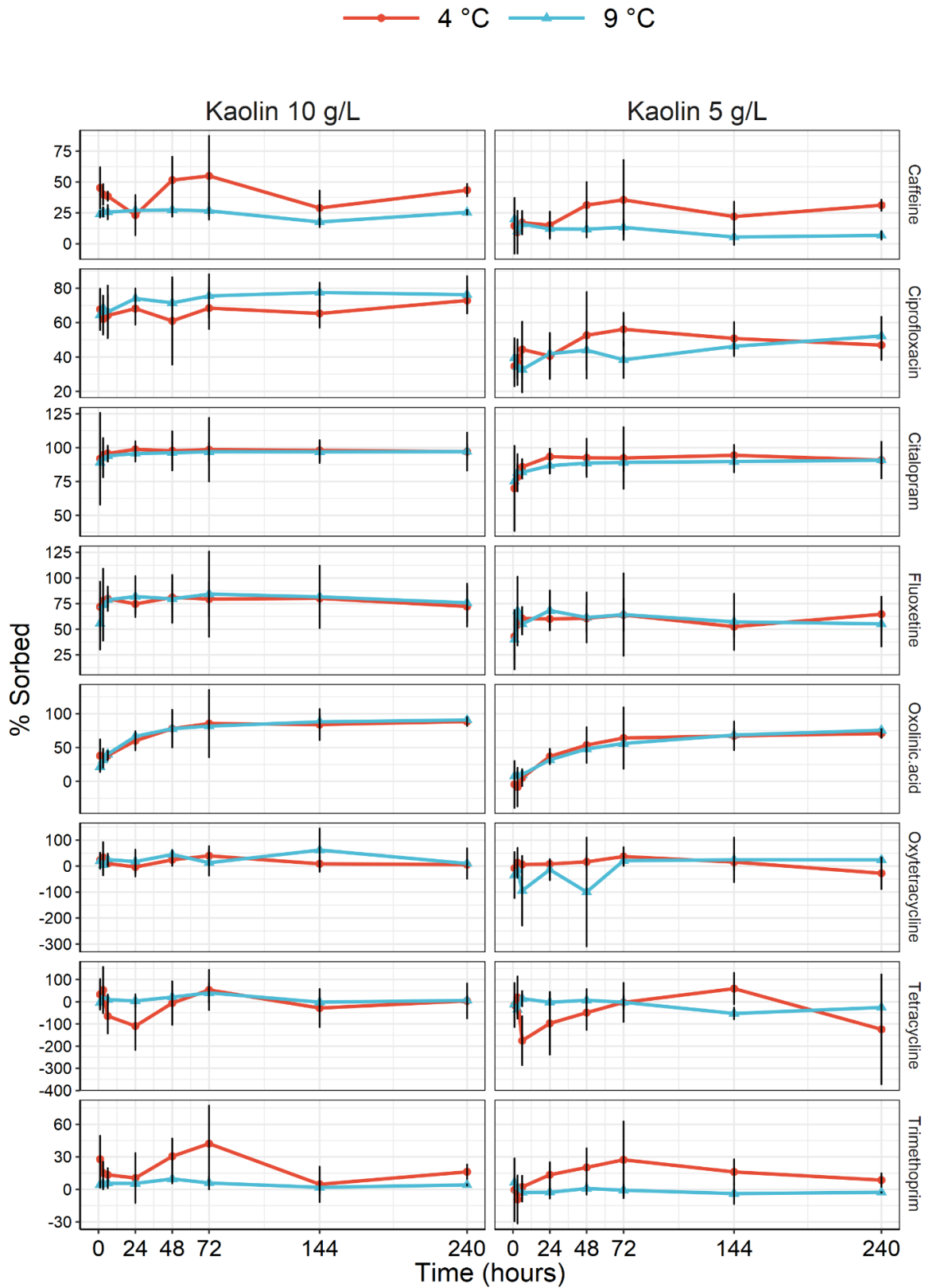
Figure 6: Sorption percentage over time for selected pharmaceuticals that showed adsorption tendencies to kaolin

4.3.1 Adsorption kinetic models

Adsorption kinetic models were assessed by calculating the adsorbed amount of pharmaceuticals, q_t, for samples taken at different time intervals using equation 1 and the data in appendix 7.4. The initial concentration, C_0, are set as the mean of the concentrations in the three control sample triplicates measured after 1 hour, since there was no measurement made immediately after samples were made. The q_t values were plotted against time. In an attempt to compare model parameters like q_{max} with other literature on the field, the concentrations were divided by 1000 to go from ng/mL (or µg/L) to mg/L before calculating kinetics and isotherm data. However, due to the q_{max} being highly related to the initial concentrations in the system, this change in units does not necessarily provide comparable numbers due to the difference in initial concentrations used in the experiments.

The kinetic models were applied using the Solver add-in in Excel, by iterating until the optimum adsorption parameters (k and q_e) were obtained. The kinetic models were optimized by minimizing the HYBRID error function, since the use of this to estimate adsorption isotherms led to the lowest overall SNE values for the isotherm data, which is discussed more in detail later. The PFO and PSO model parameters, the R^2 and the HYBRID error are presented in Table 11 and Table 12. The R^2 is provided despite it not being statistically valid for non-linear curves, as it is still vastly used for kinetic model fitting and is therefore also used to assess some results in this thesis, but with caution (Spiess and Neumeyer, 2010).

Table 11: Pseudo-first order model kinetics parameters

Amount of kaolin	Model parameters	4 °C			9 °C		
		CIP	CIT	FLU	CIP	CIT	FLU
5 g/L	k (h^{-1})	0,9531	1,3848	1,0344	2,0892	2,0453	1,1829
	q_e (mg/g)	0,0049	0,0055	0,0028	0,0043	0,0054	0,0011
	R^2	0,4767	0,7144	0,6114	0,0016	0,4808	0,0723
	HYBRID	0,0097	0,0016	0,0026	0,0142	0,0019	0,0060
10 g/L	k (h^{-1})	3,2611	2,8461	2,3647	2,0584	2,7208	1,1517
	q_e (mg/g)	0,0032	0,0030	0,0018	0,0037	0,0030	0,0008
	R^2	0,0392	0,7359	0,2657	0,3786	0,5970	0,3871
	HYBRID	0,0014	$4,4*10^{-5}$	0,0006	0,0012	0,0001	0,0012

Table 12: Pseudo-second order model kinetics parameters

Amount of kaolin	Model parameters	4 °C			9 °C		
		CIP	CIT	FLU	CIP	CIT	FLU
5 g/L	k (g/mg*h)	313,09	485,77	675,34	614,58	925,51	2222,7
	q_e (mg/g)	0,0051	0,0057	0,0029	0,0045	0,0055	0,0011
	R^2	0,5862	0,9044	0,6630	0,1992	0,8361	0,0738
	HYBRID	0,0085	0,0007	0,0020	0,0116	0,0005	0,0062
10 g/L	k (g/mg*h)	5953,9	4678,6	5458,5	1320,0	3744,3	2509,3
	q_e (mg/g)	0,0032	0,0030	0,0018	0,0038	0,0030	0,0008
	R^2	0,3205	0,9827	0,7168	0,7251	0,9573	0,5611
	HYBRID	0,0013	$1,2*10^{-5}$	0,0006	0,0007	$3*10^{-5}$	0,0009

From the data in table 11 and 12, we see that the equilibrium adsorption capacity, q_e, is highest when 5 g/L kaolin is added to the bottles, and lowest when 10 g/L kaolin is used. This is because the adsorption capacity is calculated by dividing by the mass of adsorbent in the system, meaning that when the amount of kaolin is doubled, it is divided by a twice as large number, see equation 1. The same trend was observed in some of the literature on the subject (Maged et al., 2021).

For all data sets except one (fluoxetine at 9 °C with 5 g/L kaolin) the HYBRID error was lower for the PSO model than the PFO model. Simultaneously, the R^2 was higher for all data sets when using PSO instead of PFO. When comparing plots of PFO and PSO, it can seem like the PFO model reaches equilibrium too quickly, and estimates a q_e that is too low, and therefore introduces more error between the experimental and the modelled data. An example of this is shown in Figure 7. Literature has found both PSO and PFO to fit adsorption kinetics data of pharmaceutical adsorption onto various adsorbents. Since the HYBRID error, the R^2 and the plots imply that the PSO is the best fit, that is the model that will be used to assess the adsorption kinetic parameters further.
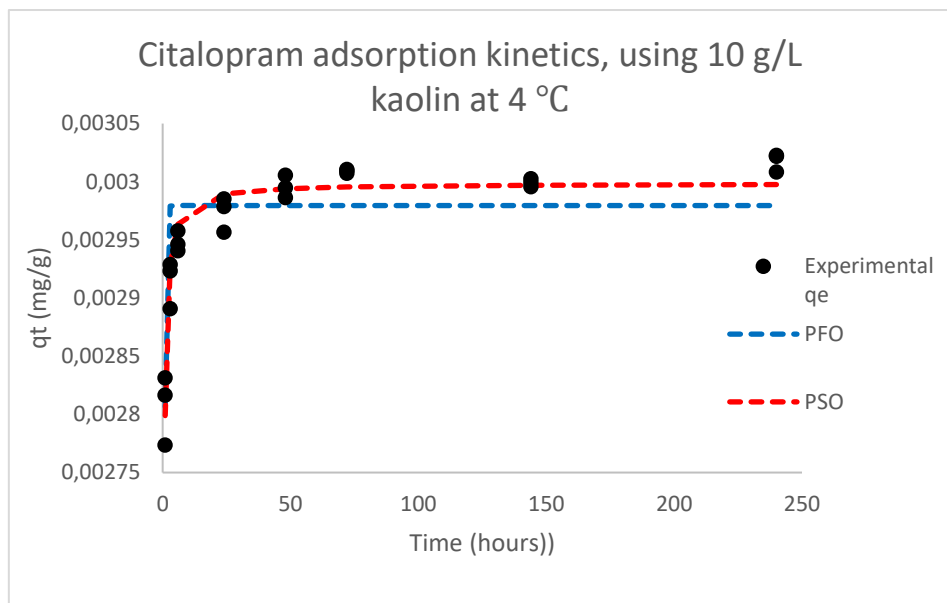
Figure 7: Citalopram adsorption kinetics

For all compounds, the use of 10 g/L kaolin gave higher rate constants and lower q_e values. As more adsorbent is added to the system, the adsorbate has more particle surface to react with, and a higher reaction rate is therefore logical. What is more surprising is the rapid increase in the rate when the adsorbent amount is increased. The rate is more than doubled for many of the data sets. For ciprofloxacin at 4 °C, the reaction rate at 10 g/L kaolin (5953,9 g/mg*h) is more than 10 times higher than for 5 g/L (313,09 g/mg*h) kaolin.

4.4 Adsorption isotherms

Raw data from the isotherm experiments are provided in appendix 7.5. Calculations of q_e were done by using the control samples at each concentration as C_0, because they are assumed to be taking adsorption to glass and degradation into consideration. Since some of the control sample concentrations were not the same as the theoretical added amount, the actual measured amount of the control samples were used as C_0. Each individual sample concentration, C_e, is subtracted from the mean of the concentration samples at the same concentration level and multiplied with the volume of the solution and divided by the mass of kaolin as shown in equation 1. Each triplicate was treated individually, in contrast to sorption percentage calculations, in order to have more data points to approximate an isotherm from. Some outliers were removed, either based on the size of the deviations between the triplicates, or the visual fit for the isotherm, and the implications the outlier had for the isotherm fitting. The outliers are marked in the raw data

49

tables. The isotherm data was used to calculate adsorption parameters using different isotherm models.

4.4.1 Effect of different error functions and SNE

In order to assess which error functions were most likely to give the most accurate isotherm parameters, SNE values were calculated. The results are provided in appendix 7.6, and the lowest SNE values and the accompanying isotherm parameters are written in bold in the tables. SNE calculations were made using MPSD, HYBRID, EABS and ARE. Due to the fact that R^2 is a value to be maximized, and the rest of the error functions to be minimised, in order to optimize the adsorption, R^2 could not be included in the SNE calculations. It was considered to use a modified value of R^2 in order to include it in the SNE analysis, like $1/R^2$ or $1-R^2$ but this was not supported by any literature.

The SNE calculations revealed that for 17 out of 24 data sets, the HYBRID error function provided the lowest SNE values. For the 7 other data sets, the ARE was the error function giving the lowest overall error. Figure 8 shows the optimization of the Sips isotherm for ciprofloxacin at 4 °C using different error functions.
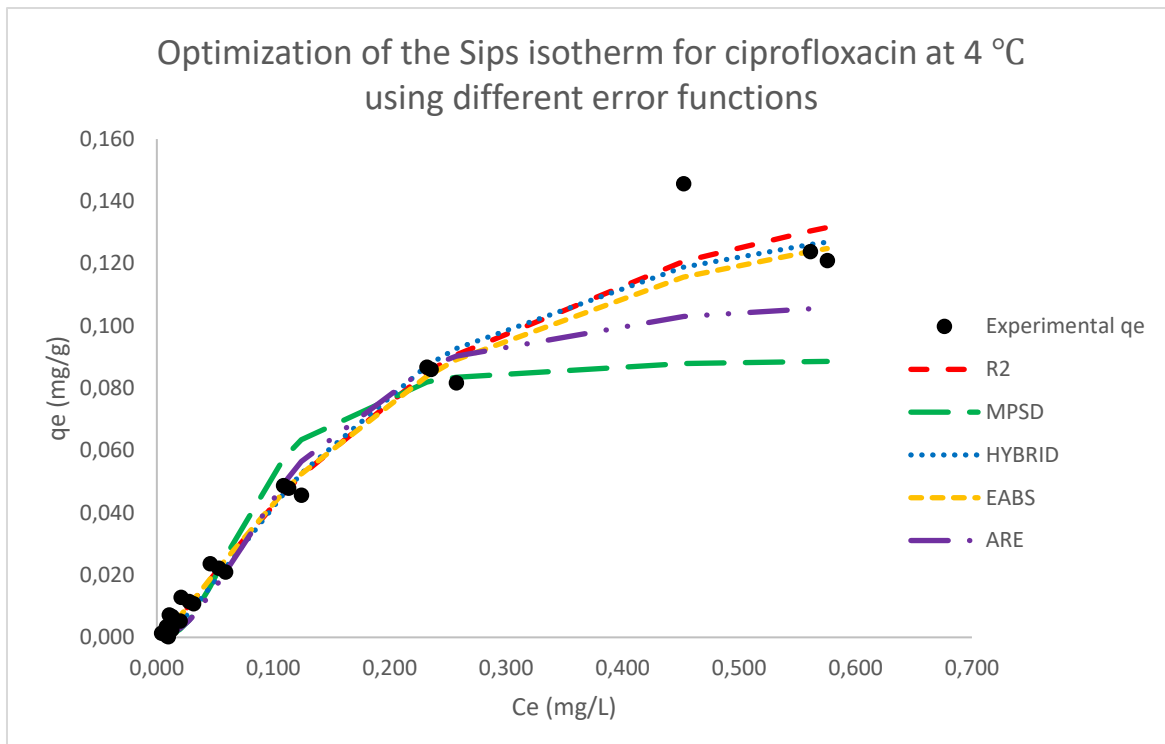
Figure 8: The Sips isotherm for ciprofloxacin at 4°C, optimized by different error functions

Visually, the R^2, EABS and HYBRID error functions seems to provide the least amount of deviations between the experimental and modelled data, while MPSD and ARE deviated from the experimental data at the highest concentrations. An interesting observation is that for this data set specifically, the ARE provided the lowest SNE value, meaning it is supposedly the best error function for minimizing the difference between the experimental and modelled data. Visually, this does not seem to be the case, as it deviates from the highest experimental concentration points. According to Fallou et al, the ARE error function had shown some weaknesses when applied to low-concentration studies (Fallou et al., 2016). Despite the R^2 being statistically invalid, it does a good job at following the curvature of the experimental data, compared to ARE and MPSD. The HYBRID and EABS error functions also seem to provide a good fit.

The HYBRID error function is the function providing the lowest SNE values for the majority of the data sets. Visually, it also seems to provide a good fit between the experimental and the modelled q_e values. It is therefore assumed that it is the best error function for minimizing the error for this study.

4.4.2 Effect of different isotherm models

Since the HYBRID error function provided the lowest SNE values for most data sets, it was assumed to be the best error function to minimize in order to get the best fitting isotherm parameters and models for the experimental data. Figure 9 to 14 shows the effect of using different isotherm models, all optimized by the HYBRID error function.
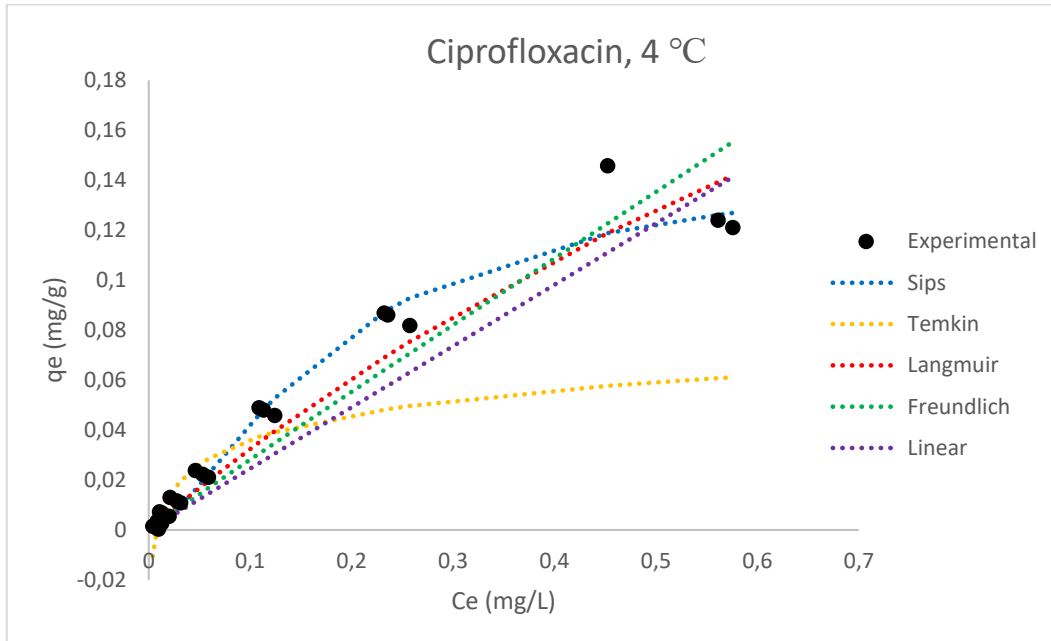
Figure 9: Comparison of isotherm models for ciprofloxacin at 4 °C, optimized by HYBRID
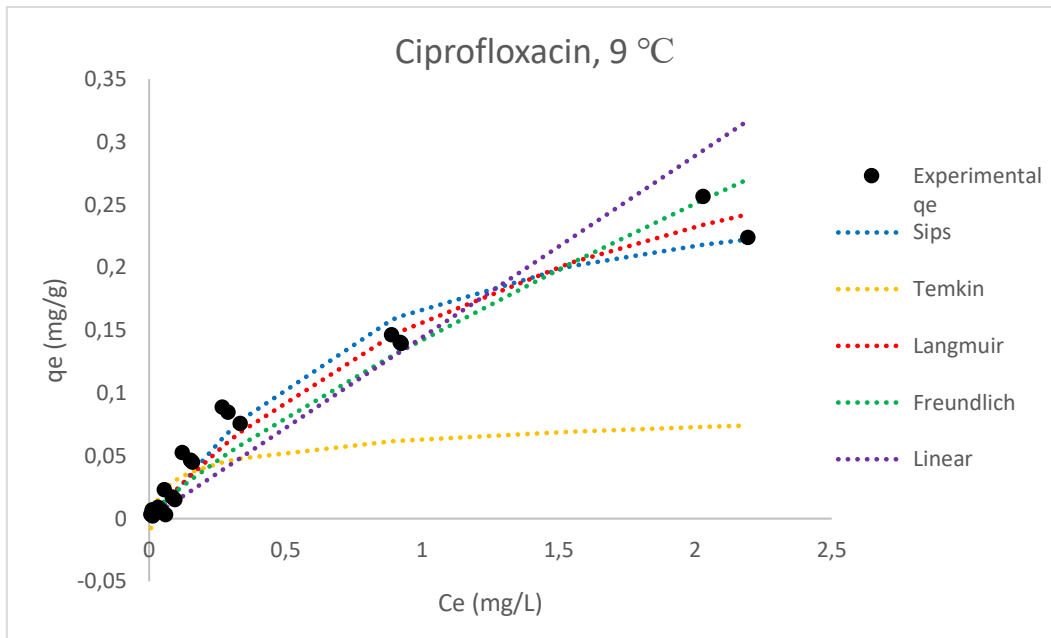
Figure 10: Comparison of isotherm models for ciprofloxacin at 9 °C, optimized by HYBRID
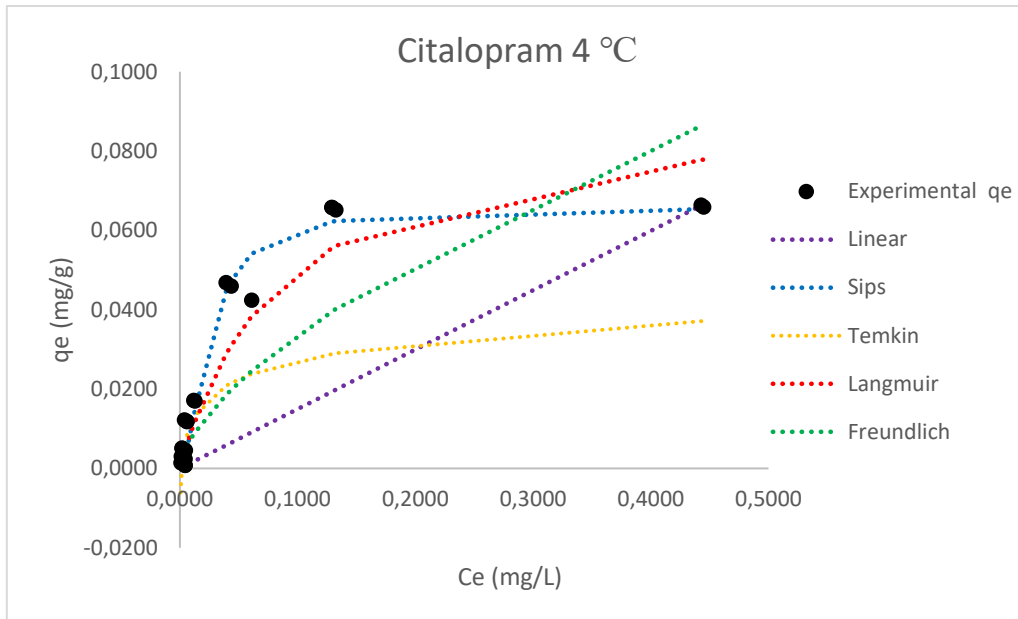
Figure 11: Comparison of isotherm models for citalopram at 4 ℃, optimized by HYBRID
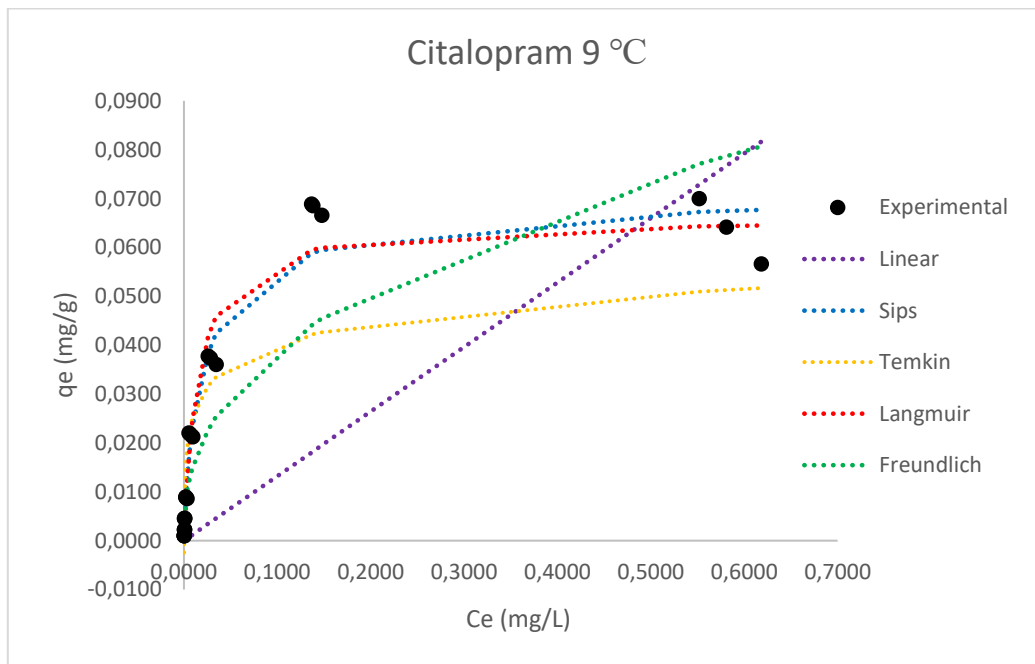
Figure 12: Comparison of isotherm models for citalopram at 9 ℃, optimized by HYBRID
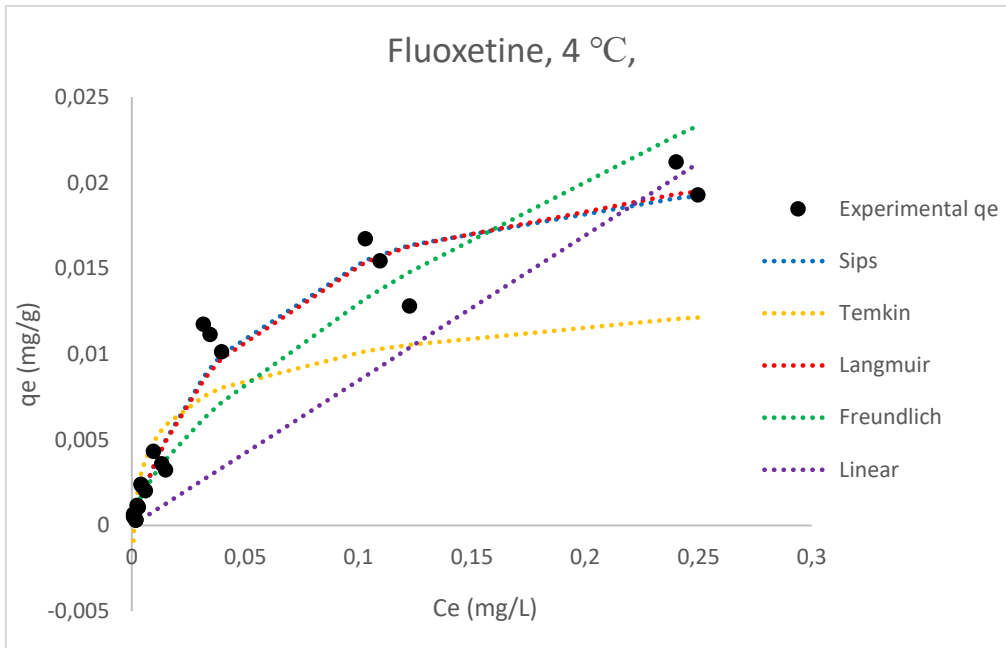
Figure 13: Comparison of isotherm models for fluoxetine at 4 ℃, optimized by HYBRID
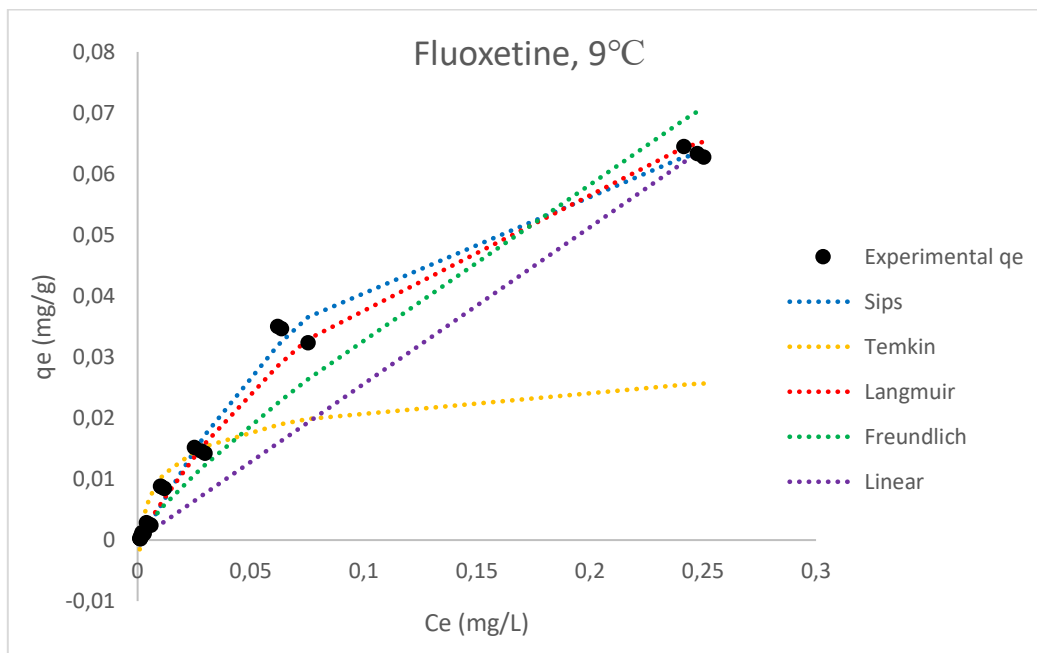
Figure 14: Comparison of isotherm models for fluoxetine at 9 ℃, optimized by HYBRID

Initial observations are that the linear model does not fit the experimental data well, especially not for citalopram, which exhibits the most curvature. The model might have a good fit for the lowest concentration range, but as the experimental data has curvature, the linear model falls short, which was expected. The Temkin model is the non-linear model that deviates the most from the experimental data at the high concentrations. In addition, at low concentrations the

Temkin graph begins at negative q_e values. This is not physically possible, as q_e cannot be negative. The Temkin model therefore seems not be applicable to the data. This might be due to some of the assumptions of the model not being true for the system, such as the assumption of multilayer adsorption, the rate at which the adsorption occurs or how the adsorption changes throughout the layering of adsorbate.

From the experimental data, citalopram seems to have reached a visible saturation limit, as the graphs appear to become completely flat at the end of the isotherm. This implies that the Langmuir or the Sips isotherm is the most applicable models, as they are both based on monolayer adsorption and a maximum limit of adsorbate on the adsorbent. For some data sets, for example for fluoxetine at 4 °C, the Sips and the Langmuir isotherms are almost identical, which is due to the n value being close to 1 (1,04). The Freundlich model seems not to be applicable to citalopram adsorption in the given system, given that the Freundlich isotherm does in theory not saturate completely.

Ciprofloxacin and fluoxetine seemed to have less curving of their data, but the Sips and Langmuir models still appear to fit the data the best, by visual investigation. As the Sips model is a combination of the Langmuir and Freundlich models, which are based on two different adsorption mechanisms, it is difficult to assess which adsorption mechanism is occurring in the system. Though, when comparing the Sips isotherm with both Langmuir and Freundlich individually, it seems to visually be most similar to the Langmuir isotherm, which implies a monolayer adsorption. Whether this directly implies chemical adsorption is unknown, whereas the literature suggests that a model can fit the data the best, but the assumptions of the model do not always match. This has been the case for some studies on ciprofloxacin and tetracycline adsorption, where the Langmuir model fit the data the best, but the mechanism of adsorption was declared to be ion exchange, a physisorption mechanism (Li et al., 2011, Wu et al., 2019).

HYBRID, ARE and R^2 errors are presented in Table 44 in appendix 7.6. For ciprofloxacin and citalopram, the HYBRID and ARE error is lowest overall, and R^2 highest overall, using the Sips isotherm model. For fluoxetine, the HYBRID error is lowest using the Langmuir isotherm, while the ARE error is lowest and R^2 highest using the Sips isotherm. This implies that the Sips isotherm successfully models the adsorption isotherms of all three compounds, since it creates the least amount of error when assessing the difference between experimental data and models. The 2-parameter model that best fits the data is the Langmuir model. As expected from visual inspection of the isotherms, the error generally tends to be the highest

for the linear model and the Temkin models, which add to the claim that they don't fit the experimental data well.

4.5 Effect of chemical properties and environmental conditions on adsorption

4.5.1 Adsorption and chemical properties

Some compounds showed signs of degradation after 10 days, as the concentrations in both control samples and kaolin samples started to decrease. The sorption percentage was therefore assessed at 6 days (144 hours). Table 13 shows sorption percentages after 6 days along with molecular mass, pK_a and log K_{OW} values. The standard deviations are also included, which are calculated using a combination of equation 20 and 21.

Large variations in log K_{OW} for the adsorbed compounds indicate that the adsorption cannot solely be explained by hydrophobic behaviour, as there is no clear relationship between the Log K_{OW} and the adsorption. For example, diclofenac is highly hydrophobic with a Log K_{OW} value of 4,51, but it did not adsorb significantly to the kaolin particles as e.g. citalopram and fluoxetine, which also have high log K_{OW}. Caffeine, with a log K_{OW} of -0,07 slightly adsorbed, but not as much as for example citalopram and fluoxetine.

pK_a is also a factor affecting the adsorption of pharmaceuticals to particles. At the experimental pH (here: 7), compounds with $pK_a < 7$ will tend to be in their neutral forms, while compounds with lower pK_a values will be deprotonated at pH higher than their pK_a. There is however no clear relation between pK_a and adsorption from the results in the kinetics experiments. For example, atenolol and citalopram have the same pK_a values, but only citalopram appears to adsorb to kaolin. Diclofenac has a low pK_a and is deprotonated and an anion at neutral pH, which can explain why it did not adsorb to the kaolin. This is the same reason that diclofenac does not adsorb to sludge (Sun et al., 2017). Another example is oxolinic acid and nicotine, which have similar pK_a values but only oxolinic acid appears to adsorb.

The molecular mass of the adsorbate molecules did not appear to impact the adsorption, as for example oxolinic acid and atenolol has similar molecular masses, but only oxolinic acid adsorbed.

Table 13: Sorption percentage of pharmaceuticals onto kaolin after 6 days. NS = No sorption observed. SD = standard deviation

| Compound | Sorption at 6 days (%) (± SD) | | | | Molecular weight (g/mol) | pK$_A$ | Log K$_{OW}$ |
| | 4 °C | | 9°C | | | | |
	5 g/L	10 g/L	5 g/L	10 g/L			
Atenolol	NS	2 (± 3)	NS	NS	266,34	9,6	0,16
Caffeine	22 (± 16)	29 (± 14)	4 (± 20)	18 (± 4)	194,19	10,4	- 0,07
Ciprofloxacin	52 (± 12)	67 (± 8)	46 (± 6)	78 (± 6)	331,34	1: 3,01 2: 6,14 3: 8,70 4: 10,58	0,280
Citalopram	94 (± 8)	98 (± 8)	90 (± 9)	97 (± 8)	324,4	9,6	3,04
Diclofenac	2 (± 6)	2 (± 7)	NS	NS	296,10	4,1	4,51
Fluoxetine	52 (± 16)	80 (± 5)	57 (± 27)	82 (± 30)	309,33	10,1	4,05
Nicotine	80 (± 9)	NS	NS	NS	162,23	6,16	1,17
Oxolinic acid	67 (± 26)	84 (± 23)	69 (± 13)	88 (± 11)	261,23	5,94	0,940
Oxytetracycline	12 (± 18)	7 (± 30)	24 (± 219)	62 (± 83)	460,40	1: 3,22 2: 7,46 3: 8,94	-0,9
Paracetamol	1 (± 3)	1 (± 3)	NS	NS	151,16	9,38	0,460
Tetracycline	10 (± 34)	NS	NS	NS	444,40	1: 3,32 2: 7,78 3: 9,58	-1,30
Trimethoprim	16 (± 3)	5 (± 16)	NS	2 (± 6)	290,32	1: 3,23 2: 6,76	0,91

According to the literature, the adsorption can both be increased and decreased with temperature, depending on the adsorbent and the adsorbate in the system. In this study, a decrease in temperature from 9 to 4 °C seemed to increase the sorption percentage for some compounds, and decrease it for others. For example, a decrease in temperature increased the adsorption of citalopram from 90 to 94 % (with 5 g/L kaolin). The same seems to be the case for caffeine and trimethoprim. The opposite seemed to occur for fluoxetine and oxolinic acid, as the sorption % degreased with decreasing temperature. The same seems to be for

oxytetracycline, though it comes with large standard deviations and the results might not be reliable. The inclusion of another temperature could have helped determine the effects of temperature. The sorption % is only an estimation of the adsorption, and kinetics modelling is a better way of determining the maximum adsorption capacities of different compounds at different temperatures.

4.5.2 Kinetic models and temperature

Figure 15 to 20 shows the PSO adsorption at different temperatures and different amounts of kaolin.

Regarding temperature changes and the kinetics parameters shown in Table 12, the effects are varying. When 5 g/L kaolin was used, the reaction rates increased with increasing temperature for all compounds. When 10 g/L kaolin was used, the opposite effects are observed for all compounds, as the rate constants decreased when the temperature increases from 4 to 9 ℃. A similar inconsistency occurs for the q_e; when 5 g/L kaolin is used, the q_e is higher for all compounds at 4 ℃. At 10 g/L kaolin, the effects are varying. For ciprofloxacin, the q_e increases slightly when the temperature is increased. For citalopram, the q_e is almost equal for 4 and 9 ℃, and for fluoxetine the q_e is lower at 9 ℃. These trends also appear in the plots below. It is unclear whether this is due to different adsorption mechanisms taking place, or if it is due to thermodynamic properties or conditions that are beyond the scope of this thesis.
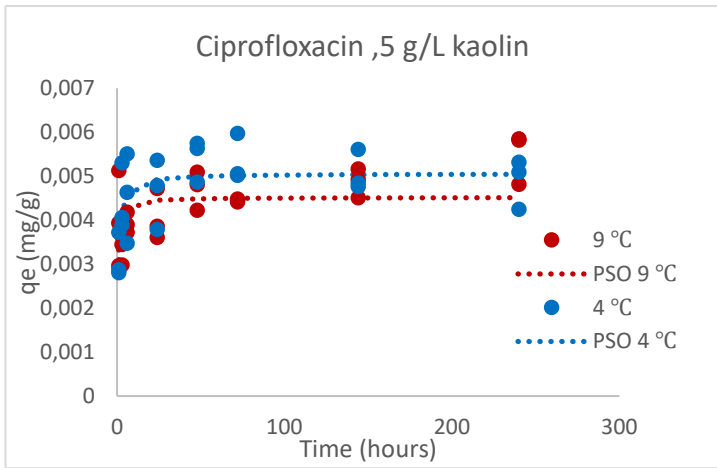
Figure 15: Ciprofloxacin adsorption kinetics by PSO model, 5 g/L kaolin
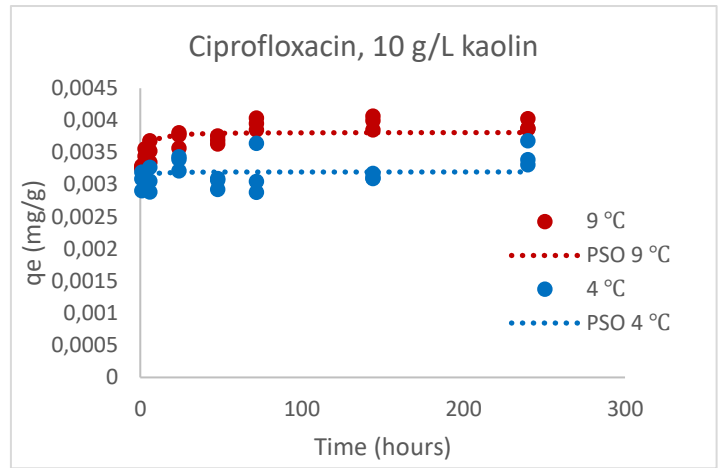
Figure 16: Ciprofloxacin adsorption kinetics by PSO model, 10 g/L kaolin
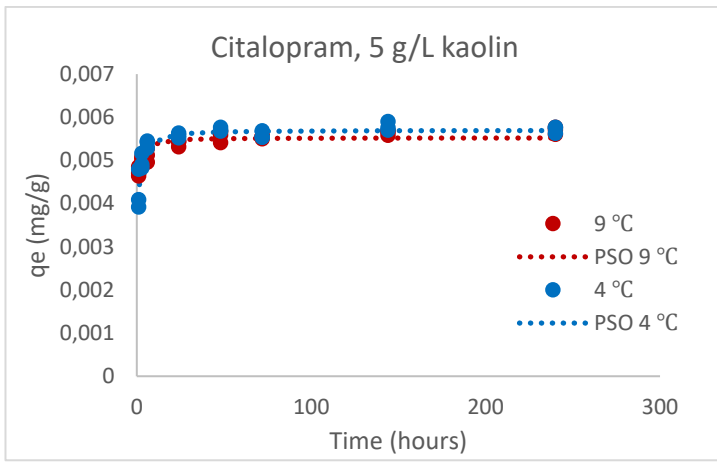
Figure 17: Citalopram adsorption kinetics by PSO model, 5 g/L kaolin
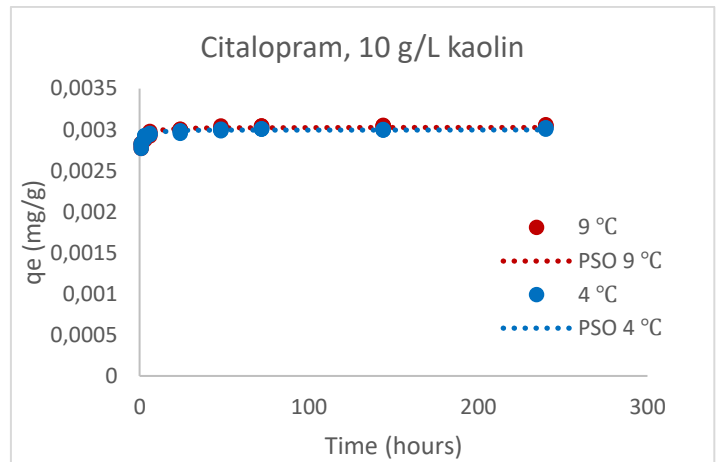
Figure 18: Citalopram adsorption kinetics by PSO model, 10 g/L kaolin
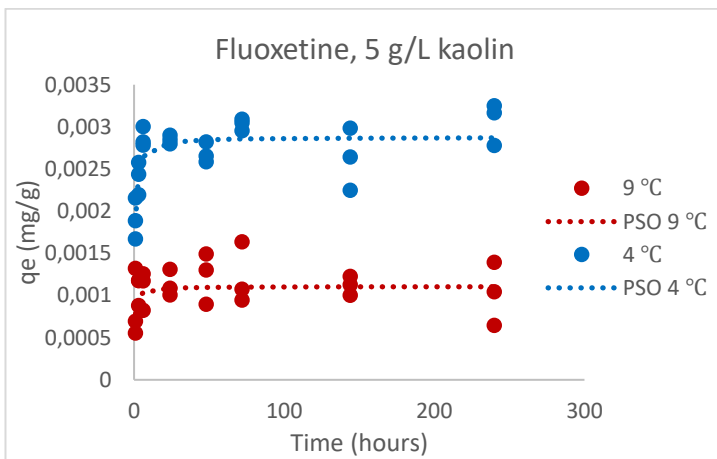
Figure 19: Fluoxetine adsorption kinetics by PSO model, 5 g/L kaolin
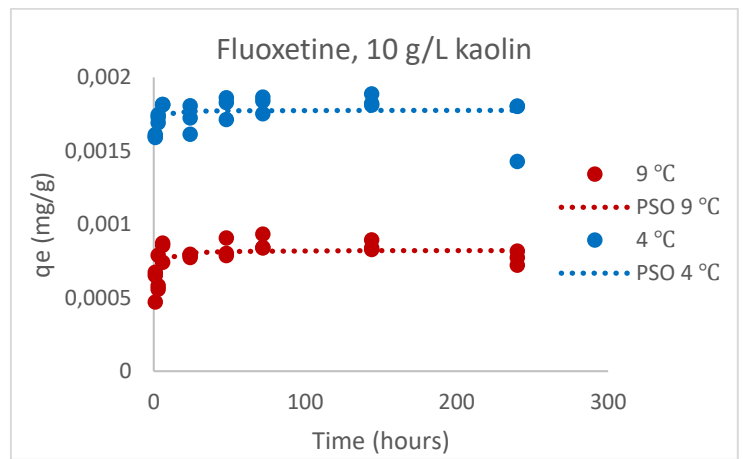
Figure 20: Fluoxetine adsorption kinetics by PSO model, 10 g/L kaolin

Above are the kinetics plots all compounds at 4 and 9 °C, using the PSO kinetics model. From the sorption % data, fluoxetine adsorption was highest at 9 °C. From the kinetics plots and the data in Table 12, the opposite trend appears. An increase in temperature for fluoxetine apparently makes the q_e (the equilibrium concentration of fluoxetine adsorbed to the kaolin particles) decrease. It is unknown why this trend appears, as one would expect the adsorbed amount of fluoxetine to be higher at 9 °C, according to the sorption percentages. The citalopram plot reveals that the two temperatures give very equal adsorption kinetics, which was also the case when assessing the sorption percentage. It seems as it is not greatly affected by the temperatures in these experiments, but larger temperature variations between experiments could have helped shed light on the temperature dependence. Ciprofloxacin seems to have a mixed trend when it comes to temperature. Using 5 g/L kaolin, the q_e increases slightly with a decrease in temperature, while at 10 g/L kaolin, the q_e increases with the increase in temperature. The same mixed trend was observed for the sorption percentage of ciprofloxacin. Fluoxetine is therefore the only compound deviating from observations made by the sorption percentage calculations.

4.5.3   Sips model and temperature

Table 14 summarizes the Sips isotherm parameters obtained by the HYBRID error function. From the table, it seems that the lower the temperature, the higher the affinity constant, K_s. Th maximum adsorption capacity is pretty equal for citalopram, while it increases with temperature for both ciprofloxacin and fluoxetine. The high affinity of citalopram to kaolin is also reflected in the sorption percentage, as almost all citalopram was adsorbed from the solution. The n-factor is between 0 and 2 for all compounds, which is relatively low compared to Silva et al who had an n-value of 6,74 (Silva et al., 2020). This can explain why the Langmuir isotherm was the 2-parameter model best fitted to the data, as an n-value of 1 will reduce the Sips isotherm to the Langmuir isotherm.

Table 14: Sips model parameters, optimised by the HYBRID error function

	Parameters	**CIP**	**CIT**	**FLU**
4 °C	K_s (L^n*mg^{-n})	12,59	672,8	22,42
	q_{max} (mg/g)	0,1501	0,0657	0,0229
	n	1,510	1,776	1,044

9 °C	K_s (L^n*mg^{-n})	1,565	22,67	17,25
	q_{max} (mg/g)	0,2754	0,0721	0,0825
	n	1,254	0,8216	1,190

Contrary to the kinetic experiments, the Sips isotherm data show a clear temperature dependence when it comes to the maximum adsorption capacity, q_{max}. For all compounds, the q_{max} is highest at 9 °C. The difference is smallest for citalopram, and highest for fluoxetine. This is also shown in figure 21-23. Ciprofloxacin shows the highest maximum adsorption capacity of 0,2754 mg/g at 9 °C. Fluoxetine has the lowest q_{max}, 0,0825 mg/g, out of the three compounds, at 4 °C.
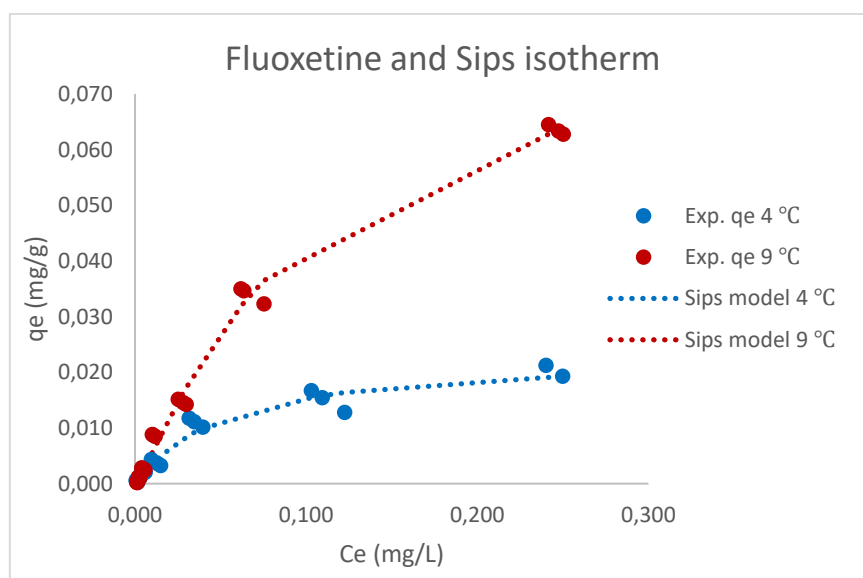
Figure 21: Fluoxetine adsorption by the Sips isotherm model at different temperatures

According to Figure 21, the adsorption of fluoxetine is much higher for 9 °C than for 4 °C. According to the literature, this is the case when the adsorbate clay molecules swell as a result of increased temperature. Diffusion into pores of the adsorbent can also increase with increasing temperature. The favourable adsorption of fluoxetine at higher temperatures correspond to the results from the sorption percentage calculations.
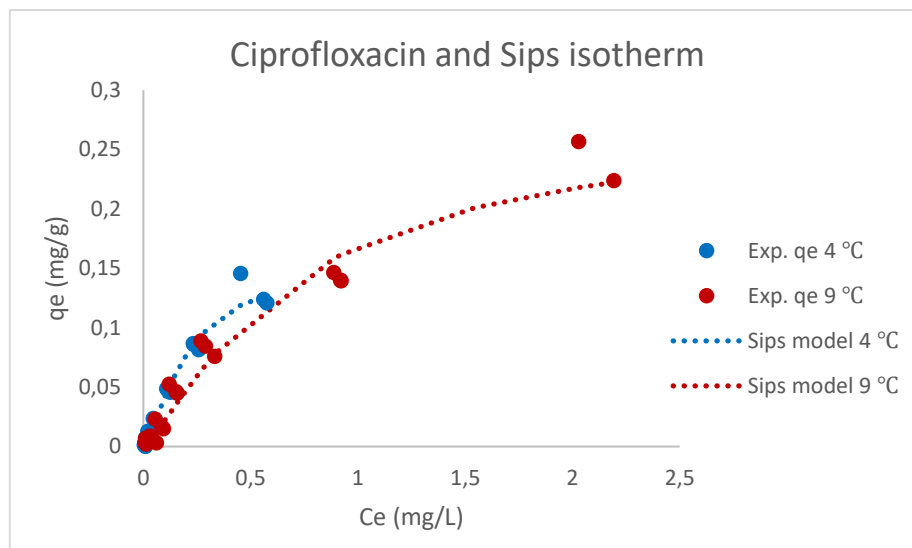
Figure 22: Ciprofloxacin adsorption by the Sips isotherm model at different temperatures

The adsorption isotherm for ciprofloxacin, shown in Figure 22, is shorter at 4 °C than at 9 °C. The reason for this could be inaccuracies during preparations of the samples, due to many manual pipetting that have been mentioned earlier. Another source of error could be degradation of internal standards or pharmaceutical standards. The 9 °C experiment was performed prior to the 4 °C experiment, and it is possible that the standard has started to degrade or that the repeated thawing of frozen standard has affected its concentration. These are both factors that could influence the concentrations of ciprofloxacin in the control samples of the isotherm experiment, which makes one of the isotherms shorter than the other.
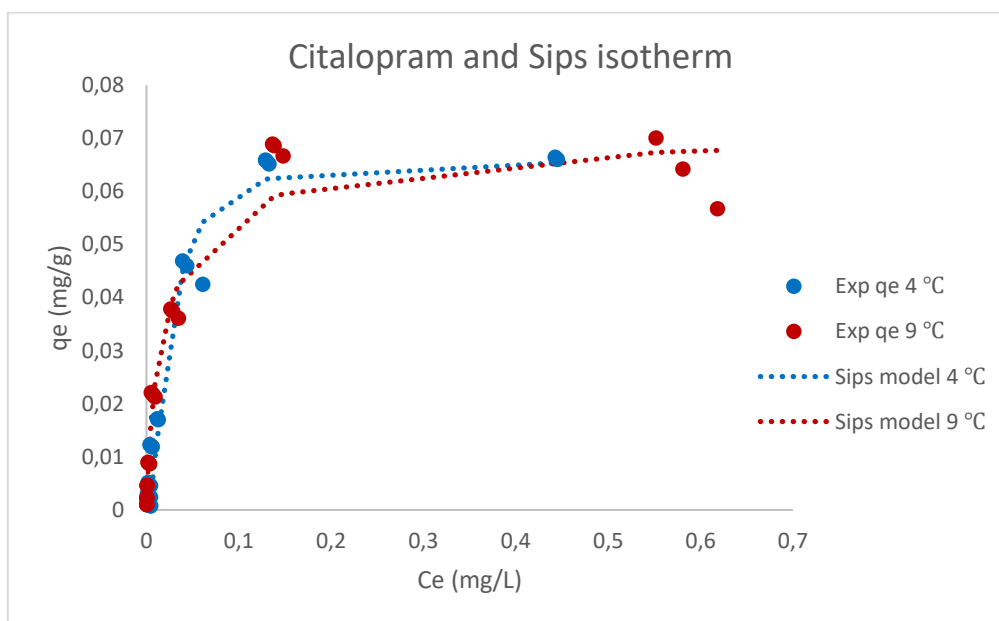
Figure 23: Citalopram adsorption by the Sips isotherm model at different temperatures

Citalopram appears to be little influenced by the change in temperature, according to Figure 23. This was also expressed by both the sorption percentage, which was high at both 4 and 9 °C. The kinetics results also showed that the q_e values were similar at 4 and 9 °C.

4.5.4 Adsorption compared to literature

The literature and the results of this study do not correspond for all analytes. Several pharmaceuticals that were reported to adsorb to kaolin or other sediments did not show adsorption in this thesis. Hu et al reported fast and high adsorption of atenolol onto kaolin particles, while no significant adsorption of atenolol was observed in this study (Hu et al., 2015). High adsorption was also reported for paracetamol and diclofenac. The pH and salinity of the liquid phase are properties that could have negative effects on the adsorption.

Because many of the studies in the literature use higher concentrations of pharmaceuticals (in the mg/L range), it is difficult to directly compare q_{max} values between literature and this thesis, as the initial concentration of adsorbate is highly important for the outcome of an adsorption study and the maximum adsorption capacity that is calculated.

The Sips isotherm model successfully described fluoxetine adsorption onto pine bark (Silva et al., 2020). In that study, the K_s was calculated to be 15,8 L/g. Some articles include the n-values of the Freundlich and Sips models in the unit of their constants, while others don't, which makes it difficult to compare between models. The obtained Sips affinity constants in this project were 22,42 and 17,53 L^n*mg^{-n} for 4 and 9 °C, respectively, for fluoxetine.

Citalopram have fitted well to the Freundlich isotherm, in addition to the PFO and PSO kinetic models, in the literature. However, in this thesis the citalopram adsorption was clearly better fitted to the Langmuir or Sips model, as the adsorption had a clear maximum adsorption capacity. The obtained affinity constants for citalopram were 672,8 and 22,67 L^n*mg^{-n} for citalopram at 4 and 9 °C, respectively, which is a very large increase in the affinity constant from 9 to 4 °C.

Ciprofloxacin was mostly fitted to the Langmuir isotherm according to the literature. Wu et al reported a K_L value of 262 L/mmol, which corresponds to 791 L/g, or 0,791 L/mg. This value is relatively close to the K_L value obtained by this study using the Langmuir isotherm, $K_L =$ 0,704 L/mg at 4 °C, which means that the partitioning coefficients are comparable, even if the initial concentrations are different. As the Sips affinity constant, K_s, has other units then K_L, it

is difficult to compare directly between models. The Sips affinity constants for ciprofloxacin were 12,59 and 1,57 L^n*mg^{-n}.

Adsorption from an environmental perspective

Whether or not the compounds that adsorb strongly to sediments pose a smaller or greater risk of impacting marine life is still unknown. Pollutants can cause harm both when they are dissolved in water or adsorbed to solid particles. One can imagine that sediment bound pharmaceuticals are less likely to be transported by ocean currents, but this will be dependent on the sediment particle sizes and whether or not is suspended in the liquid phase or sedimented at the bottom. An accumulation can be more probable in sediments due to the possibility of increased persistence one the pharmaceutical is adsorbed (Hektoen et al., 1995), and can cause damage for organisms feeding of sediments.

In the environment, the adsorption process is much more complex than in the lab, and many factors contribute. Changes in the weather can affect the degradation of compounds, and the wind speed can affect the turbulence of the water. The release point of wastewater can be important in terms of distance from the ocean and depth. If the waste is disposed close to the surface, the adsorption can differ from locations where it is disposed close to the bottom. Different types of sediments are present at different locations, which can affect the adsorption. In addition, the concentrations in the environment are much smaller than what has been used in most adsorption studies.

Despite all the factors mentioned above, the data in this thesis still contributes to a higher understanding of the adsorption mechanisms that occur and the information can hopefully be used to improve the models that assess the transport of pharmaceuticals in the ocean.

4.6 Further work

Experiments described in this thesis were also performed at 18 °C, in addition to 4 and 9. However, due to limited time to analyse all the planned samples, the adsorption at 18 °C was not assessed. Analysis of samples 4 and 9 °C experiments was prioritised due to them being most relevant to Scandinavian and Arctic sea temperatures. The 18 °C samples should be analysed for the sake of the Pharmarine project in order to gain a deeper understanding of the adsorption at different temperatures, as some the results from 4 and 9 °C were conflicting.

Because of the higher temperature gap, data from 18 °C could provide more distinct temperature relationships and trends.

Experiments including algae (*Rhodomonas Baltica*) were performed, but these samples were not analysed either, due to time constraints. These samples are also of interest to analyse in order to assess the adsorption of pharmaceuticals to algae surfaces. Since these species of algae are found in the Arctic and are food for other species, it is interesting to quantify the amounts of pharmaceuticals that adsorb to it, as it can possibly be accumulated in the food chain.

In order to fully assess the adsorption mechanisms that occur, more measurements and calculations are possible to make. These include FT-IR, which was performed in many of the relevant studies on the subject, in order to assess the differences in bonds in the adsorbate before and after adsorption. Thermodynamic calculations can also be performed in order to assess the energy of the bond formation and get a sense of the strength of the interaction, which is related to the type of adsorption mechanism.

Other compounds, such as metabolites of pharmaceuticals, are interesting for adsorption studies due to the fact that many pharmaceuticals are transformed either in the body or by hydrolysis or degradation in the environment. Their adsorption behaviour in environmental conditions is therefore an interesting topic. The use of other sediment types, or even natural sediment collected in the environment, can also be an interesting approach for more understanding of the environmental fate of these compounds.

5   Conclusion

The adsorption of pharmaceuticals onto the sediment kaolin was studied in this thesis, by kinetics and isotherm modelling. HPLC-MS/MS measurements of remaining pharmaceuticals in a seawater/sediment system was measured after specific time intervals and at different initial concentrations of pharmaceuticals.

Experimental adsorption data was fitted to the Pseudo-first and -second order kinetics models. The PSO model provided the best fit and revealed that the increase of the amount of particles heavily impacted the rate of the adsorption, and that a doubling in sediment mass led to more than 10 times higher rate constants for the pseudo-second order model at 4 °C. The highest rate was obtained for ciprofloxacin at 4 °C, which was 5953,9 g/mg*h. The equilibrium concentrations had a varying impact from increasing temperature and adsorbent mass.

Different error functions were implemented in order to minimize the error between experimental and modelled data. The HYBRID error function provided the lowest SNE values for most of the data sets, and visual inspection also showed that it fit well to the experimental data. The HYBRID error revealed that the Sips isotherm model was the best fit for all compounds, as it gave the lowest error and a good visual fit.

The 3-parameter Sips isotherm model performed well for all compounds, with regard to visual fit and error. Sips isotherm data revealed that citalopram was little influenced by temperature changes with regard to the q_{max}. The Sips affinity constant however, changed drastically from 22,67 to 672,8 L^n*mg^{-n} for citalopram when the temperature decreased from 9 to 4 °C. The affinity constant for fluoxetine increased less, only from 17,25 to 22,42 L^n*mg^{-n} with increasing temperature. The maximum adsorption capacity for all compounds was highest at 9 °C, which indicates favourable adsorption at higher temperatures.

Adsorption is a complicated phenomenon that is dependent on many factors. The results from this thesis can hopefully contribute to improve the current modelling of pharmaceutical pollution in the ocean. Research into the fate and transport of pharmaceuticals in the ocean is important, as the increase in their use can have implications for marine life.

6 Bibliography

AKCAY, G. & YURDAKOC, K. 2008. Removal of nicotine and its pharmaceutical derivatives from aqueous solution by raw bentonite and dodecylammonium-bentonite. *Journal of scientific & industrial research (New Delhi, India : 1963),* 67**,** 451-454.

AL-GHOUTI, M. A. & DA'ANA, D. A. 2020. Guidelines for the use and interpretation of adsorption isotherm models: A review. *J Hazard Mater,* 393**,** 122383-122383.

AL-KHAZRAJY, O. S. A. & BOXALL, A. B. A. 2016. Impacts of compound properties and sediment characteristics on the sorption behaviour of pharmaceuticals in aquatic systems. *J Hazard Mater,* 317**,** 198-209.

ALMAZROO, O. A., MIAH, M. K. & VENKATARAMANAN, R. 2017. Drug Metabolism in the Liver. Philadelphia :.

ÁNGEL, V.-O., KELLY, J. F.-L. & RODRIGO, O.-T. 2022. Kinetics and Adsorption Equilibrium in the Removal of Azo-Anionic Dyes by Modified Cellulose. *Sustainability (Basel, Switzerland),* 14**,** 3640.

APPEL, C., MA, L. Q., DEAN RHUE, R. & KENNELLEY, E. 2003. Point of zero charge determination in soils and minerals via traditional methods and detection of electroacoustic mobility. *Geoderma,* 113**,** 77-93.

ARMBRUSTER, D. A. & PRY, T. 2008. Limit of blank, limit of detection and limit of quantitation. *Clin Biochem Rev,* 29 Suppl 1**,** S49-S52.

BAKIR, A., ROWLAND, S. J. & THOMPSON, R. C. 2012. Competitive sorption of persistent organic pollutants onto microplastics in the marine environment. *Mar Pollut Bull,* 64**,** 2782-2789.

BAVUMIRAGIRA, J. P., GE, J. N. & YIN, H. 2022. Fate and transport of pharmaceuticals in water systems: A processes review. *Sci Total Environ,* 823**,** 153635-153635.

BEIRAS, R. & SCHÖNEMANN, A. M. 2021. Water quality criteria for selected pharmaceuticals and personal care products for the protection of marine ecosystems. *Sci Total Environ,* 758**,** 143589-143589.

BOTTONI, P., CAROLI, S. & CARACCIOLO, A. B. 2010. Pharmaceuticals as priority water contaminants. *Toxicological and environmental chemistry,* 92**,** 549-565.

BROOKS, B. W., TURNER, P. K., STANLEY, J. K., WESTON, J. J., GLIDEWELL, E. A., FORAN, C. M., SLATTERY, M., LA POINT, T. W. & HUGGETT, D. B. 2003. Waterborne and sediment toxicity of fluoxetine to select organisms. *Chemosphere,* 52**,** 135-142.

BRUMOVSKÝ, M., BEČANOVÁ, J., KOHOUTEK, J., BORGHINI, M. & NIZZETTO, L. 2017. Contaminants of emerging concern in the open sea waters of the Western Mediterranean. *Environ Pollut,* 229**,** 976-983.

CHEMICAL ABSTRACTS SERVICE 2021. SciFinder. Columbus, Ohio: American Chemical Society.

CHEN, J., Y. 2017a. Adsorption Properties of Activated Carbon Fibers. Elsevier.

CHEN, J. Y. 2017b. Activated carbon fiber and textiles. Amsterdam, Netherlands: Woodhead Publishing.

CHENG, K. & HEIDARI, Z. 2018. A new method for quantifying cation exchange capacity in clay minerals. *Applied clay science,* 161**,** 444-455.

CIBOROWSKI, P. & SILBERRING, J. 2016. *Proteomic Profiling and Analytical Chemistry: The Crossroads,* Oxford, Oxford: Elsevier.

COSTA JUNIOR, I. L., MACHADO, C. S., PLETSCH, A. L. & TORRES, Y. R. 2022. Sorption and desorption behavior of residual antidepressants and caffeine in freshwater sediment and sewage sludge. *International journal of sediment research,* 37**,** 346-354.

COUTO JR, O. M., MATOS, I., DA FONSECA, I. M., ARROYO, P. A., DA SILVA, E. A. & DE BARROS, M. A. S. D. 2015. Effect of solution pH and influence of water hardness on caffeine adsorption onto activated carbons. *Can. J. Chem. Eng,* 93**,** 68-77.

DABROWSKI, A. 2001. Adsorption — from theory to practice. *Adv Colloid Interface Sci,* 93**,** 135-224.

DASTMALCHI, S., RASHIDI, M. R. & RASSI, M. M. B. Simultaneous determination of the pKa and octanol/water partition coefficient (Pm) of acetaminophen. 1995.

EEA 2022. Transport via ocean currents of human pharmaceutical products and their impact on marine biota in the European Arctic. University of Gdansk.

EL-SAID IBRAHIM, E. S. H. A.-L. A. S. A.-S. 2012. Ciprofloxacin adsorption from aqueous solution onto chemically prepared carbon from date palm leaflets. *Journal of Environmental Sciences,* 24**,** 1579-1586.

EPA 2008. Aquatic Life Criteria for Contaminants of Emerging Concern: Part 1 General Challenges and Recommendations. United States Environmental Protection Agency.

FALLOU, H., CIMETIÈRE, N., GIRAUDET, S., WOLBERT, D. & LE CLOIREC, P. 2016. Adsorption of pharmaceuticals onto activated carbon fiber cloths – Modeling and extrapolation of adsorption isotherms at very low concentrations. *J Environ Manage,* 166**,** 544-555.

FATTA, D., ACHILLEOS, A., NIKOLAOU, A. & MERIÇ, S. 2007. Analytical methods for tracing pharmaceutical residues in water and wastewater. *TrAC, Trends in analytical chemistry (Regular ed.),* 26**,** 515-533.

FENT, K., WESTON, A. A. & CAMINADA, D. 2006. Ecotoxicology of human pharmaceuticals. *Aquat Toxicol,* 76**,** 122-159.

FERRER, I., ZWEIGENBAUM, J. A. & THURMAN, E. M. 2010. Analysis of 70 Environmental Protection Agency priority pharmaceuticals in water by EPA Method 1694. *J Chromatogr A,* 1217**,** 5674-5686.

GILL, M. K. 2016. The History of Pharmaceuticals. Britannica Educational Publishing.

GIMBERT, F., MORIN-CRINI, N., RENAULT, F., BADOT, P.-M. & CRINI, G. 2008. Adsorption isotherm models for dye removal by cationized starch-based material in a single component system: Error analysis. *J Hazard Mater,* 157**,** 34-46.

GONZALEZ-REY, M., MATTOS, J. J., PIAZZA, C. E., BAINY, A. C. D. & BEBIANNO, M. J. 2014. Effects of active pharmaceutical ingredients mixtures in mussel Mytilus galloprovincialis. *Aquat Toxicol,* 153**,** 12-26.

GROS, M., RODRÍGUEZ-MOZAZ, S. & BARCELÓ, D. 2012. Fast and comprehensive multi-residue analysis of a broad range of human and veterinary pharmaceuticals and some of their metabolites in surface and treated waters by ultra-high-performance liquid chromatography coupled to quadrupole-linear ion trap tandem mass spectrometry. *Journal of Chromatography A,* 1248**,** 104-121.

HALLING-SØRENSEN, B., NORS NIELSEN, S., LANZKY, P. F., INGERSLEV, F., HOLTEN LÜTZHØFT, H. C. & JØRGENSEN, S. E. 1998. Occurrence, fate and effects of pharmaceutical substances in the environment- A review. *Chemosphere,* 36**,** 357-393.

HAO, C., ZHAO, X. & YANG, P. 2007. GC-MS and HPLC-MS analysis of bioactive pharmaceuticals and personal-care products in environmental matrices. *TrAC, Trends in analytical chemistry (Regular ed.),* 26**,** 569-580.

HEKTOEN, H., BERGE, J. A., HORMAZABAL, V. & YNDESTAD, M. 1995. Persistence of antibacterial agents in marine sediments. *Aquaculture,* 133**,** 175-184.

HELBÆK, M. 2011. *Statistikk : kort og godt,* Oslo, Universitetsforl.

HO, Y.-S. 2004. Selection of optimum sorption isotherm. *Carbon (New York),* 42**,** 2115-2116.

HO, Y. S. & MCKAY, G. 1999. Pseudo-second order model for sorption processes. *Process biochemistry (1991),* 34**,** 451-465.

HORSFALL, M. & SPIFF, A. I. 2005. Effects of temperature on the sorption of Pb^{2+} and Cd^{2+} from aqueous solution by Caladium bicolor (Wild Cocoyam) biomass. *Electronic Journal of Biotechnology,* 8**,** 162-169.

HOUNFODJI, J. W., KANHOUNNON, W. G., KPOTIN, G., ATOHOUN, G. S., LAINÉ, J., FOUCAUD, Y. & BADAWI, M. 2021. Molecular insights on the adsorption of some pharmaceutical residues from wastewater on kaolinite surfaces. *Chemical engineering journal (Lausanne, Switzerland : 1996),* 407**,** 127176.

HOVSBAKKEN, I. A. 2021. Analytical method performance, stability and particle adsorption of pharmaceuticals and pesticides in seawater.

HU, Y., FITZGERALD, N. M., LV, G., XING, X., JIANG, W.-T. & LI, Z. 2015. Adsorption of Atenolol on Kaolinite. *Advances in materials science and engineering,* 2015**,** 1-8.

IQVIA 2022. The Global Use of Medicines 2022: Outlook to 2026.

IVANIĆ, M., VDOVIĆ, N., BARRETO, S. D. B., BERMANEC, V. & SONDI, I. 2015. Mineralogy, surface properties and electrokinetic behaviour of kaolin clays derived from naturally occurring pegmatite and granite deposits. *Geologia Croatica,* 68**,** 139-145.

JIN, Q., HUANG, L., LI, A. & SHAN, A. 2017. Quantification of the limitation of Langmuir model used in adsorption research on sediments via site energy heterogeneity. *Chemosphere,* 185**,** 518-528.

KALINENKO, V. V. 2001. Clay Minerals in Sediments of the Arctic Seas. *Lithology and mineral resources,* 36**,** 362-372.

KHAN, H. K., REHMAN, M. Y. A. & MALIK, R. N. 2020. Fate and toxicity of pharmaceuticals in water environment: An insight on their occurrence in South Asia. *Journal of environmental management,* 271**,** 111030-111030.

KIM, H.-Y., LEE, I.-S. & OH, J.-E. 2017. Human and veterinary pharmaceuticals in the marine environment including fish farms in Korea. *Sci Total Environ,* 579**,** 940-949.

KLEMENT, A., KODEŠOVÁ, R., BAUEROVÁ, M., GOLOVKO, O., KOČÁREK, M., FÉR, M., KOBA, O., NIKODEM, A. & GRABIC, R. 2018. Sorption of citalopram, irbesartan and fexofenadine in soils: Estimation of sorption coefficients from soil properties. *Chemosphere,* 195**,** 615-623.

KLOEPFER, A., QUINTANA, J. B. & REEMTSMA, T. 2005. Operational options to reduce matrix effects in liquid chromatography–electrospray ionisation-mass spectrometry analysis of aqueous environmental samples. *J Chromatogr A,* 1067**,** 153-160.

KUMAR, K. V., PORKODI, K. & ROCHA, F. 2008. Comparison of various error functions in predicting the optimum isotherm by linear and non-linear regression analysis for the sorption of basic red 9 by activated carbon. *J Hazard Mater,* 150**,** 158-165.

KÜMMERER, K. 2008. Pharmaceuticals in the Environment : Sources, Fate, Effects and Risks. 3rd ed. 2008. ed. Berlin, Heidelberg: Springer Berlin Heidelberg : Imprint: Springer.

LE GUET, T., HSINI, I., LABANOWSKI, J. & MONDAMERT, L. 2018. Sorption of selected pharmaceuticals by a river sediment: role and mechanisms of sediment or Aldrich humic substances. *Environ Sci Pollut Res Int,* 25**,** 14532-14543.

LEDIEU, L., SIMONNEAU, A., THIEBAULT, T., FOUGERE, L., DESTANDAU, E., CERDAN, O. & LAGGOUN, F. 2021. Spatial distribution of pharmaceuticals within the particulate phases of a peri-urban stream. *Chemosphere,* 279**,** 130385-130385.

LENZI, G. G., FUZIKI, M. E. K., FIDELIS, M. Z., FÁVARO, Y. B., RIBEIRO, M. A., CHAVES, E. S. & LENZI, E. K. 2020. Caffeine adsorption onto Bentonite clay in suspension and immobilized. *Braz. arch. biol. technol,* 63.

LI, J. & ZHANG, H. 2017. Factors influencing adsorption and desorption of trimethoprim on marine sediments: mechanisms and kinetics. *Environ Sci Pollut Res Int,* 24**,** 21929-21937.

LI, Z., HONG, H., LIAO, L., ACKLEY, C. J., SCHULZ, L. A., MACDONALD, R. A., MIHELICH, A. L. & EMARD, S. M. 2011. A mechanistic study of ciprofloxacin removal by kaolinite. *Colloids Surf B Biointerfaces,* 88**,** 339-344.

LI, Z., SCHULZ, L., ACKLEY, C. & FENSKE, N. 2010. Adsorption of tetracycline on kaolinite with pH-dependent surface charges. *J Colloid Interface Sci,* 351**,** 254-260.

LIANG, Y., GUAN, T., ZHOU, Y., LIU, Y., XING, L., ZHENG, X., DAI, C., DU, P., RAO, T., ZHOU, L., YU, X., HAO, K., XIE, L. & WANG, G. 2013. Effect of mobile phase additives on qualitative and quantitative analysis of ginsenosides by liquid chromatography hybrid quadrupole-time of flight mass spectrometry. *Journal of Chromatography A,* 1297**,** 29-36.

LORPHENSRI, O., INTRAVIJIT, J., SABATINI, D. A., KIBBEY, T. C. G., OSATHAPHAN, K. & SAIWAN, C. 2006. Sorption of acetaminophen, 17 α-ethynyl estradiol, nalidixic acid, and norfloxacin to silica, alumina, and a hydrophobic medium. *Water research (Oxford),* 40**,** 1481-1491.

LUNDANES, E., REUBSAET, L. & GREIBROKK, T. 2014. *Chromatography : basic principles, sample preparations and related methods,* Weinheim, Wiley-VCH.

LUO, T., XU, J., CHENG, W., ZHOU, L., MARSAC, R., WU, F., BOILY, J.-F. & HANNA, K. 2022. Interactions of Anti-Inflammatory and Antibiotic Drugs at Mineral Surfaces Can Control Environmental Fate and Transport. *Environ Sci Technol,* 56**,** 2378-2385.

MA, C. & EGGLETON, R. A. 1999. Cation Exchange Capacity of Kaolinite. *Clays and clay minerals,* 47**,** 174-180.

MAGED, A., DISSANAYAKE, P. D., YANG, X., PATHIRANNAHALAGE, C., BHATNAGAR, A. & OK, Y. S. 2021. New mechanistic insight into rapid adsorption of pharmaceuticals from water utilizing activated biochar. *Environmental research,* 202**,** 111693-111693.

MARANHO, L. A., BAENA-NOGUERAS, R. M., LARA-MARTÍN, P. A., DELVALLS, T. A. & MARTÍN-DÍAZ, M. L. 2014. Bioavailability, oxidative stress, neurotoxicity and genotoxicity of pharmaceuticals bound to marine sediments. The use of the polychaete Hediste diversicolor as bioindicator species. *Environ Res,* 134**,** 353-365.

MARQUES, B. S., FRANTZ, T. S., SANT'ANNA CADAVAL JUNIOR, T. R., DE ALMEIDA PINTO, L. A. & DOTTO, G. L. 2018. Adsorption of a textile dye onto piaçava fibers: kinetic, equilibrium, thermodynamics, and application in simulated effluents. *Environ Sci Pollut Res Int,* 26**,** 28584-28592.

MEIERJOHANN, A., KORTESMÄKI, E., BROZINSKI, J.-M. & KRONBERG, L. 2017. An online SPE LC-MS/MS method for the analysis of antibiotics in environmental water. *Environ Sci Pollut Res Int,* 24**,** 8692-8699.

NAM, S.-W., CHOI, D.-J., KIM, S.-K., HER, N. & ZOH, K.-D. 2014. Adsorption characteristics of selected hydrophilic and hydrophobic micropollutants in water using activated carbon. *J Hazard Mater,* 270**,** 144-152.

NATIONAL LIBRARY OF MEDICINE 2021. PubChem.

NESSE, W. D. 2000. *Introduction to mineralogy,* New York, Oxford University Press.

NG, J. C. Y., CHEUNG, W. H. & MCKAY, G. 2002. Equilibrium Studies of the Sorption of Cu(II) Ions onto Chitosan. *J Colloid Interface Sci,* 255**,** 64-74.

NÄSLUND, J., HEDMAN, J. E. & AGESTRAND, C. 2008. Effects of the antibiotic ciprofloxacin on the bacterial community structure and degradation of pyrene in marine sediment. *Aquat Toxicol,* 90**,** 223-227.

PAROLINI, M., BINELLI, A., MATOZZO, V. & MARIN, M. G. 2010. Persistent organic pollutants in sediments from the Lagoon of Venice—a possible hazard for sediment-dwelling organisms. *Journal of soils and sediments,* 10**,** 1362-1379.

PAROLO, M. E., AVENA, M. J., PETTINARI, G. R. & BASCHINI, M. T. 2012. Influence of Ca2+ on tetracycline adsorption on montmorillonite. *J Colloid Interface Sci,* 368**,** 420-426.

PATEL, M., KUMAR, R., KISHOR, K., MLSNA, T., PITTMAN, C. U. & MOHAN, D. 2019. Pharmaceuticals of Emerging Concern in Aquatic Systems: Chemistry, Occurrence, Effects, and Removal Methods. *Chem. Rev,* 119**,** 3510-3673.

PAVLOVIC, D. M., CURKOVIC, L., GRCIC, I., SIMIC, I. & ZUPAN, J. 2017. Isotherm, kinetic, and thermodynamic study of ciprofloxacin sorption on sediments. *Environ Sci Pollut Res Int,* 24**,** 10091-10106.

PEREIRA, C. D. S., MARANHO, L. A., CORTEZ, F. S., PUSCEDDU, F. H., SANTOS, A. R., RIBEIRO, D. A., CESAR, A. & GUIMARÃES, L. L. 2016. Occurrence of pharmaceuticals and cocaine in a Brazilian coastal zone. *Sci Total Environ,* 548-549**,** 148-154.

PI, K., XIA, M., WU, P., YANG, M., CHEN, S., LIU, D. & GERSON, A. R. 2015. Effect of oxidative modification of activated carbon for the adsorption behavior of nicotine. *Journal of industrial and engineering chemistry (Seoul, Korea),* 31**,** 112-117.

POOLE, C. F. 2003. *The essence of chromatography,* Amsterdam, Elsevier.

POULIQUEN, H. & LE BRIS, H. 1996. Sorption of oxolinic acid and oxytetracycline to marine sediments. *Chemosphere (Oxford),* 33**,** 801-815.

PUTRO, J. N., JU, Y.-H., SOETAREDJO, F. E., SANTOSO, S. P. & ISMADJI, S. 2021. *Biosorption of dyes,* Amsterdam, Netherlands :.

QIANG, Z. & ADAMS, C. 2004. Potentiometric determination of acid dissociation constants (p Ka) for human and veterinary antibiotics. *Water Res,* 38**,** 2874-2890.

RAKIĆ, V., RAJIĆ, N., DAKOVIĆ, A. & AUROUX, A. 2013. The adsorption of salicylic acid, acetylsalicylic acid and atenolol from aqueous solutions onto natural zeolites and clays: Clinoptilolite, bentonite and kaolin. *Microporous and mesoporous materials,* 166**,** 185-194.

RATEEV, M. A., SADCHIKOVA, T. A. & SHABROVA, V. P. 2011. Clay minerals in recent sediments of the World Ocean and their relation to types of lithogenesis. *Lithology and mineral resources,* 43**,** 125-135.

REVELLAME, E. D., FORTELA, D. L., SHARP, W., HERNANDEZ, R. & ZAPPI, M. E. 2020. Adsorption kinetic modeling using pseudo-first order and pseudo-second order rate laws: A review. *Cleaner Engineering and Technology,* 1**,** 100032.

SCHOONHEYDT, R. A., JOHNSTON, C. T. & BERGAYA, F. 2018. Clay Minerals and their surfaces. *Surface and Interface Chemistry of Clay Minerals.* Elsevier Ltd.

SHIKUKU, V. O., ZANELLA, R., KOWENJE, C. O., DONATO, F. F., BANDEIRA, N. M. G. & PRESTES, O. D. 2018. Single and binary adsorption of sulfonamide antibiotics onto iron-modified clay: linear and nonlinear isotherms, kinetics, thermodynamics, and mechanistic studies. *Applied water science,* 8**,** 1-12.

SILVA, B., MARTINS, M., ROSCA, M., ROCHA, V., LAGO, A., NEVES, I. C. & TAVARES, T. 2020. Waste-based biosorbents as cost-effective alternatives to commercial adsorbents for the retention of fluoxetine from water. *Separation and purification technology,* 235**,** 116139.

SIMS, R. A., HARMER, S. L. & QUINTON, J. S. 2019. The role of physisorption and chemisorption in the oscillatory adsorption of organosilanes on aluminium oxide. *Polymers (Basel),* 11**,** 410.

SINGH, N. B., NAGPAL, G., AGRAWAL, S. & RACHNA 2018. Water purification by using Adsorbents: A Review. *Environmental technology & innovation,* 11**,** 187-240.

SONG, Y., SACKEY, E. A., WANG, H. & WANG, H. 2019. Adsorption of oxytetracycline on kaolinite. *PloS one,* 14**,** e0225335-e0225335.

SPIESS, A.-N. & NEUMEYER, N. 2010. An evaluation of R2 as an inadequate measure for nonlinear models in pharmacological and biochemical research: A Monte Carlo approach. *BMC Pharmacol,* 10**,** 6-6.

STACKELBERG, P. E., GIBS, J., FURLONG, E. T., MEYER, M. T., ZAUGG, S. D. & LIPPINCOTT, R. L. 2007. Efficiency of conventional drinking-water-treatment processes in removal of pharmaceuticals and other organic compounds. *Sci Total Environ,* 377**,** 255-272.

STUMM, W. & MORGAN, J. J. 1996. *Aquatic chemistry : chemical equilibria and rates in natural waters,* New York, Wiley.

SUN, K., SHI, Y., WANG, X., RASMUSSEN, J., LI, Z. & ZHU, J. 2017. Organokaolin for the uptake of pharmaceuticals diclofenac and chloramphenicol from water. *Chemical engineering journal (Lausanne, Switzerland : 1996),* 330**,** 1128-1136.

SAADI, R., SAADI, Z., FAZAELI, R. & FARD, N. E. 2015. Monolayer and multilayer adsorption isotherm models for sorption from aqueous media. *The Korean journal of chemical engineering,* 32**,** 787-799.

THE NORWEGIAN MEDICINES AGENCY 2020. Definisjon på ulike typer legemidler.

TRAN, H. N., YOU, S.-J., HOSSEINI-BANDEGHARAEI, A. & CHAO, H.-P. 2017. Mistakes and inconsistencies regarding adsorption of contaminants from aqueous solutions: A critical review. *Water Res,* 120**,** 88-116.

UMPUCH, C. & SAKAEW, S. 2013. Removal of methyl orange from aqueous solutions by adsorption using chitosan intercalated montmorillonite. *Wārasān Songkhlā Nakharin,* 35**,** 451-459.

UNESCO, H. 2017. Pharmaceuticals in the aquatic environment of the Baltic Sea region - A status report. *UNESCO Emerging Pollutants in Water Series.* Paris: UNESCO.

VEERASINGAM, S., VENKATACHALAPATHY, R. & RAMKUMAR, T. 2014. Distribution of clay minerals in marine sediments off Chennai, Bay of Bengal, India : Indicators of sediment sources and transport processes. *International Journal of Sediment Research,* 29**,** 11-23.

VERLICCHI, P., AL AUKIDY, M. & ZAMBELLO, E. 2012. Occurrence of pharmaceutical compounds in urban wastewater: Removal, mass load and environmental risk after a secondary treatment—A review. *Sci Total Environ,* 429**,** 123-155.

WANG, H., XI, H., XU, L., JIN, M., ZHAO, W. & LIU, H. 2021. Ecotoxicological effects, environmental fate and risks of pharmaceutical and personal care products in the water environment: A review. *The Science of the total environment,* 788**,** 147819-147819.

WANG, J. & GUO, X. 2020a. Adsorption isotherm models: Classification, physical meaning, application and solving method. *Chemosphere (Oxford),* 258**,** 127279-127279.

WANG, J. & GUO, X. 2020b. Adsorption kinetic models: Physical meanings, applications, and solving methods. *J Hazard Mater,* 390**,** 122156-122156.

WANG, R., ZHANG, L., ZHANG, Z. & TIAN, Y. 2016. Comparison of ESI– and APCI–LC–MS/MS methods: A case study of levonorgestrel in human plasma. *J Pharm Anal,* 6**,** 356-362.

WANG, W. & WANG, J. 2018. Different partition of polycyclic aromatic hydrocarbon on environmental particulates in freshwater: Microplastics in comparison to natural sediment. *Ecotoxicol Environ Saf,* 147**,** 648-655.

WEST, D. M., HOLLER, F. J., CROUCH, S. R. & SKOOG, D. A. 2014. *Fundamentals of analytical chemistry,* Boston, Brooks/Cole Cengage Learning.

WHO 2012. Pharmaceuticals in drinking-water.

WILLIAMS, A. J., GRULKE, C. M., EDWARDS, J., MCEACHRAN, A. D., MANSOURI, K., BAKER, N. C., PATLEWICZ, G., SHAH, I., WAMBAUGH, J. F., JUDSON, R. S. & RICHARD, A. M. 2017. The CompTox Chemistry Dashboard: a community data resource for environmental chemistry. *J Cheminform.* Cham: Cham: Springer International Publishing.

WU, M., ZHAO, S., JING, R., SHAO, Y., LIU, X., LV, F., HU, X., ZHANG, Q., MENG, Z. & LIU, A. 2019. Competitive adsorption of antibiotic tetracycline and ciprofloxacin on montmorillonite. *Applied clay science,* 180**,** 105175.

WU, X., XIAO, B., LI, R., WANG, C., HUANG, J. & WANG, Z. 2011. Mechanisms and Factors Affecting Sorption of Microcystins onto Natural Sediments. *Environ. Sci. Technol,* 45**,** 2641-2647.

YAMAMOTO, H., TAKEMOTO, K., TAMURA, I., SHIN-OKA, N., NAKANO, T., NISHIDA, M., HONDA, Y., MORIGUCHI, S. & NAKAMURA, Y. 2016. Contribution of inorganic and organic components to sorption of neutral and ionizable pharmaceuticals by sediment/soil. *Environ Sci Pollut Res Int,* 25**,** 7250-7261.

YUAN, L., ZHANG, D., JEMAL, M. & AUBRY, A.-F. 2012. Systematic evaluation of the root cause of non-linearity in liquid chromatography/tandem mass spectrometry bioanalytical assays and strategy to predict and extend the linear standard curve range. *Rapid Commun. Mass Spectrom,* 26**,** 1465-1474.

ZHOU, D., CHEN, B., WU, M., LIANG, N., ZHANG, D., LI, H. & PAN, B. 2014. Ofloxacin sorption in soils after long-term tillage: The contribution of organic and mineral compositions. *Sci Total Environ,* 497-498**,** 665-670.

ZUTHER, M., BROCKAMP, O. & CLAUER, N. 2000. Composition and origin of clay minerals in Holocene sediments from the south-eastern North Sea. *Sedimentology,* 47**,** 119-134.

7 Appendixes

7.1 Material and method data

Table 15: Overview of pharmaceutical standards

Compound	Solvent
Atenolol	Ethanol
Atenolol_d7	Methanol
Caffeine	Ethanol/methanol/Milli-Q
Ciprofloxacin	0,1 M HCl
Ciprofloxacin_d8	Methanol
Citalopram	Methanol
Diclofenac	Ethanol
Diclofenac_d4	Methanol
Fluoxetine	Methanol
Fluoxetine_d6	Methanol
Nicotine	Ethanol
Oxolinic acid	0,5 M NaOH
Oxytetracycline	MeOH
Paracetamol	Ethanol
Paracetamol_d4	Methanol
Tetracycline	Methanol
Tetracycline_d6	Methanol
Trimethoprim	Methanol

Table 16: Column and mobile phase details for the different sample batches

Sample batch	Column	Mobile phase pH	Dilution of samples
5 °C kinetics	Agilent Poroshell 120 EC-C18 2.1x50mm, 2.7um	8,5	1:10 in Milli-Q
5 °C isotherm	Agilent Poroshell 120 EC-C18 2.1x50mm, 2.7um	7,3	1:10 in Milli-Q
9 °C kinetics	Agilent Poroshell 120 EC-C18 2.1x50mm, 1.9um	8,5	No, pure seawater

| 9 °C isotherm | Agilent Poroshell HPH-C18 2.1x50mm, 1.9um | 8,5 | 1:10 in Milli-Q |
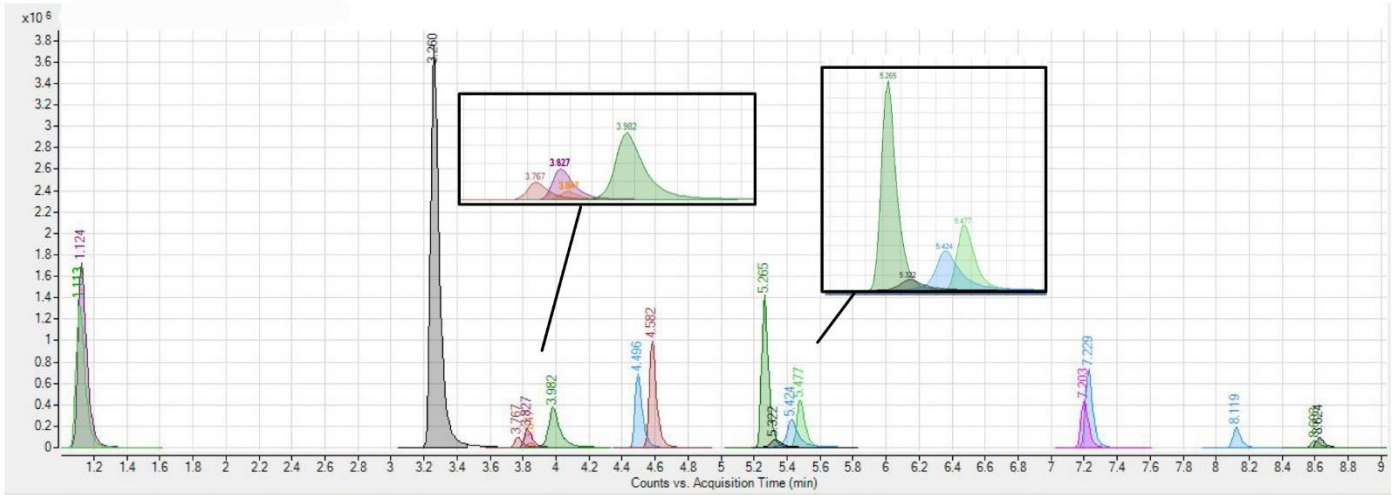
Figure 24: Total ion chromatogram of quantifier ions. Retention times correspond to the values in table 9

7.2 Calibration curves

Calibration curves in figure 25 to 36 are from the run of the 4 °C kinetics sample batch
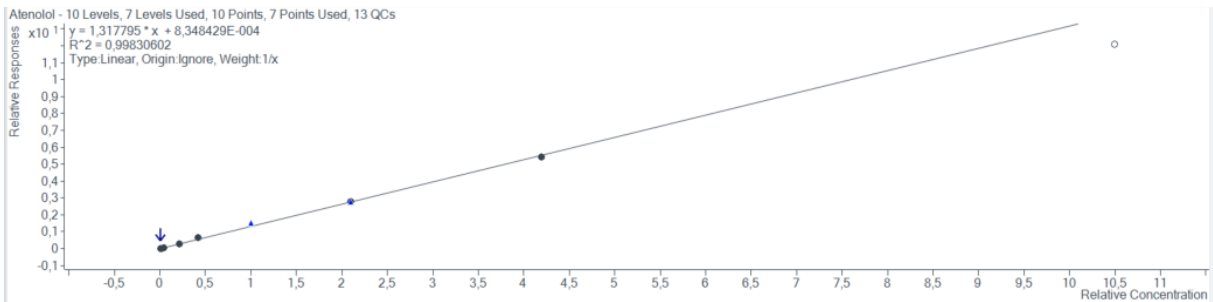
Figure 25: Calibration curve for atenolol (with IS atenolol_d7)
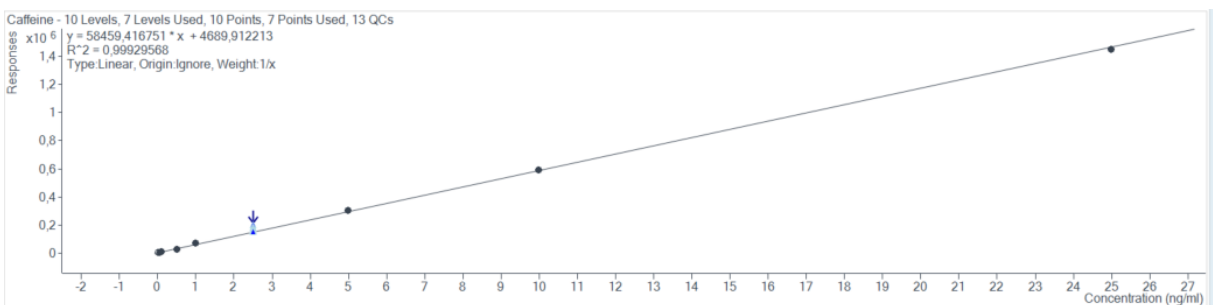
Figure 26: Calibration curve for caffeine
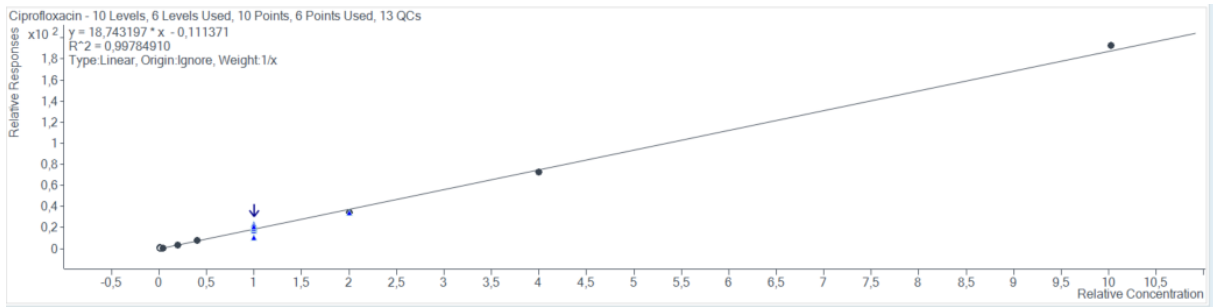
Figure 27: Calibration curve for ciprofloxacin (with IS ciprofloxacin_d8)
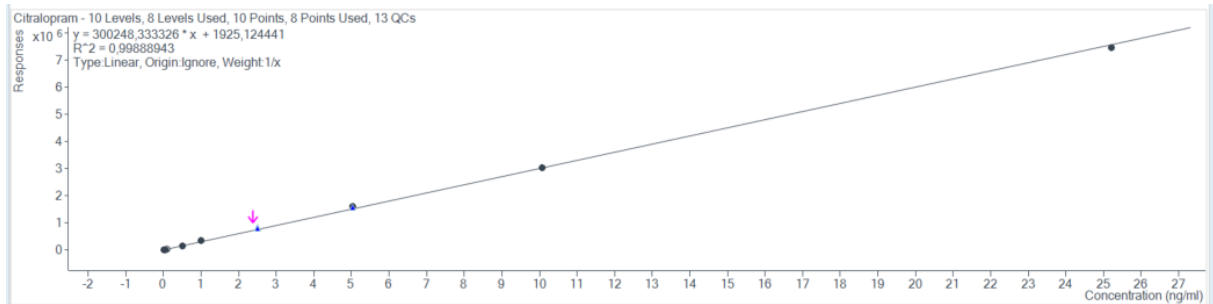
Figure 28: Calibration curve for citalopram
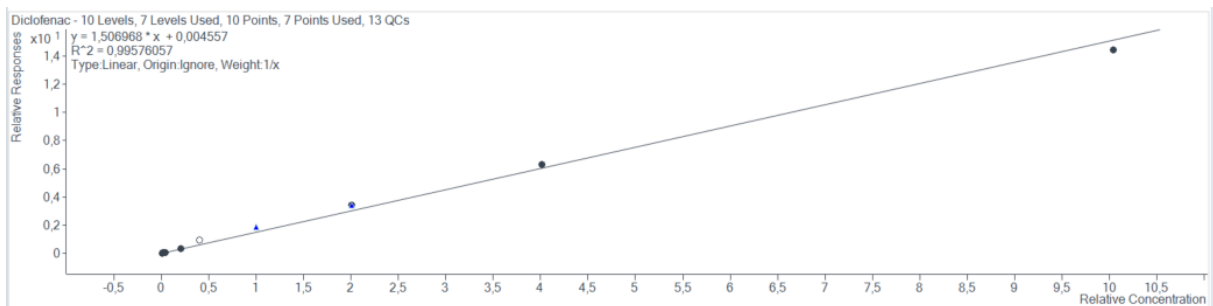
Figure 29: Calibration curve for diclofenac (with IS diclofenac_d4)
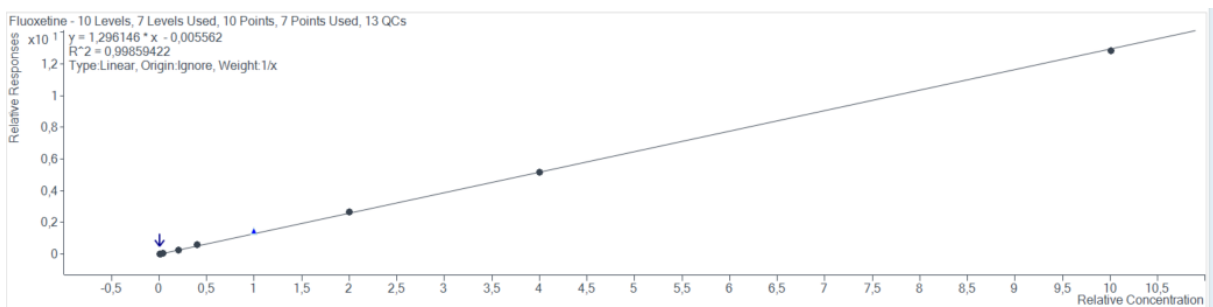
Figure 30: Calibration curve for fluoxetine (with IS fluoxetine_d6)
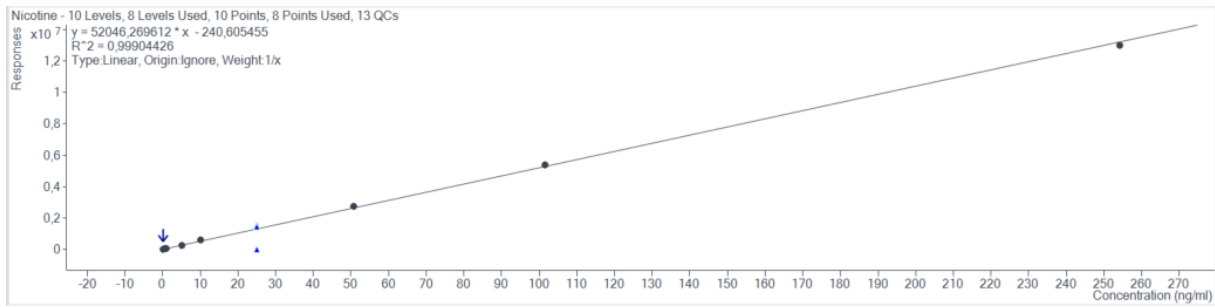
Figure 31: Calibration curve for nicotine
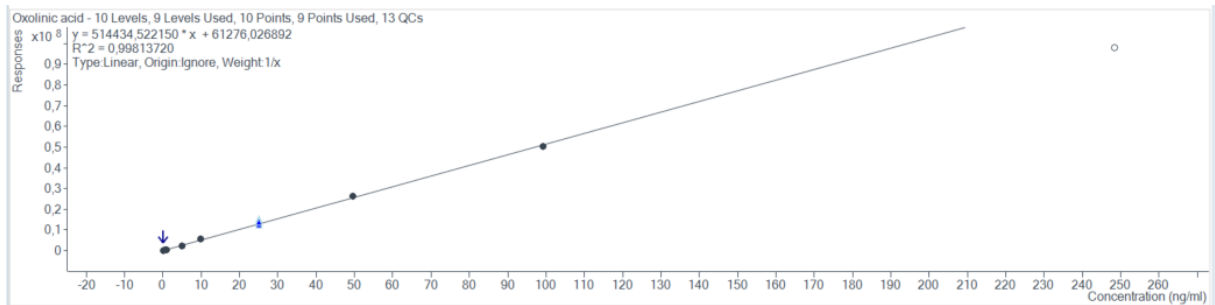
Figure 32: calibration curve for oxolinic acid
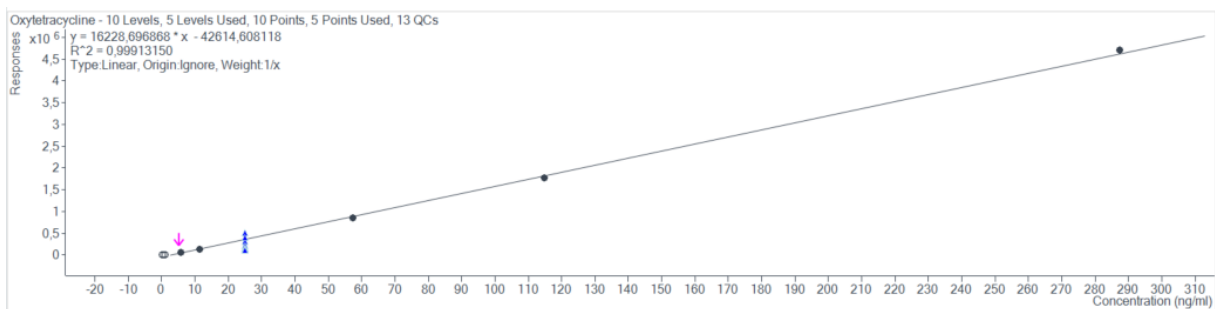
Figure 33: Calibration curve for oxytetracycline
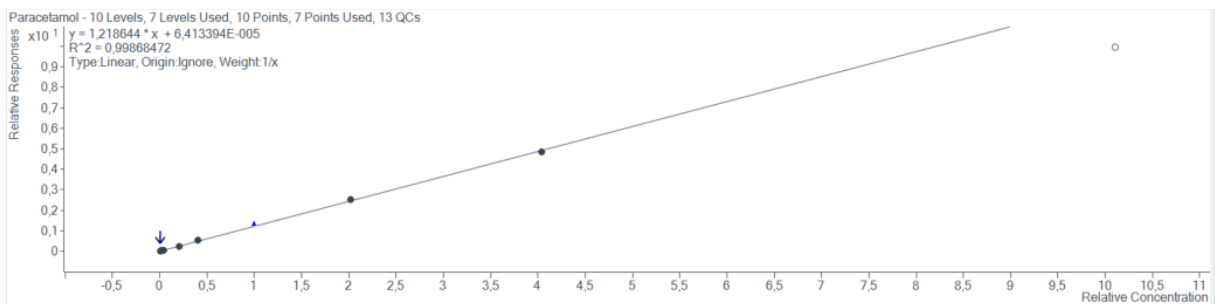
Figure 34: Calibration curve for paracetamol (with IS paracetamol_d4)
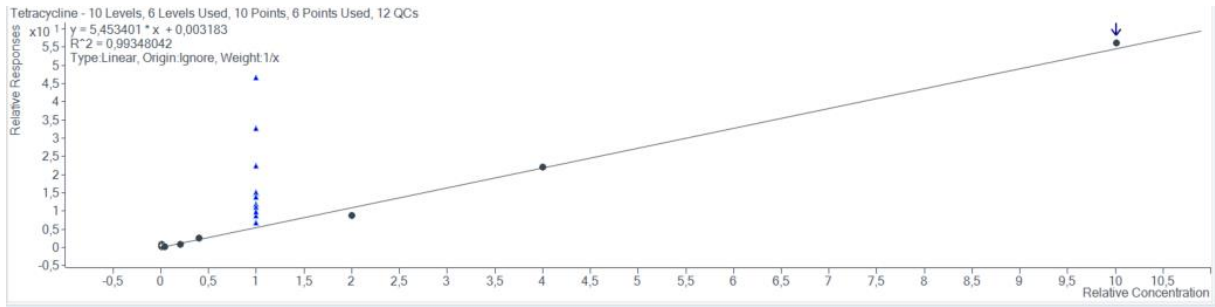
Figure 35: Calibration curve for tetracycline (with IS tetracycline_d6)
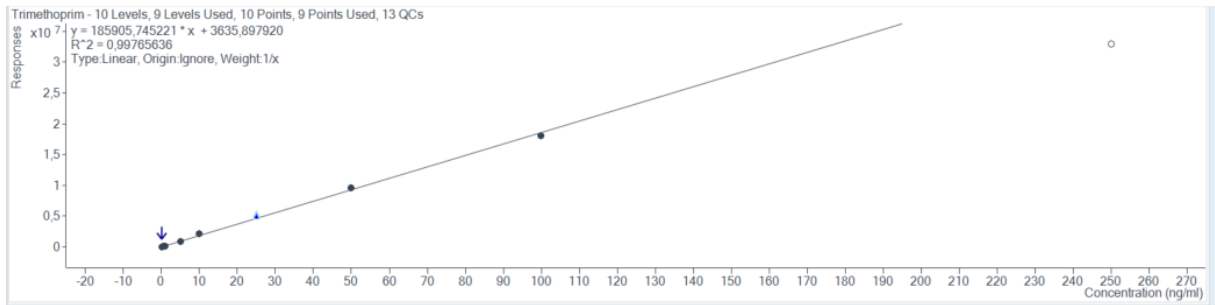
Figure 36: Calibration curve for trimethoprim

7.3 QC data

Table 17: 9 °C kinetics QC data

Compound	Linear range (ng/mL)	R^2	LOQ* (ng/mL)	Linear curve parameters (origin and weighing)
Atenolol (w/IS)	0,1 – 100	0,999	0,1	Ignore 1/x
Caffeine	0,05 – 10*	0,997	0,5	Include 1/x
Ciprofloxacin (w/IS)	0,1 - 100	0,999	0,1	Ignore 1/x
Citalopram	0,05 – 25*	0,998	0,5	Ignore 1/x
Diclofenac (w/IS)	0,5 - 250	0,999	0,5	Ignore 1/x
Fluoxetine (w/IS)	0,1 - 250	0,999	1	Ignore none
Nicotine	0,1 - 250	0,999	0,1	Ignore 1/x
Oxolinic acid	0,1 – 100	0,995	0,1	Ignore 1/x
Oxytetracycline	0,5 – 250	0,994	0,5	Ignore 1/x
Paracetamol (w/IS)	0,5 - 250	0,999	0,5	Ignore 1/x
Tetracycline (w/IS)	0,5 - 250	0,996	0,5	Ignore 1/x
Trimethoprim	0,1 - 100	0,997	0,1	Ignore 1/x

*Other concentrations of caffeine and citalopram were added to the calibration standards, therefore their linear range is different

Table 18: 4 °C kinetic QC data

Compound	Linear range (ng/mL)	R^2	LOQ* (ng/mL)	Linear curve parameters (origin and weighing)
Atenolol (w/IS)	0,1 - 100	0,998	0,1	Ignore 1/x
Caffeine	0,05 – 25*	0,999	0,05	Ignore 1/x
Ciprofloxacin (w/IS)	1– 250	0,998	1	Ignore 1/x
Citalopram	0,005 – 25*	0,999	0,005	Ignore 1/x
Diclofenac (w/IS)	0,1 - 250	0,998	0,1	Ignore 1/x
Fluoxetine (w/IS)	0,5 – 250	0,999	0,5	Ignore 1/x
Nicotine	0,1 - 250	0,999	0,1	Ignore 1/x
Oxolinic acid	0,02 - 100	0,998	0,1	Ignore 1/x
Oxytetracycline	5 - 250	0,999	5	Ignore 1/x
Paracetamol (w/IS)	0,1 - 100	0,999	0,1	Ignore 1/x
Tetracycline (w/IS)	1 - 250	0,993	5	Ignore 1/x
Trimethoprim	0,02 - 100	0,998	0,02	Ignore 1/x

*Other concentrations of caffeine and citalopram were added to the calibration standards, therefore their linear range is different

Table 19: Isotherm 9 ℃ QC data

Compound	Linear range (ng/mL)	R2	LOQ (ng/mL)	Calibration parameters (origin and weighing)
Ciprofloxacin	0,5 – 100	0,993	0,5	Ignore 1/x
Citalopram	0,05 – 25 *	0,994	0,5	Include 1/x
Fluoxetine	0,5 - 250	0,995	0,5	Ignore 1/x

Table 20: Isotherm 4 ℃ QC data

Compound	Linear range (ng/mL)	R2	LOQ (ng/mL)	Calibration parameters (origin and weighing)
Ciprofloxacin	0,5 - 250	0,998	0,5	Ignore 1/x
Citalopram	0,05 - 25	0,998	0,05	Ignore 1/x
Fluoxetine	1 - 250	0,999	1	Ignore None

7.4 Experimental data, kinetics experiments

Table 21: Atenolol raw kinetics data

4 °C

Time	Triplicate	CTRL	5 g/L	10 g/L
		Concentration (ng/mL)		
1	1	46,5	44,8	44,4
	2	45,1	52,6	44,2
	3	47,8	45,4	43,9
3	1	46,2	45,1	41,1
	2	45,5	44,2	44,5
	3	43,8	45,4	46,0
6	1	47,8	46,3	44,7
	2	44,2	45,3	43,7
	3	44,4	45,9	45,5
24	1	44,4	45,8	44,8
	2	44,9	44,3	44,1
	3	45,0	45,3	45,3
48	1	46,1	46,1	44,9
	2	45,1	45,0	45,1
	3	44,9	45,5	45,0
72	1	46,6	44,7	44,8
	2	44,9	45,0	44,6
	3	45,6	45,2	46,0
144	1	47,0	46,6	44,2
	2	44,9	45,2	44,7
	3	44,8	45,2	45,6
240	1	44,7	43,3	43,1
	2	43,9	43,8	42,9
	3	43,2	41,7	44,5

RSD

Time	CTRL	5 g/L	10 g/L
1	2,9 %	9,1 %	0,7 %
3	2,7 %	1,3 %	5,7 %
6	4,4 %	1,1 %	2,0 %
24	0,6 %	1,6 %	1,3 %
48	1,5 %	1,2 %	0,1 %
72	1,8 %	0,6 %	1,7 %
144	2,6 %	1,8 %	1,6 %
240	1,8 %	2,6 %	2,1 %

9 °C

Time	Triplicate	CTRL	5 g/L	10 g/L
		Concentration (ng/mL)		
1	1	41,4	43,6	43,8
	2	44,9	42,5	44,9
	3	41,1	45,2	44,5
3	1	43,7	45,2	43,4
	2	43,4	43,1	43,7
	3	39,9	44,0	44,3
6	1	42,6	44,1	44,7
	2	42,4	41,9	44,4
	3	38,3	44,0	43,7
24	1	43,4	45,2	43,5
	2	42,3	44,5	44,5
	3	41,5	45,7	46,4
48	1	44,3	45,7	44,9
	2	43,3	44,6	45,9
	3	41,8	45,6	45,8
72	1	44,0	47,0	45,9
	2	45,1	45,2	45,5
	3	42,6	46,0	45,2
144	1	44,9	46,2	45,5
	2	44,4	45,7	46,0
	3	42,8	47,2	45,2
240	1	27,1	27,9	28,0
	2	27,1	27,3	29,0
	3	26,3	28,3	32,3

RSD

Time	CTRL	5 g/L	10 g/L
1	5,0 %	3,1 %	1,3 %
3	4,9 %	2,3 %	1,1 %
6	5,9 %	2,8 %	1,2 %
24	2,2 %	1,4 %	3,3 %
48	2,9 %	1,3 %	1,2 %
72	2,9 %	2,0 %	0,8 %
144	2,5 %	1,7 %	0,9 %
240	1,7 %	1,8 %	7,6 %

Caffeine

Table 22: Caffeine raw kinetics data

4 °C

		Concentration (ng/mL)		
Time	Triplicate	CTRL	5 g/L	10 g/L
1	1	52,1	48,9	24,9
	2	44,7	32,4	25,0
	3	56,6	49,8	34,2
3	1	43,7	41,9	23,5
	2	39,2	38,2	23,7
	3	38,2	29,6	25,5
6	1	39,0	29,7	24,2
	2	40,3	36,9	25,8
	3	39,7	32,1	23,3
24	1	42,2	34,3	36,6
	2	44,9	37,2	30,7
	3	46,2	29,2	24,0
48	1	60,9	32,9	27,0
	2	44,5	39,5	23,1
	3	49,4	34,0	24,9
72	1	72,3	42,6	25,6
	2	63,2	40,7	27,7
	3	40,1	30,1	26,0
144	1	39,2	32,9	28,2
	2	47,4	32,4	27,7
	3	38,7	32,4	33,1
240	1	40,5	29,8	26,6
	2	37,9	30,9	24,7
	3	40,2	31,1	24,3

RSD			
Time	CTRL	5 g/L	10 g/L
1	11,7 %	22,4 %	19,2 %
3	7,3 %	17,3 %	4,6 %
6	1,7 %	11,2 %	5,1 %
24	4,6 %	12,1 %	20,6 %
48	16,3 %	10,1 %	7,8 %
72	28,4 %	17,9 %	4,3 %
144	11,6 %	0,9 %	10,0 %
240	3,7 %	2,3 %	4,8 %

9 °C

		Concentration (ng/mL)		
Time	Triplicate	CTRL	5 g/L	10 g/L
1	1	42,8	33,3	31,7
	2	42,5	30,6	32,4
	3	40,9	37,2	31,7
3	1	41,7	37,0	30,9
	2	42,8	36,9	31,3
	3	40,0	37,9	30,3
6	1	42,4	36,9	31,7
	2	45,9	35,5	31,9
	3	44,2	39,0	34,9
24	1	43,6	36,3	28,2
	2	42,3	36,7	31,1
	3	41,7	39,3	33,9
48	1	42,8	38,0	31,9
	2	46,1	40,6	32,1
	3	42,0	36,8	31,0
72	1	47,2	38,5	34,2
	2	42,8	37,8	30,4
	3	44,6	40,4	34,1
144	1	42,2	41,7	35,8
	2	41,3	36,7	32,5
	3	41,0	39,3	34,2
240	1	42,7	41,2	32,2
	2	43,5	41,7	32,3
	3	44,6	39,0	33,0

RSD			
Time	CTRL	5 g/L	10 g/L
1	2,4 %	9,9 %	1,2 %
3	3,4 %	1,5 %	1,8 %
6	3,9 %	4,8 %	5,5 %
24	2,3 %	4,4 %	9,1 %
48	5,0 %	4,9 %	1,9 %
72	4,9 %	3,5 %	6,6 %
144	1,6 %	6,4 %	4,8 %
240	2,2 %	3,6 %	1,3 %

Table 23: Ciprofloxacin raw kinetics data

4 °C

Time	Triplicate	CTRL	Concentration (ng/mL) 5 g/L	10 g/L
1	1	49,1	25,5	13,2
	2	40,9	29,8	15,1
	3	42,4	30,1	12,2
3	1	38,6	17,6	13,2
	2	33,1	24,7	12,7
	3	35,2	23,8	12,4
6	1	40,4	16,6	15,3
	2	42,6	26,7	11,5
	3	35,4	21,0	13,6
24	1	37,1	25,2	9,8
	2	37,9	20,2	12,0
	3	32,9	17,3	10,2
48	1	45,9	16,0	14,8
	2	36,1	15,4	13,4
	3	29,5	19,8	13,2
72	1	43,7	18,9	13,6
	2	41,1	19,0	7,7
	3	38,4	14,2	15,3
144	1	40,0	19,9	12,4
	2	41,5	20,3	13,1
	3	36,2	16,1	13,2
240	1	40,2	18,6	7,3
	2	37,2	17,6	11,0
	3	36,6	22,9	10,3

Time	CTRL	RSD 5 g/L	10 g/L
1	9,9 %	9,0 %	10,9 %
3	7,8 %	17,5 %	3,2 %
6	9,4 %	23,8 %	14,3 %
24	7,5 %	19,1 %	11,0 %
48	22,2 %	14,1 %	6,5 %
72	6,4 %	15,6 %	32,7 %
144	7,0 %	12,4 %	3,3 %
240	5,1 %	14,3 %	20,5 %

9 °C

Time	Triplicate	Concentration (ng/mL) CTRL	5 g/L	10 g/L
1	1	52,5	31,1	17,9
	2	51,3	25,2	18,3
	3	48,7	36,0	18,1
3	1	53,5	32,6	16,4
	2	53,6	33,6	17,5
	3	48,4	35,9	15,2
6	1	52,6	29,9	15,6
	2	44,9	32,2	17,3
	3	41,4	31,3	14,0
24	1	54,7	27,2	12,7
	2	52,5	31,5	15,1
	3	50,3	32,8	13,1
48	1	53,4	26,8	13,2
	2	44,1	25,3	14,5
	3	48,5	29,7	13,9
72	1	46,8	28,7	11,3
	2	50,6	28,4	12,3
	3	41,5	28,5	10,4
144	1	47,9	25,0	10,1
	2	51,6	26,2	12,3
	3	48,3	28,3	10,8
240	1	52,8	21,7	10,5
	2	49,4	21,6	12,2
	3	44,3	26,7	12,1

Time	CTRL	RSD 5 g/L	10 g/L
1	3,8 %	17,6 %	1,2 %
3	5,7 %	5,0 %	7,1 %
6	12,4 %	3,7 %	10,7 %
24	4,2 %	9,5 %	9,5 %
48	9,6 %	8,1 %	4,5 %
72	9,9 %	0,5 %	8,2 %
144	4,2 %	6,3 %	9,8 %
240	8,7 %	12,6 %	7,9 %

Table 24: Citalopram raw kinetics data

4 °C						9 °C				
		Concentration (ng/mL)						Concentration (ng/mL)		
			5						5	
Time	Triplicate	CTRL	g/L	10 g/L		Time	Triplicate	CTRL	g/L	10 g/L
1	1	36,7	10,1	2,4		1	1	32,9	8,3	3,8
	2	22,0	6,6	2,3			2	31,1	8,0	3,4
	3	33,0	10,9	2,8			3	30,8	7,2	3,2
3	1	25,6	6,4	1,3		3	1	33,0	6,9	2,7
	2	28,7	6,1	1,3			2	39,2	6,1	2,5
	3	25,2	4,7	1,7			3	32,5	6,3	2,5
6	1	25,3	3,5	1,0		6	1	32,8	6,7	1,7
	2	26,7	4,1	1,2			2	33,3	5,1	2,2
	3	24,7	3,3	1,1			3	31,4	5,9	2,0
24	1	30,7	3,0	1,0		24	1	35,5	4,9	1,5
	2	28,6	2,6	0,8			2	32,8	4,3	1,5
	3	30,8	2,4	0,7			3	33,5	4,3	1,4
48	1	29,2	2,2	0,6		48	1	34,8	4,4	1,3
	2	26,6	2,0	0,5			2	31,4	3,6	1,4
	3	23,8	1,7	0,7			3	31,4	3,1	1,0
72	1	38,7	2,9	0,5		72	1	37,0	4,0	1,0
	2	37,1	2,9	0,5			2	34,1	3,7	1,2
	3	28,0	2,1	0,5			3	34,2	3,7	1,0
144	1	26,9	2,1	0,6		144	1	33,4	3,6	1,0
	2	29,8	1,1	0,6			2	33,5	3,1	1,1
	3	29,0	1,8	0,6			3	30,1	3,2	0,9
240	1	29,0	1,8	0,4		240	1	32,0	3,5	0,9
	2	26,2	1,7	0,5			2	31,5	2,6	1,0
	3	32,3	2,4	0,4			3	33,8	2,9	1,0

	RSD					RSD		
Time	CTRL	5 g/L	10 g/L		Time	CTRL	5 g/L	10 g/L
1	25,0 %	25,1 %	11,9 %		1	3,6 %	6,9 %	8,7 %
3	7,1 %	15,8 %	14,3 %		3	10,7 %	6,2 %	5,7 %
6	4,0 %	11,8 %	7,9 %		6	3,1 %	13,5 %	13,2 %
24	4,2 %	10,6 %	17,8 %		24	4,2 %	7,9 %	3,1 %
48	10,3 %	11,2 %	15,4 %		48	6,0 %	17,8 %	15,4 %
72	16,6 %	16,7 %	3,5 %		72	4,7 %	4,3 %	8,2 %
144	5,3 %	31,2 %	5,8 %		144	5,9 %	8,2 %	5,3 %
240	10,5 %	19,7 %	20,0 %		240	3,8 %	13,9 %	8,9 %

Table 25: Diclofenac raw kinetics data

4 °C					9 °C				
		Concentration (ng/mL)					Concentration (ng/mL)		
Time	Triplicate	CTRL	5 g/L	10 g/L	Time	Triplicate	CTRL	5 g/L	10 g/L
1	1	60,0	58,3	56,9	1	1	35,6	39,0	39,7
	2	62,7	67,2	59,0		2	35,7	39,9	39,2
	3	62,5	57,7	56,1		3	33,1	37,8	38,2
3	1	64,3	59,2	51,8	3	1	35,5	38,2	40,0
	2	59,5	59,4	57,3		2	35,7	38,3	39,4
	3	56,6	58,6	61,6		3	33,0	39,6	40,2
6	1	60,1	54,4	58,7	6	1	36,1	41,1	38,2
	2	57,0	57,5	56,9		2	36,6	36,9	38,8
	3	55,5	52,1	59,2		3	33,6	39,7	37,9
24	1	57,9	59,3	57,4	24	1	34,3	39,2	39,7
	2	56,4	60,5	55,6		2	34,0	37,0	36,6
	3	56,5	55,5	58,0		3	34,5	39,6	39,9
48	1	62,9	57,6	59,8	48	1	36,3	38,1	38,9
	2	59,3	58,7	53,7		2	36,2	38,0	39,6
	3	59,1	55,4	56,1		3	34,6	36,9	40,2
72	1	55,5	55,1	53,5	72	1	37,1	37,9	38,2
	2	56,7	61,8	56,6		2	36,7	38,1	42,5
	3	57,9	55,5	58,7		3	35,8	38,5	41,3
144	1	61,2	56,0	55,0	144	1	37,5	40,5	40,9
	2	58,4	56,2	56,9		2	36,1	38,8	39,9
	3	54,4	58,7	59,0		3	34,2	39,1	38,7
240	1	55,7	53,6	55,3	240	1	23,4	26,3	25,8
	2	52,9	53,4	53,1		2	24,9	25,4	26,1
	3	55,8	54,1	58,4		3	23,9	26,1	29,2

		RSD					RSD		
Time	CTRL	5 g/L	10 g/L		Time	CTRL	5 g/L	10 g/L	
1	2,5 %	8,7 %	2,6 %		1	4,2 %	2,8 %	1,9 %	
3	6,5 %	0,7 %	8,6 %		3	4,4 %	2,0 %	1,1 %	
6	4,1 %	5,0 %	2,1 %		6	4,6 %	5,4 %	1,1 %	
24	1,5 %	4,5 %	2,2 %		24	0,7 %	3,7 %	4,7 %	
48	3,6 %	2,9 %	5,5 %		48	2,7 %	1,7 %	1,7 %	
72	2,1 %	6,6 %	4,7 %		72	1,8 %	0,9 %	5,5 %	
144	5,9 %	2,7 %	3,5 %		144	4,6 %	2,3 %	2,8 %	
240	3,0 %	0,7 %	4,8 %		240	3,0 %	1,8 %	6,9 %	

Table 26: Fluoxetine raw kinetics data

4 ℃						9 ℃				
		Concentration (ng/mL)						Concentration (ng/mL)		
Time	Triplicate	CTRL	5 g/L	10 g/L		Time	Triplicate	CTRL	5 g/L	10 g/L
1	1	17,7	12,8	6,1		1	1	13,3	8,0	6,0
	2	26,5	11,4	6,3			2	9,5	7,3	4,2
	3	22,3	13,9	6,2			3	9,5	4,2	4,0
3	1	22,8	11,2	5,3		3	1	13,2	6,4	4,9
	2	22,7	9,3	4,9			2	21,8	4,9	2,9
	3	21,5	10,0	4,8			3	14,9	4,9	5,2
6	1	21,6	8,1	4,1		6	1	12,1	6,6	2,1
	2	17,9	8,3	4,1			2	11,6	4,9	3,3
	3	20,3	7,2	4,1			3	11,9	4,5	2,2
24	1	20,3	8,2	5,0		24	1	16,0	5,7	2,8
	2	18,4	8,0	6,1			2	13,6	5,3	2,9
	3	20,9	7,7	4,1			3	18,6	4,2	3,0
48	1	25,1	8,9	5,1		48	1	14,4	6,3	2,7
	2	20,8	8,1	3,9			2	10,6	4,2	2,9
	3	20,8	9,3	3,6			3	10,9	3,3	1,7
72	1	16,6	6,8	3,8		72	1	14,2	6,0	2,4
	2	20,1	7,4	3,6			2	8,5	5,4	2,3
	3	21,5	7,0	4,7			3	16,5	2,6	1,4
144	1	19,5	7,3	4,1		144	1	12,6	5,7	1,8
	2	19,6	11,0	3,4			2	14,6	5,1	2,5
	3	18,3	9,0	4,0			3	9,0	4,6	2,4
240	1	22,2	6,0	7,9		240	1	12,7	7,5	2,6
	2	16,9	6,4	4,2			2	10,6	3,8	3,0
	3	19,4	8,3	4,2			3	14,4	5,5	3,5

	RSD					RSD		
Time	CTRL	5 g/L	10 g/L		Time	CTRL	5 g/L	10 g/L
1	19,8 %	9,6 %	1,6 %		1	20,2 %	31,5 %	23,2 %
3	3,3 %	9,5 %	5,6 %		3	27,4 %	16,1 %	29,4 %
6	9,3 %	7,6 %	0,4 %		6	2,3 %	21,6 %	27,9 %
24	6,7 %	3,2 %	19,4 %		24	15,4 %	15,5 %	3,7 %
48	11,0 %	6,9 %	18,4 %		48	17,7 %	33,0 %	27,1 %
72	13,0 %	4,9 %	14,6 %		72	31,6 %	39,2 %	26,3 %
144	3,7 %	20,2 %	10,7 %		144	23,5 %	10,8 %	16,1 %
240	13,8 %	18,2 %	40,0 %		240	15,1 %	33,3 %	15,6 %

Table 27: Nicotine raw kinetics data

4 °C					9 °C				
		Concentration (ng/mL)					Concentration (ng/mL)		
Time	Triplicate	CTRL	5 g/L	10 g/L	Time	Triplicate	CTRL	5 g/L	10 g/L
1	1	105,4	115,7	70,3	1	1	81,5	74,1	81,6
	2	87,6	74,5	70,3		2	80,8	72,8	83,9
	3	113,8	113,9	97,1		3	76,9	82,8	82,4
3	1	84,2	93,4	70,4	3	1	81,9	80,8	79,8
	2	72,5	90,5	70,9		2	81,2	82,2	81,5
	3	73,2	71,0	80,4		3	76,3	84,6	83,0
6	1	76,0	69,6	75,0	6	1	81,4	86,2	82,1
	2	80,3	89,2	74,8		2	82,2	78,4	82,7
	3	76,2	78,6	70,5		3	77,9	85,7	86,9
24	1	80,8	78,3	106,4	24	1	82,9	84,9	80,6
	2	86,5	84,7	81,8		2	80,5	80,7	80,1
	3	85,3	72,1	74,2		3	78,9	86,0	82,2
48	1	116,9	76,2	81,0	48	1	81,6	84,6	81,4
	2	88,1	97,1	70,1		2	81,8	82,1	82,0
	3	89,3	78,6	73,9		3	78,5	80,9	79,0
72	1	137,2	99,3	71,3	72	1	84,3	83,6	82,0
	2	122,6	98,8	81,2		2	81,6	82,0	83,6
	3	76,9	71,0	78,4		3	77,1	86,8	82,0
144	1	78,0	76,7	81,5	144	1	82,2	88,6	82,9
	2	90,7	75,0	82,3		2	80,1	79,9	83,6
	3	75,4	73,3	98,0		3	77,8	83,9	81,4
240	1	78,1	72,3	78,5	240	1	81,4	82,8	81,8
	2	73,8	74,0	68,3		2	79,8	84,3	82,0
	3	76,8	72,8	72,7		3	79,7	82,6	82,8

	RSD					RSD		
Time	CTRL	5 g/L	10 g/L		Time	CTRL	5 g/L	10 g/L
1	13,1 %	23,0 %	19,5 %		1	3,1 %	7,1 %	1,4 %
3	8,6 %	14,4 %	7,7 %		3	3,8 %	2,3 %	2,0 %
6	3,1 %	12,4 %	3,5 %		6	2,9 %	5,3 %	3,1 %
24	3,6 %	8,0 %	19,2 %		24	2,5 %	3,3 %	1,3 %
48	16,6 %	13,6 %	7,4 %		48	2,3 %	2,3 %	2,0 %
72	28,0 %	18,0 %	6,6 %		72	4,5 %	2,9 %	1,1 %
144	10,1 %	2,2 %	10,7 %		144	2,8 %	5,2 %	1,4 %
240	2,9 %	1,1 %	7,0 %		240	1,2 %	1,1 %	0,6 %

Table 28: Oxolinic acid raw kinetics data

4 °C

Time	Triplicate	CTRL	5 g/L	10 g/L
		Concentration (ng/mL)		
1	1	68,6	75,3	30,6
	2	50,6	42,3	33,5
	3	65,2	75,1	50,2
3	1	53,3	59,7	31,1
	2	46,6	55,7	31,2
	3	41,0	37,5	30,5
6	1	42,8	37,3	27,5
	2	47,3	46,7	29,1
	3	43,0	42,1	25,8
24	1	54,0	38,1	31,3
	2	60,0	40,9	20,5
	3	59,1	30,2	17,6
48	1	77,0	24,7	13,5
	2	55,0	34,8	12,3
	3	52,7	26,2	15,1
72	1	101,8	31,0	10,0
	2	84,8	30,0	13,1
	3	45,1	22,3	10,7
144	1	49,3	17,2	7,6
	2	63,9	18,4	8,1
	3	46,5	16,6	9,9
240	1	46,6	12,4	5,8
	2	43,1	13,2	5,2
	3	48,3	14,8	5,1

Time	CTRL	5 g/L	10 g/L
	RSD		
1	15,5 %	29,6 %	27,8 %
3	13,1 %	23,1 %	1,3 %
6	5,6 %	11,3 %	6,1 %
24	5,5 %	15,2 %	31,3 %
48	21,8 %	19,0 %	10,4 %
72	37,7 %	17,2 %	14,2 %
144	17,5 %	5,2 %	13,7 %
240	5,7 %	9,2 %	7,2 %

9 °C

Time	Triplicate	CTRL	5 g/L	10 g/L
		Concentration (ng/mL)		
1	1	48,4	41,2	37,0
	2	47,4	43,7	37,7
	3	46,3	46,1	37,1
3	1	48,3	42,9	31,9
	2	48,5	43,6	32,0
	3	45,7	44,1	34,0
6	1	48,4	45,9	28,0
	2	49,5	39,4	28,4
	3	46,3	44,6	29,7
24	1	50,0	34,3	17,1
	2	48,6	31,6	15,7
	3	46,6	33,1	15,8
48	1	49,5	26,8	10,9
	2	50,0	25,3	11,1
	3	47,0	24,2	10,4
72	1	50,2	21,2	8,9
	2	48,7	20,9	9,3
	3	46,9	22,0	8,5
144	1	53,4	16,7	6,1
	2	47,3	14,5	5,8
	3	46,2	15,2	5,8
240	1	49,0	11,7	4,6
	2	48,3	12,0	4,5
	3	48,6	11,9	4,4

Time	CTRL	5 g/L	10 g/L
	RSD		
1	2,2 %	5,6 %	1,0 %
3	3,3 %	1,4 %	3,6 %
6	3,4 %	8,0 %	3,1 %
24	3,5 %	4,2 %	4,8 %
48	3,3 %	5,2 %	3,5 %
72	3,4 %	2,4 %	4,8 %
144	8,0 %	7,5 %	2,9 %
240	0,7 %	1,3 %	1,9 %

Table 29: Oxytetracyline raw kinetics data

4 °C					9 °C				
		Concentration (ng/mL)					Concentration (ng/mL)		
Time (h)	Triplicate	CTRL	5 g/L	10 g/L	Time	Triplicate	CTRL	5 g/L	10 g/L
1	1	73,9	67,6	45,3	1	1	145,7	87,8	85,9
	2	58,0	54,0	46,9		2	146,3	322,2	156,1
	3	58,8	81,6	64,6		3	124,4	150,5	91,9
3	1	53,4	60,9	49,4	3	1	127,8	112,4	76,2
	2	102,4	68,7	50,2		2	108,9	161,1	99,6
	3	48,2	53,9	50,6		3	114,1	130,9	162,1
6	1	54,8	50,4	45,7	6	1	142,8	254,3	143,6
	2	53,4	52,5	51,6		2	152,7	102,1	91,9
	3	51,0	49,5	50,3		3	135,6	482,9	88,0
24	1	59,7	61,6	54,1	24	1	148,4	193,6	177,4
	2	64,1	55,2	79,9		2	116,3	95,0	72,0
	3	55,6	51,6	50,2		3	134,1	164,6	79,9
48	1	71,3	50,4	46,7	48	1	135,5	619,4	97,4
	2	53,0	57,7	49,5		2	155,9	113,2	70,6
	3	55,6	49,4	50,5		3	130,1	109,6	65,9
72	1	78,2	52,4	47,9	72	1	155,8	104,8	83,5
	2	89,4	52,1	54,5		2	136,6	119,8	190,4
	3	51,3	49,4	46,5		3	113,2	96,2	79,8
144	1	56,4	56,4	55,0	144	1	379,8	269,4	70,1
	2	68,7	48,9	49,7		2	112,7	91,9	92,7
	3	44,3	44,5	53,7		3	137,0	116,1	78,6
240	1	50,0	45,5	49,0	240	1	86,4	62,0	141,0
	2	48,4	45,3	46,3		2	85,0	72,7	46,7
	3	47,3	83,5	44,6		3	91,4	65,2	49,4

	RSD					RSD		
Time	CTRL	5 g/L	10 g/L		Time	CTRL	5 g/L	10 g/L
1	14 %	20 %	21 %		1	9,0 %	64,9 %	35,0 %
3	44 %	12 %	1 %		3	8,3 %	18,2 %	18,9 %
6	4 %	3 %	6 %		6	6,0 %	68,5 %	28,8 %
24	7 %	9 %	26 %		24	12,1 %	33,5 %	53,5 %
48	16 %	9 %	4 %		48	9,7 %	104,5 %	21,8 %
72	27 %	3 %	9 %		72	15,8 %	11,1 %	53,3 %
144	22 %	12 %	5 %		144	70,4 %	60,5 %	14,2 %
240	3 %	38 %	5 %		240	3,9 %	8,3 %	67,9 %

Table 30: Paracetamol raw kinetics data

4 °C						9 °C				
		Concentration (ng/mL)						Concentration (ng/mL)		
			5			Time		CTRL		
Time	Triplicate	CTRL	g/L	10 g/L			Triplicate		5 g/L	10 g/L
1	1	40,9	40,2	39,7		1	1	48,4	50,9	51,7
	2	40,1	46,9	39,7			2	51,9	48,3	52,1
	3	41,1	40,7	39,9			3	47,9	52,9	52,3
3	1	41,5	39,8	36,5		3	1	49,6	53,4	51,2
	2	40,3	39,5	40,0			2	49,6	50,9	51,7
	3	38,8	40,4	41,5			3	46,5	50,7	51,0
6	1	41,6	40,9	40,6		6	1	49,3	50,4	51,3
	2	39,8	40,7	39,9			2	48,2	49,0	51,2
	3	39,8	39,9	41,0			3	44,1	50,5	49,9
24	1	39,9	40,9	40,0		24	1	48,8	51,1	49,6
	2	40,0	39,1	39,7			2	48,6	51,1	51,8
	3	40,1	40,0	40,4			3	47,1	51,8	53,4
48	1	41,3	40,7	40,3		48	1	49,7	50,9	51,3
	2	40,2	40,5	40,1			2	48,6	50,6	53,1
	3	39,7	40,6	40,7			3	47,1	52,2	52,6
72	1	41,5	40,1	39,6		72	1	49,4	53,0	52,0
	2	40,2	40,2	39,8			2	50,7	51,0	51,4
	3	40,1	40,3	40,7			3	47,3	52,6	51,1
144	1	41,3	40,9	40,0		144	1	49,5	51,8	51,4
	2	40,2	39,9	39,4			2	49,9	51,2	52,8
	3	39,8	39,8	41,0			3	47,8	53,9	51,5
240	1	39,6	38,6	38,1		240	1	31,3	32,5	32,7
	2	38,0	38,9	38,2			2	31,3	31,7	33,7
	3	38,6	37,6	39,1			3	30,1	32,9	38,0
		RSD						RSD		
Time	CTRL	5 g/L	10 g/L			Time	CTRL	5 g/L	10 g/L	
1	1,3 %	8,8 %	0,3 %			1	4,4 %	4,5 %	0,6 %	
3	3,4 %	1,1 %	6,6 %			3	3,6 %	2,9 %	0,8 %	
6	2,6 %	1,3 %	1,4 %			6	5,8 %	1,7 %	1,5 %	
24	0,2 %	2,2 %	0,8 %			24	2,0 %	0,8 %	3,7 %	
48	1,9 %	0,3 %	0,8 %			48	2,7 %	1,6 %	1,8 %	
72	1,9 %	0,2 %	1,5 %			72	3,4 %	2,0 %	0,9 %	
144	1,9 %	1,5 %	2,0 %			144	2,2 %	2,8 %	1,5 %	
240	2,0 %	1,8 %	1,3 %			240	2,2 %	2,0 %	8,1 %	

Table 31: Tetracycline raw kinetics data

4 °C

		Concentration (ng/mL)		
Time	Triplicate	CTRL	5 g/L	10 g/L
1	1	33,5	50,1	30,4
	2	33,4	24,9	30,8
	3	25,2	35,1	27,1
3	1	33,9	36,2	26,8
	2	34,1	34,0	25,7
	3	23,3	27,0	25,3
6	1	29,6	22,1	21,8
	2	21,8	34,3	23,3
	3	19,8	30,5	22,5
24	1	22,8	35,5	42,3
	2	37,9	35,6	46,4
	3	21,6	23,3	11,2
48	1	30,2	17,8	23,0
	2	39,4	16,5	27,6
	3	29,4	37,6	21,7
72	1	29,9	39,7	33,8
	2	32,7	26,5	16,2
	3	18,4	12,6	23,1
144	1	28,3	28,4	50,7
	2	29,6	24,4	17,7
	3	22,6	19,6	18,8
240	1	19,6	15,7	12,3
	2	20,6	30,9	14,7
	3	13,0	40,4	20,4

	RSD		
Time	CTRL	5 g/L	10 g/L
1	15,5 %	34,5 %	6,8 %
3	20,4 %	14,9 %	2,9 %
6	21,8 %	21,4 %	3,3 %
24	33,0 %	22,4 %	57,8 %
48	16,8 %	49,4 %	12,9 %
72	28,1 %	51,7 %	36,3 %
144	14,0 %	18,3 %	64,5 %
240	23,3 %	42,9 %	26,7 %

9 °C

		Concentration (ng/mL)		
Time	Triplicate	CTRL	5 g/L	10 g/L
1	1	79,9	79,0	74,6
	2	71,8	58,6	78,8
	3	53,6	91,1	61,8
3	1	74,0	80,8	62,6
	2	60,0	85,7	68,3
	3	49,7	83,7	16,4
6	1	76,5	36,0	71,8
	2	70,2	74,3	55,1
	3	54,3	62,6	54,7
24	1	84,2	38,5	65,8
	2	57,3	75,8	54,9
	3	50,5	82,1	64,3
48	1	77,8	27,6	48,5
	2	65,5	76,2	51,3
	3	46,0	72,4	49,7
72	1	86,4	73,5	57,5
	2	67,5	66,3	17,5
	3	48,5	67,6	46,4
144	1	33,9	65,5	44,6
	2	54,0	70,4	48,6
	3	47,1	70,5	44,3
240	1	41,9	40,6	28,2
	2	27,8	40,9	30,9
	3	30,7	44,6	35,2

	RSD		
Time	CTRL	5 g/L	10 g/L
1	19,7 %	21,6 %	12,3 %
3	19,9 %	3,0 %	6,1 %
6	17,1 %	34,0 %	16,2 %
24	27,8 %	36,0 %	9,6 %
48	25,4 %	46,1 %	2,8 %
72	28,1 %	5,6 %	51,1 %
144	22,7 %	4,2 %	5,3 %
240	22,3 %	5,4 %	11,2 %

Table 32: Trimethoprim raw kinetics data

4 °C					9 °C				
		Concentration (ng/mL)					Concentration (ng/mL)		
Time	Triplicate	CTRL	5 g/L	10 g/L	Time	Triplicate	CTRL	5 g/L	10 g/L
1	1	47,1	51,9	27,7	1	1	31,1	27,6	28,9
	2	38,4	31,4	27,9		2	30,8	28,2	29,9
	3	48,7	51,4	41,2		3	29,9	30,1	29,0
3	1	38,1	43,3	27,9	3	1	31,2	30,5	29,0
	2	33,0	40,1	28,9		2	32,1	30,7	28,9
	3	32,6	29,9	31,2		3	29,6	31,6	30,3
6	1	33,6	29,9	29,0	6	1	31,3	34,2	28,5
	2	35,0	36,8	31,6		2	31,9	29,3	29,4
	3	33,7	33,2	27,9		3	31,0	33,3	31,0
24	1	38,6	35,3	46,6	24	1	32,1	33,1	30,0
	2	41,7	39,3	32,9		2	31,3	30,3	28,7
	3	41,3	30,6	29,2		3	30,4	32,9	29,9
48	1	51,0	32,0	32,0	48	1	31,5	33,0	29,3
	2	39,8	39,6	27,2		2	32,5	31,1	28,8
	3	40,3	32,9	31,9		3	30,8	29,9	27,5
72	1	65,7	42,0	27,4	72	1	33,9	31,9	29,4
	2	57,7	41,6	33,1		2	31,4	31,9	31,2
	3	33,6	30,5	30,2		3	30,9	33,1	29,9
144	1	34,9	33,0	33,5	144	1	33,2	34,9	31,2
	2	42,0	29,7	32,4		2	30,6	30,3	30,0
	3	35,3	31,4	40,9		3	29,7	31,9	30,5
240	1	34,9	31,0	31,0	240	1	31,2	32,5	30,3
	2	32,9	31,5	28,3		2	31,6	32,2	29,7
	3	37,1	33,2	28,6		3	31,5	32,1	30,4

4 °C					9 °C				
	RSD					RSD			
Time	CTRL	5 g/L	10 g/L		Time	CTRL	5 g/L	10 g/L	
1	12,4 %	26,1 %	24,0 %		1	2,0 %	4,5 %	1,8 %	
3	8,9 %	18,6 %	5,7 %		3	4,2 %	2,0 %	2,7 %	
6	2,4 %	10,3 %	6,4 %		6	1,5 %	8,1 %	4,3 %	
24	4,1 %	12,5 %	25,2 %		24	2,8 %	4,8 %	2,5 %	
48	14,4 %	12,0 %	9,1 %		48	2,7 %	5,0 %	3,3 %	
72	31,9 %	17,2 %	9,5 %		72	5,0 %	2,1 %	3,0 %	
144	10,6 %	5,3 %	13,0 %		144	5,9 %	7,3 %	1,8 %	
240	5,9 %	3,6 %	5,1 %		240	0,6 %	0,6 %	1,3 %	

7.5 Experimental data, isotherm experiments

Table 33: Ciprofloxacin raw isotherm data, 4 ℃

C0	Triplicate	CTRL (ng/mL)	C_e (ng/mL)	C_e (mg/L)	q_e	SD (q_e)
8	1	11,6	8,3	0,008311	0,0005	2,96E-05
	2	10,6	9,6	0,009606	0,0003	1,48E-05
	3	10,5	3,9	0,003854	0,0014	8,03E-05
16	1	31,0	8,2	0,008207	0,0034	0,000716
	2	24,1	10,0	0,010005	0,0031	0,00064
	3	20,6	12,7	0,012704	0,0025	0,000527
31	1	54,2	10,5	0,010452	0,0072	0,001286
	2	37,8	20,0	0,019975	0,0053	0,000948
	3	48,0	13,1	0,013135	0,0067	0,00119
63	1	84,8	31,3	0,031335	0,0108	0,000396
	2	88,8	20,7	0,020749	0,0129	0,000473
	3	82,6	27,5	0,027549	0,0116	0,000424
125	1	158,4	58,8	0,058835	0,0211	0,001493
	2	177,5	45,7	0,045749	0,0237	0,001678
	3	156,5	53,1	0,053091	0,0222	0,001574
250	1	338,0	124,2	0,124186	0,0457	0,002769
	2	342,9	113,0	0,113041	0,0479	0,002904
	3	377,2	108,7	0,108706	0,0488	0,002957
500	1	740,9	257,1	0,257087	0,0817	0,008009
	2	623,7	231,9	0,231906	0,0868	0,008502
	3	632,6	235,3	0,235331	0,0861	0,008435
1000	1	1135,1	452,3	0,452286	0,1457	0,008825
	2	1144,2	561,2	0,561164	0,1239	0,007506
	3	1263,3	575,8	0,575769	0,1210	0,00733

Table 34: Citalopram raw isotherm data, 4 ℃

C_0	Triplicate	CTRL (ng/mL)	C_e (ng/mL)	C_e (mg/L)	q_e (mg/g)	SD (q_e)
8	1	7,9	0,7	0,000701	0,00149	4,00009E-05
	2	8,3	4,2	0,004189	0,00079	2,12213E-05
	3	8,2	4,2	0,004238	0,00078	2,0958E-05
16	1	15,9	*			
	2	19,4	4,3	0,004293	0,00239	0,000439353
	3	13,5	1,0	0,001014	0,00305	0,000559907
31	1	30,3	1,5	0,001530	0,00517	0,000736092
	2	22,9	1,9	0,001943	0,00508	0,000724322
	3	28,9	4,5	0,004478	0,00458	0,000652082
63	1	71,7	3,8	0,003792	0,01229	0,001142831

	2	64,4	5,8	0,005777	0,01189	0,001105915
	3	59,6	6,0	0,006024	0,01184	0,001101311
125	1	83,5	*			
	2	119,1	12,7	0,012658	0,01700	0,00329128
	3	90,3	11,7	0,011731	0,01719	0,003327189
250	1	178,3	39,0	0,038998	0,04686	0,015157645
	2	353,1	43,3	0,043346	0,04599	0,014876305
	3	288,5	60,9	0,060921	0,04248	0,013739358
500	1	596,6	128,9	0,128899	0,06587	0,017229783
	2	386,6	132,4	0,132443	0,06516	0,017044402
	3	391,5	129,5	0,129521	0,06575	0,017197268
1000	1	763,7	442,6	0,442628	0,06640	0,001541613
	2	795,4	444,8	0,444789	0,06597	0,00153158
	3	764,8	537,5	0,537533	0,04742**	

*Faulty samples   ** Outlier

Table 35: Fluoxetine raw isotherm data, 4 ℃

C_0	Triplicate	CTRL (ng/mL)	C_e (ng/mL)	C_e (mg/L)	q_e (mg/g)	SD (q_e)
8	1	3,08	1,66	0,00166	0,00032	3,00E-05
	2	3,13	1,67	0,001666	0,00032	2,98E-05
	3	3,63	0,77	0,000768	0,00050	4,64E-05
16	1	3,43	1,19	0,001191	0,00057	7,65E-05
	2	4,40	0,72	0,000722	0,00067	8,90E-05
	3	4,32	1,04	0,001037	0,00060	8,06E-05
31	1	7,89	2,30	0,002298	0,00118	2,69E-04
	2	10,23	2,86	0,002864	0,00107	2,43E-04
	3	6,54	2,62	0,002623	0,00112	2,54E-04
63	1	18,27	4,48	0,004479	0,00232	3,89E-04
	2	16,95	4,05	0,004045	0,00241	4,04E-04
	3	13,08	5,95	0,00595	0,00203	3,40E-04
125	1	18,33	14,91	0,014906	0,00326	1,18E-03
	2	39,50	9,54	0,009536	0,00433	1,57E-03
	3	35,72	13,16	0,013164	0,00360	1,30E-03
250	1	82,41	31,51	0,031506	0,01176	1,37E-03
	2	102,28	34,53	0,034531	0,01116	1,30E-03
	3	86,25	39,62	0,039618	0,01014	1,18E-03
500	1	226,94	102,98	0,102978	0,01674	3,85E-03
	2	191,54	122,53	0,122531	0,01283	2,95E-03
	3	141,54	109,41	0,109414	0,01545	3,55E-03
1000	1	355,39	324,36**	0,32463	0,00438	3,40 E-04
	2	315,98	240,08	0,24008	0,02124	1,65E-03
	3	367,41	249,76	0,249761	0,01930	1,50E-03

** Outlier

Table 36: Ciprofloxacin raw isotherm data, 9 °C

C_0	Parallel	CTRL (mg/L)	C_e (mg/L)	q_e (mg/g)	Sd (q_e)
8	1	0,02072	0,0079	0,0032	0,0016
	2	0,03120	0,0063	0,0035	0,0017
	3	0,01912	0,0128	0,0022	0,0011
16	1	0,03993	0,0228	0,0046	0,0023
	2	0,05291	0,0489**		
	3	0,04487	0,0104	0,0071	0,0036
31	1	0,07757	0,0315	0,0090	0,004499
	2	0,07145	0,0599	0,0033	0,001653
	3	0,08033	0,0434	0,0066	0,003307
63	1	0,15858	0,0935	0,0152	0,007618
	2	0,16796	0,0842	0,0171	0,008552
	3	0,18263	0,0544	0,0231	0,011536
125	1	0,39048	0,1202	0,0526	0,024789
	2	0,37570	0,1509	0,0464	0,021894
		0,07494**	0,1577	0,0451	0,02125
250	1	0,73456	0,3328	0,0759	0,03794
	2	0,69109	0,2675	0,0889	0,044466
	3	0,71087	0,2888	0,0847	0,042337
500	1	1,51813	0,8878	0,1465	0,073255
	2	1,73628	0,9191	0,1403	0,07013
	3	1,60671	0,9220	0,1397	0,069842
1000	1	3,36539	2,0284	0,2568	0,181553
		1,49658**	2,1922	0,2240	0,158387
	3	3,25897	1,5451	0,3534	0,249899

** outliers

Table 37: Citalopram raw isotherm data, 9 °C

C_0	Parallel	CTRL (mg/L)	C_e (mg/L)	q_e (mg/g)	SD (q_e)
8	1	0,00541	0,0002	0,0010	0,0005
	2	0,00517	0,0001	0,0010	0,0005
	3	0,00497	0,0002	0,0010	0,0005
16	1	0,01105	0,0004	0,0023	0,0011
	2	0,01196	0,0003	0,0023	0,001138
	3	0,01208	0,0003	0,0023	0,0011
31	1	0,02685	0,0005	0,0046	0,002302
	2	0,02064	0,0006	0,0046	0,002294
	3	0,02321	0,0008	0,0046	0,002279
63	1	0,04220	0,0017	0,0089	0,004474
	2	0,04895	0,0032	0,0086	0,004323

	3	0,04820	0,0019	0,0089	0,004457
125	1	0,11819	0,0093	0,0212	0,010014
	2	0,11288	0,0070	0,0217	0,010233
		0,02542**	0,0052	0,0221	0,010406
250	1	0,22109	0,0346	0,0361	0,018049
	2	0,21149	0,0281	0,0374	0,018693
	3	0,21263	0,0260	0,0378	0,018907
500	1	0,43915	0,1364	0,0689	0,034434
	2	0,51828	0,1380	0,0685	0,034274
	3	0,48485	0,1477	0,0666	0,033311
1000	1	0,91953	0,5517	0,0700	0,049499
		0,47910**	0,5809	0,0642	0,045369
	3	0,88382	0,6183	0,0567	0,040079

*outliers

Table 38: fluoxetine raw isotherm data, 9 ℃

C_0	Parallel	CTRL (mg/L)	C_e (mg/L)	q_e (mg/g)	SD (q_e)
8	1	0,00249	0,0012	0,0002	0,0001
	2	0,00212	0,0012	0,0002	0,0001
	3	0,00236	0,0009	0,0003	0,0001
16	1	0,00429	0,0016	0,0006	0,0003
	2	0,00436	0,0016	0,0006	0,0003
	3	0,00490	0,0014	0,0006	0,0003
31	1	0,00909	0,0029	0,0011	0,00053
	2	0,00767	0,0026	0,0011	0,000552
	3	0,00771	0,0019	0,0012	0,000622
63	1	0,01461	0,0053	0,00255	0,001276
	2	0,02019	0,0038	0,00284	0,001421
	3	0,01929	0,0058	0,00245	0,001224
125	1	0,05335	0,0118	0,00848	0,003995
	2	0,05494	0,0100	0,00882	0,004159
	3	0,01299**	0,0106	0,00871	0,004108
250	1	0,11695	0,0251	0,01517	0,007587
	2	0,08913	0,0280	0,01459	0,007293
	3	0,09685	0,0298	0,01423	0,007117
500	1	0,18369	0,0635	0,03466	0,017329
	2	0,27829	0,0753	0,03231	0,016156
	3	0,24852	0,0619	0,03499	0,017495
1000	1	0,60900	0,2416	0,06451	0,045612
	2	0,26547**	0,2474	0,06334	0,044788
	3	0,51923	0,2503	0,06276	0,044381

** Outliers

7.6   Isotherm model data

Table 39: Isotherm parameters for the linear isotherm model (Henrys Law), using linear regression

	Parameter	CIP	CIT	FLU
4 °C				
	K_D (L/g)	0,2454	0,1497	0,0846
	R^2	0,8837	0,1717	0,6695
	MPSD	182,1	79,78	71,08
	HYBRID	0,4691	1,350	0,1781
	EABS	0,2625	0,3371	0,0622
	ARE	77,40	71,34	65,02
9 °C				
	K_D (L/g)	0,1340	0,1320	0,2562
	R^2	0,8873	0,1799	0,8896
	MPSD	54,57	89,47	47,47
	HYBRID	0,8063	1,380	0,2292
	EABS	0,4660	0,3991	0,1014
	ARE	42,52	83,87	41,91

Table 40: Langmuir model parameters and SNE after optimization by different error functions

		R^2	MPSD	HYBRID	EABS	ARE
4 °C						
CIP	K_L (L/mg)	2,2254	0,0242	0,7044	2,4721	**0,0305**
	q_{max} (mg/g)	0,2385	2,6050	0,4916	0,2133	**6,480**
	SNE	-	2,83	1,70	2,38	**1,69**
CIT	K_L (L/mg)	28,52	1,893	**11,49**	28,37	4,303
	q_{max} (mg/g)	0,0770	0,1715	**0,0931**	0,0825	0,1013
	SNE	-	2,64	**1,92**	3,28	2,34
FLU	K_L (L/mg)	20,4843	12,3568	**17,221**	19,4998	15,354
	q_{max} (mg/g)	0,02320	0,0268	**0,0240**	0,0233	0,0254
	SNE	-	3,81	**3,55**	3,65	3,56
9 °C						
CIP	K_L (L/mg)	0,8148	0,0366	0,5503	0,8496	**0,3695**
	q_{max} (mg/g)	0,3669	3,6818	0,4433	0,3443	**0,5533**
	SNE	-	3,59	2,81	3,07	**2,73**
CIT	K_L (L/mg)	53,6	104,4	**65,7**	44,2	107,6
	q_{max} (mg/g)	0,069	0,056	**0,066**	0,073	0,058
	SNE	-	3,20	**2,98**	3,61	3,16
FLU	K_L (L/mg)	7,399	0,6026	**5,441**	7,223	2,157
	q_{max} (mg/g)	0,0986	0,5405	**0,1133**	0,0988	0,1883
	SNE	-	3,04	**2,22**	2,64	2,29

Table 41: Freundlich model parameters and SNE after optimization by different error functions

		R^2	MPSD	HYBRID	EABS	ARE
4 °C						
CIP	K_F ($L^{1/n}$*$mg^{1-1/n}$/g)	0,2063	0,4081	**0,2663**	0,2366	0,4462
	n	1,43	0,70	**1,02**	1,28	0,71
	SNE	-	2,45	**1,88**	3,36	2,48
CIT	K_F ($L^{1/n}$*$mg^{1-1/n}$/g)	0,1086	0,1808	**0,1448**	0,1090	0,1441
	n	2,66	1,10	**1,58**	2,35	1,05
	SNE	-	2,62	**2,07**	2,81	2,86
FLU	K_F ($L^{1/n}$*$mg^{1-1/n}$/g)	0,0430	0,0758	0,0567	0,0497	**0,0541**
	n	2,01	1,31	1,56	1,68	**1,52**
	SNE	-	3,40	3,08	3,44	**2,92**
9 °C						
CIP	K_F ($L^{1/n}$*$mg^{1-1/n}$/g)	0,1505	0,1296	**0,1427**	0,1488	0,1560
	n	1,56	1,01	**1,23**	1,55	1,09
	SNE	-	2,62	**2,18**	3,52	2,30
CIT	K_F ($L^{1/n}$*$mg^{1-1/n}$/g)	0,087	0,115	**0,098**	0,084	0,122
	n	3,53	2,01	**2,50**	3,27	2,02
	SNE	-	2,28	**2,17**	3,71	2,29
FLU	K_F ($L^{1/n}$*$mg^{1-1/n}$/g)	0,1579	0,3645	0,2216	0,1621	**0,2622**
	n	1,58	0,970	1,22	1,49	**1,06**
	SNE	-	2,36	1,81	3,37	**1,76**

Table 42: Temkin model parameters and SNE after optimization by different error functions

		R2	MPSD	HYBRID	EABS	ARE
4 °C						
CIP	K_T (L/mg)	87,996	163,78	**123,89**	99,217	113,707
	b (kJ/mol)	83,670	2144,8	**160,87**	91,320	467,36
	SNE	-	2,62	**1,97**	3,24	2,18
CIT	K_T (L/mg)	577,32	$1,4*10^{24}$	**575,19**	673,39	14,031
	b (kJ/mol)	192,118	93548,1	**369,961**	212,583	11906,6
	SNE	-	2,51	**2,20**	3,24	2,54
FLU	K_T (L/mg)	649,84	1478,8	**929,20**	600,549	1577,8
	b (kJ/mol)	721,066	3484,27	**1112,22**	673,354	2733,14
	SNE	-	2,79	**2,08**	3,39	2,43
9 °C						
CIP	K_T (L/mg)	47,259	421,60	**92,610**	40,436	300,86
	b (kJ/mol)	61,679	1156,13	**167,93**	62,775	910,49
	SNE	-	1,78	**1,57**	3,44	1,74
CIT	K_T (L/mg)	3193,0	8886,9	**5778,1**	3140,2	8258,2
	b (kJ/mol)	263,71	794,96	**371,15**	274,52	766,90
	SNE	-	2,51	**1,80**	3,38	2,45
FLU	K_T (L/mg)	469,76	1030,1	**788,9**	598,70	936,05
	b (kJ/mol)	282,330	1772,57	**482,99**	276,33	1567,82
	SNE	-	2,12	**1,73**	3,63	2,06

Table 43: Sips model parameters and SNE after optimization by different error functions

		R2	MPSD	HYBRID	EABS	ARE
4 °C						
CIP	K_S (L^n*mg^{-n})	6,04	361,54	12,594	7,5243	**66,223**
	q_{max} (mg/g)	0,17566	0,0896	0,1501	0,15898	**0,1109**
	n	1,277	2,3971	1,5098	1,30639	**1,9938**
	SNE	-	2,86	1,70	2,43	**1,51**
CIT	K_S (L^n*mg^{-n})	107,356	235510,4	**672,81**	684,334	2718,27
	q_{max} (mg/g)	0,0703	0,0557	**0,0657**	0,0688	0,0669
	n	1,30	2,99	**1,78**	1,74	2,25
	SNE	-	3,24	**3,03**	3,28	3,06
FLU	K_S (L^n*mg^{-n})	20,6730	21,6747	**22,418**	18,3859	15,2684
	q_{max} (mg/g)	0,02316	0,02317	**0,0229**	0,02342	0,02456
	n	1,00	1,07	**1,04**	0,985	0,993
	SNE	-	3,77	**3,61**	3,84	3,67
9 °C						
CIP	K_S (L^n*mg^{-n})	0,4296	0,2831	1,5653	1,0305	**0,8638**
	q_{max} (mg/g)	0,5302	0,6545	0,2754	0,3062	**0,3370**
	n	0,835	1,12	1,25	0,977	**1,12**
	SNE	-	3,37	2,64	3,52	**2,61**
CIT	K_S (L^n*mg^{-n})	34,530	24,647	**22,673**	17,600	23,242
	q_{max} (mg/g)	0,0710	0,0701	**0,0721**	0,0761	0,0685
	n	0,904	0,834	**0,822**	0,789	0,811
	SNE	-	3,85	**3,82**	3,90	3,94
FLU	K_S (L^n*mg^{-n})	11,187	56,999	17,253	18,490	**27,057**
	q_{max} (mg/g)	0,0896	0,0630	0,0825	0,0814	**0,0773**
	n	1,09	1,39	1,19	1,19	**1,28**
	SNE	-	3,58	3,16	2,82	**2,77**

Table 44: HYBRID, ARE and R^2 error for different isotherm models, optimized for each error function (except for linear model)

	HYBRID		ARE		R^2	
	4 °C	9 °C	4 °C	9 °C	4 °C	9 °C
Linear						
CIP	0,4691	0,8063	77,40	42,52	0,8837	0,8873
CIT	1,350	1,380	71,34	83,87	0,1717	0,1799
FLU	0,1781	0,2292	65,02	41,91	0,6695	0,8896
Langmuir						
CIP	0,3763	0,4588	75,40	38,81	0,9740	0,9723
CIT	0,3968	0,0732	65,82	17,03	0,9694	0,9699
FLU	0,0128	0,0209	28,29	32,73	0,9647	0,9933
Freundlich						
CIP	0,4447	0,6107	63,10	40,66	0,9555	0,9702
CIT	0,7531	0,3545	67,79	37,07	0,8435	0,8687
FLU	0,0527	0,1139	31,01	36,87	0,9361	0,9805
Temkin						
CIP	1,4732	3,3821	83,73	67,52	0,8616	0,7246
CIT	1,4145	0,4087	82,27	40,95	0,9077	0,9176
FLU	0,1452	0,6167	51,79	52,19	0,8977	0,8511
Sips						
CIP	0,1654	0,4321	42,14	38,17	0,9778	0,9747
CIT	0,2416	0,0544	45,93	13,56	0,9773	0,9709
FLU	0,0258	0,0277	26,99	20,28	0,9647	0,9937

Ingrid Alver Hovsbakken

Master's thesis in Analytical Chemistry

NTNU
Norwegian University of
Science and Technology